ANALYSIS OF VARIABLE SCATTEROMETER WIND FIELDS IN THE BENGUELA UPWELLING REGION

By

ASHLEY STRATTON JOHNSON

Submitted in fulfillment of the requirements for the degree Master of Science in the Faculty of Science at the UNIVERSITY OF CAPE TOWN

JUNE 2001

Supervisor: Assoc. Prof. F.A. Shillington *(Dept. of Oceanography)*

Co-Supervisors: Mr. G. Nelson *(Physical and Chemical Oceanography Section, Marine and Coastal Management)*
Dr. C. Roy *(Institut de Recherche pour le Développement Research Associate at the Dept. of Oceanography)*

This dissertation is dedicated:

Firstly to my wife Jessica, my daughter Brittany, my mother Anna

and my aunts Mymoena and Claire

"Everything should be made as simple as possible,
but not simpler"
--Albert Einstein

"If nature were not beautiful, it would not be worth studying it.
And life would not be worth living"
--Henry Poincaré

"The sea is man's constant companion. It forms the tread of his
activities and, as such, binds all men to it"
--Mac Orlan

ABSTRACT

The dissertation seeked to understand the effectiveness of satellite based data collection of wind fields along the west coast of southern Africa, pertaining to particular synoptic atmospheric systems. A comparison between data from two automatic coastal weather stations and measurements obtained by the NASA scatterometer (NSCAT) for the period 1 December 1996 to 31 May 1997 yielded a correlation coefficient of 70%. NSCAT longshore wind components, as close to the coast as possible, were extracted as time series at four known areas of upwelling, namely Cape Peninsula, Cape Columbine, Hondeklip Bay and Lüderitz. Using a simple, two-layer model coastal Ekman divergence volumes were calculated in Sverdrups. The volume fluxes showed the dominance of the Lüderitz upwelling cell contributing a total of 1.23 Sv over the period 1 Dec 1996 - 28 Feb 1997. The total volume upwelled by the four areas over the 3-month summer period is 1.69 Sv.

NSCAT data were used to do a quantitative study of the South Atlantic Anticyclone (SAA) during the eastward ridging process, a cold front, a west coast trough and coastal low generation. It was found that during the eastward ridging of the SAA, highest negative/clockwise wind stress curl values derived from the wind vector components. As a result, the highest upward vertical velocity induced at the base of the Ekman layer was 1.56 $m.day^{-1}$ compared to a coastal Ekman divergence velocity of 68 $m.day^{-1}$. It was concluded that the spatial structure in the wind field produced very low values of upward vertical velocities during active phases of coastal upwelling, hence the process of wind stress curl is negligible.

It was also found that the offshore extent of topographical steering by coastal mountains around the Cape Peninsula-Cape Columbine area is approximately 200km. West coast troughs of low pressure produced low wind speeds of ≤ 5 ms^{-1} over an average distance of 120 nmiles (~ 200km) from the coast. The area of maximum wind

speed was also pushed further offshore as a result of the west coast atmospheric trough advecting down the coast from Namibia towards Cape Town. The troughs were also found to be the major atmospheric trigger of long periods of low wind speeds over the shelf during late-summer of 1996/1997. Between 27 March and 4 April 1997, a persistent trough of low pressure reduced winds along the west coast of South Africa to ~ 2 ms^{-1} for a period of nine days. During this period an anticyclone was also anomalously situated at approximately 40°S and in conjunction with the passage of a cold front produced onshore flow that advected a dense dinoflagellate bloom inshore that eventually produced the largest rock lobster mortality of 1500 tonnes.

Coastal lows were shown to form in the vicinity of either Lüderitz or Walvis Bay along the Namibian coast. The system is initiated by an offshore flow from the land being confined by an offshore band of strong equatorward wind forcing the clockwise rotation. The offshore extent of the coastal lows was approximately 200km. The systems propagated with a speed of ~11 ms^{-1}.

ACKNOWLEDGEMENTS

I wish to express my appreciation and thanks to my ex-Director: Marine and Coastal Management, Dr Andy Payne, for his continued support and permission to undertake this dissertation, my supervisors Assoc. Prof. F.A. Shillington, Dr C. Roy and Mr. G. Nelson. I sincerely thank my colleagues for their continued support, especially the technicians responsible for regular servicing of equipment. A special thank-you to Christine Illert and Neil Needham for their dedication and regular updating of the wind database. This thesis is dedicated to my wife Jessica.

The NSCAT data were obtained from the NASA Physical Oceanography Distributed Active Archive Centre at the Jet Propulsion Laboratory, California Institute of Technology.

LIST OF CONTENTS

Introduction

The Benguela, together with the California Current, Chile-Peru and North African upwelling systems, is one of four major eastern boundary current regions of the World Ocean (Hill *et al.*, 1998). Durand *et al.* (1998) estimated that their combined surface area accounts for only 0.1% of the total surface area of the world oceans. Like the other three systems, the Benguela coastal upwelling process enriches the ecosystem with nutrients. Coastal upwelling is induced by a strong equatorward wind along the coast causing an offshore directed advection. The surface offshore advection perpendicular to the coast, also termed coastal Ekman divergence, is compensated by a deeper, nutrient-rich onshore flow to satisfy conservation of mass. Coastal upwelling makes the four eastern boundary current systems important and they collectively provide almost 30% of the world's total fish catches (Durand *et al.*, 1998). Not only is the Benguela an extremely productive biological area, but also economically important due to the rich fishery it supports. As a result, a large part of marine research in South Africa has been directed towards the analysis and understanding of the ecosystem and its variability. Numerous studies during the last few decades resulted in the publishing of special volumes in the *South African Journal of Marine Science* (1987, 1992, 1998) under the Benguela Ecology Programme.

Coastal upwelling manifests itself as a sea surface temperature depression along the coast. Consequently sea surface temperature has been used as a major variable in studying environmental effects on fish populations. More recent findings have tended to examine the effects of wind action on the sea surface to explain variability in fish populations (Bakun *et al.*, 1991). The longshore, equatorward component of wind stress is not perennial in the southern Benguela (south of the Orange River; 28.5°S) and has a seasonal character. The wind stress is strongest and most consistent during summer. During summer, the wind over the continental shelf has been

shown to exhibit modulation in speed between 3 and 6 days (Nelson and Hutchings, 1983). The pulsing nature of winds in the southern Benguela suggests that there are periods of relatively low wind separating two wind maxima. Therefore, the length and timing of such low wind events are important not only for fish recruitment (Hutchings, 1992), but also for the development of large dinoflagellate blooms (Pitcher *et al.*, 1998).

A consequence of extended periods of wind quiescence is the appearance of low oxygen values or anoxia through the water column (Pollock and Bailey, 1986) that arise from extensive surface dinoflagellate concentrations during summer and autumn. On several occasions, the anoxic conditions near St Helena Bay/Lamberts Bay resulted in west coast Rock Lobster *Jasus lalandii* stranding events causing large mortalities (Newman and Pollock, 1971, 1974). Such mortality events have been recorded all along the west coast of South Africa since the middle of the twentieth century, with estimated total mortality values ranging from 3 - 60 tons per event. The most dramatic event occurred during late summer-early autumn 1997, during which an estimated 2000 tons of rock lobster were stranded around the small fishing town of Lamberts Bay (~32°S) along the west coast of South Africa. This is a considerable fraction of the total population considering that the Total Allowable Catch (TAC) for west coast rock lobster during the season 1996/97 was 1680 tons (Cockcroft *et al.*, 1999).

A causative link between the rock lobster stranding events and periods of low wind has been suggested by Pitcher *et al.* (1995). They used daily weather maps produced by the South African Weather Bureau to show that a majority of rock lobster stranding events occurred at a time when a trough of low pressure remains over the west coast for an extended period, usually between three to seven days. Such low pressure atmospheric troughs normally dominate the west coast circulation for periods shorter than three days (Preston-Whyte and Tyson, 1988). A later study by Cockcroft *et al.* (1999), using wind records from an automatic weather station at Cape Columbine, showed some decrease tendency in wind speed during rock lobster mortality events. Results were not entirely conclusive due to coastal wind records being "contaminated" by local

effects such as land-sea breezes, topography and vegetation. This raised a key question concerning the validity of a definitive relationship between low wind speeds measured at the coast and the occurrence of dense dinoflagellate blooms and subsequent rock lobster mortality events. The dynamical link between low wind events, dense dinoflagellate blooms and subsequent rock lobster mortality requires synoptic scale data.

The objectives of this dissertation are:

(1) to establish whether a clear relationship exists between the synoptic wind field dynamics and rock lobster mortality events during extended periods of low wind over the southern Benguela region

(2) to investigate wind field dynamics of dominant synoptic atmospheric systems affecting the west coast of southern Africa;

In order to achieve these objectives, two data sources were required. The wind data sources are:

(1) the NASA scatterometer (NSCAT) aboard the Japanese satellite ADEOS, covering the west coast of South Africa between latitudes 20°S - 35°S and longitudes 10°E - 20°E from December 1996 to May 1997 (Liu *et al*, 1998b).

(2) *in situ* wind speed measurements made by two automatic coastal weather stations located at Cape Columbine (32.75°S) and Cape Peninsula (34.25°S). A third automatic weather station at Port Nolloth (29.15°S) measured atmospheric air pressure.

The dissertation proceeds in the following manner:

Chapter 1 gives a broad description of main elements of the large scale Benguela Current. Several papers (Nelson and Hutchings, 1983, Shannon, 1985, Shannon and Nelson, 1996, Shillington, 1998) review the dynamics of the Benguela system. The chapter includes an overview of synoptic atmospheric forcing, on the large and small scales, in the region focussing particularly

on the main upwelling season. The process of upwelling, and its variability, along the west coast of southern Africa is addressed.

A short overview of past rock lobster mortality events is given as background to understand the interaction between the physical environment and biological succession as previously suggested by by Pitcher *et al.* (1998) and Cockcroft *et al.* (1999).

Chapter 2 focuses on the NASA scatterometer data by commencing with a brief history of the instrument, design specifications and general data handling in terms of data gaps and averaging. The data are examined at three temporal scales: namely the original daily data, three day running means and monthly averaged data. The hourly automatic coastal weather station data is also reaveraged over 24 hours to have comparable time series to NSCAT.

Chapter 3 commences with a comparison of satellite and automatic coastal weather stations, to evaluate whether coastal wind records are good proxies of the wind field over the shelf. This is followed by analyses of different synoptic atmospheric systems. The atmospheric systems considered are the South Atlantic Anticyclone, coastal lows, cold front and west coast trough of low pressure occurring during summer and early autumn. The classification uses the daily NSCAT data in conjunction with three day running mean data. Wind fields are investigated in terms of a vector analysis, speeds, vorticity (or wind stress curl) and vertical velocities at the base of the Ekman layer are evaluated for Ekman transport and Ekman pumping.

The study of wind fields associated with different synoptic systems is followed by a time series analysis, contained in **Chapter 4**, encapsulating all atmospheric systems investigated above. It shows wind field variability as one synoptic system changes to the next during the period 25 March to 10 April 1997. The Daily Weather Bulletin for March to April 1997 (SAWB) indicated that a west coast trough dominated the air circulation during this period, resulting in reduced wind speeds over the shelf. Biologically, this period was characterised by a large rock lobster mortality event (Cockcroft *et al.*, 1999). Pitcher *et al.* (1995) alluded to a dynamical link between west coast

troughs and rock lobster mortality events using SAWB Daily Weather Bulletins, but the present study uses synoptic NSCAT wind data to investigate the validity of this hypothesis.

Chapters 5 discuss the results and conclusions as well as future studies planned to tackle the problem of no scatterometer data along the coast. It is believed that the approach used will provide a better understanding of the dynamics involved in mass stranding or mortality events as well as synoptic wind field dynamics.

Chapter 1

Benguela dynamics have been the focus of marine science in South Africa for several decades. A number of review articles form the basis of the bibliography in order to gain insight into processes that control the physical, and subsequent biological, environment. This chapter will also introduce a particular biological peculiarity in the region commonly referred to as west coast rock lobster *Jasus lalandii* stranding or mortality events occurring during late summer to early autumn.

The overall aim of the chapter is to give a broad description of the Benguela system dynamics in terms of the oceanography and atmospheric controls. The chapter is divided into the following sections:

The Benguela Current System

- Geographical Setting
- Large Scale Circulation
- Coastal Upwelling

Atmospheric Forcing

Red Tides - Formation and Consequences

THE BENGUELA CURRENT SYSTEM

The dissertation primarily focuses on wind field dynamics in the Benguela Current region, but there is a need to become familiar with the large scale features and geographical setting of the system. As a result only a brief overview of the geographical setting, large scale and coastal circulation of the Benguela is given. There are recent review articles such as Shannon and Nelson (1996) and Shillington (1998) that could be referred to for supplementary reading.

Geographical Setting

On the large scale, the Benguela Current is the eastern boundary current of the South Atlantic sub-tropical gyre system. Generally it is described as the broad equatorward flowing waters located along the west coast of southern Africa between Cape Agulhas (35°S) and Cape Frio (18.4°S). Equatorward flow at the surface occurs to a depth of several hundred meters and Nelson (1989) showed typical Ekman drift velocities in the surface friction layer between 20 to 35 $cm.s^{-1}$.

Together with the California Current, Chile-Peru and North West African upwelling systems, the Benguela Current is also one of four major eastern boundary current regions of the World Ocean (Hill *et al.*, 1998). The upwelling process will be reviewed later in this chapter. The system comprises two parts that are collectively termed the Benguela Current: the equatorward flowing limb of the subtropical gyre and a more complex coastal upwelling system (Peterson and Stramma, 1987, Penven, 2000). What distinguishes the Benguela system from other systems, is that it is uniquely bounded at both equatorward and poleward ends by warm water regimes (Shannon and Nelson, 1996, and Shillington, 1998). The warm water of the poleward flowing Angola Current forms a region of confluence, the Angola-Benguela Front, with the Benguela at approximately 16°S. In the south, the warm waters of the Agulhas Current bound the Benguela.

The Agulhas Current is a major western boundary current of the Indian Ocean that follows the bathymetry of the South African continental shelf (Shillington, 1998) (Figure 1.1).

The west coast of southern Africa is a narrow coastal plain which rises to the main continental escarpment situated between 50 and 200 km inland (Penven, 2000). To the north of Cape Columbine (~32°S) the coastline is fairly regular in a north westward orientation. South of 32°S the coastline is very irregular with several capes and bays. Ambient air flow is also affected by desert-like conditions along the coast north of Cape Columbine. Stretching along the Cape Peninsula (34°S) is a 1000m high mountain range that play an important role in perturbing local wind forcing.

The continental shelf along the west coast of southern Africa is very variable in width. It can be narrow with minimum distances of 75 km and 40 km located to the south of Lüderitz, Namibia (~26.5°S) and in front of the Cape Peninsula, respectively. A maximum width of 180 km, for the continental shelf, occurs off the Orange River mouth. The shelf break is deep (200 m) and quasi-rectangular (Penven, 2000), running north westward and roughly parallel to the coastline.

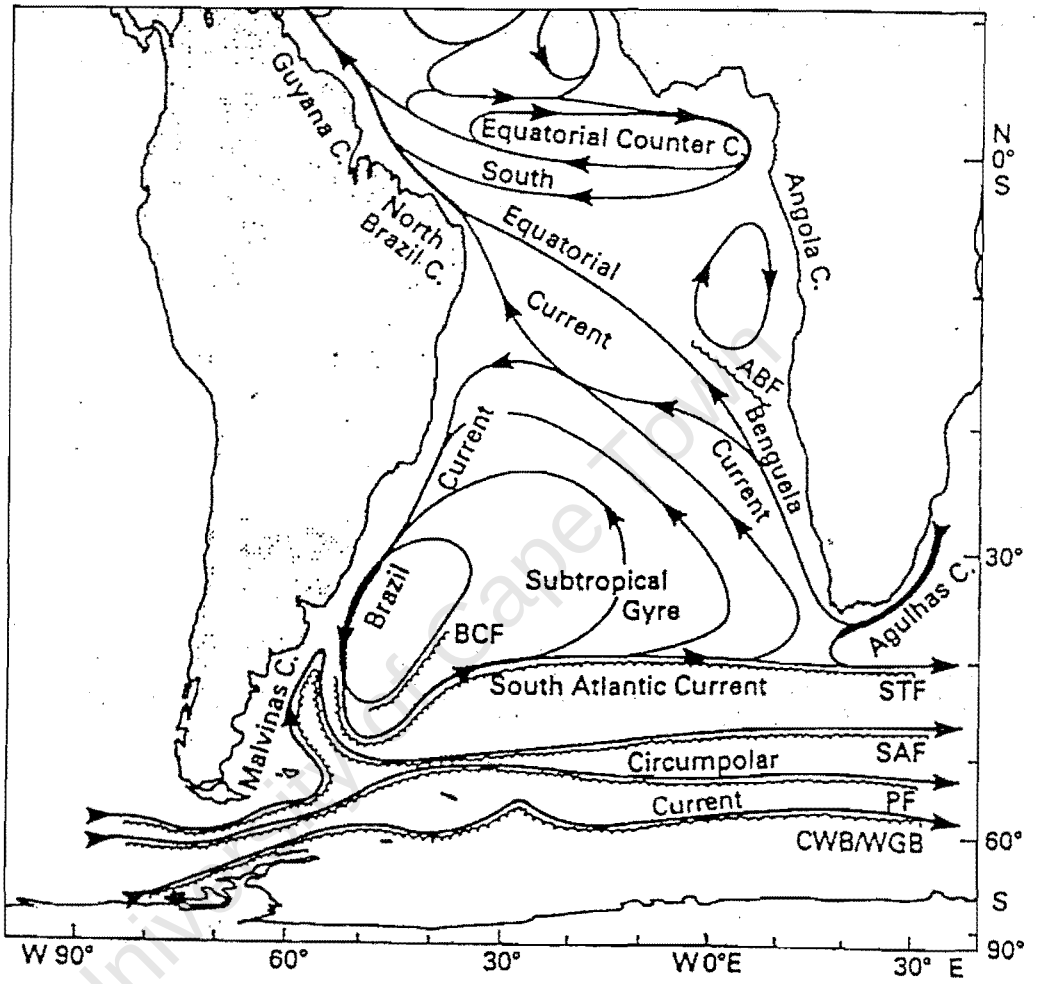

FIGURE 1.1: Surface currents of the South Atlantic Ocean. Abbreviations are used for the Angola-Benguela Front (ABF), Brazil Current Front (BCF), Sub-tropical Front (STF), Sub-antarctic Front (SAF), Polar Front (PF) and Continental Water Boundary/Wedell Gyre Boundary (CWB/WGB). Adapted from Tomczak and Godfrey (1994).

Large Scale Circulation

A Potential Temperature-Salinity or θ-S diagram taken from Shannon and Nelson (1996) expresses the principal water masses and their "core" characteristics in the Benguela Current system (Figure 1.2). The linear part of the curve from 6°C to 16°C corresponding to 34.5 - 35.5 psu includes the thermocline waters, which upwells along the coast. The thermocline water typically constitutes the shelf waters of the Benguela, but often appear in a highly modified form. There are three types of thermocline water present in the Benguela: South Atlantic Central Water (SACW), South Indian Central Water (SICW) and Tropical Atlantic Central Water (TACW). The differences between the coastal waters and true South Atlantic thermocline waters are clearly seen in Figure 1.2. Water warmer than 10°C, along the linear part of the θ-S diagram, is fresher by 0.2 psu or more and is associated with the upwelling system (Shannon and Nelson, 1996).

Thermocline water overlies Antarctic Intermediate Water (AAIW). In the Benguela the core of AAIW is in the salinity range 34.2 - 34.5 psu, and potential temperatures of 4 -5°C (Shannon and Hunter, 1988, Valentine *et al.*, 1993). The core occupies an average depth of 700-800 m in the SE Atlantic and 1100 m in the South Indian Ocean and Agulhas retroflection. Shannon and Hunter (1988) have described general features and circulation characteristics of AAIW around southern Africa. On a volumetric basis, AAIW accounts for 52% of the water masses present above 1500 m off southern Africa (Valentine *et al.*, 1993). Stramma and Petersen (1989) have estimated that the Benguela Current, in a broad sense, transports a total volume of 4 - 5 Sv of AAIW northwards, all of which turns westward to cross the Greenwich Meridian south of 24°S.

Around southern Africa AAIW display variations, in terms of salinity, potential temperature and oxygen, depending on modification prior to entering the Benguela. AAIW originating in the Indian Ocean is more saline (typically > 34.45 psu) and less well oxygenated (typically < 4.5 $ml.l^{-1}$) than that originating from the South Atlantic Current. The latter is

dominant in the SE Atlantic. In the same way, AAIW from the tropical Atlantic is saltier than the South Atlantic AAIW and is characterised by low concentrations of dissolved oxygen (<4-5 $ml.l^{-1}$). Of these three "types", Gordon *et al.* (1992) estimated that about 50% of AAIW in the Benguela area are of Indian Ocean origin. According to the review article of Shannon and Nelson (1996) this might be an overestimate.

Underneath the AAIW, North Atlantic Deep Water (NADW) is found with a potential temperature <3°C and salinity typically > 34.8 psu. NADW is relatively warm and saline, spreading southward in a thick layer between 1000m and 3500m at the equator (Reid, 1989). This author's monograph is a comprehensive treatment of NADW.

For depths greater than 3800m, Antarctic Bottom Water (AABW) dominates the circulation underlying NADW. The Walvis Ridge acts as a physical barrier to the northward passage of AABW producing a cyclonic circulation in the Cape Basin. This cyclonic circulation produces a poleward flow along the continental margin of the Benguela as reported by Reid (1994) and Nelson (1989). In the Cape Basin, AABW has a typical salinity < 34.82 psu and potential temperature <1.4°C (Shannon and Chapman, 1991).

Stramma and Petersen (1989) provides an overview of the greater Benguela Current, whereas Shannon (1985) and Chapman and Shannon (1985) addressed various aspects of surface and thermocline circulation in the Benguela region. Stramma and Petersen's (1989) calculations suggested a northward transport of surface water by the Benguela at 32°S of 21 Sv and at about 28°S of about 18 Sv. When considering surface-thermocline water transported northward together with Antarctic Intermediate Water (AAIW) a total of 25 Sv is gained. This total is higher than previous estimates including a recent estimate provided by Garzoli *et al.* (1992). A large proportion (7 Sv) of the total northward transport is of Indian Ocean origin via Agulhas rings, but this will not be elaborated on and the study of Van Ballegooyen *et al.* (1994) can be referred to.

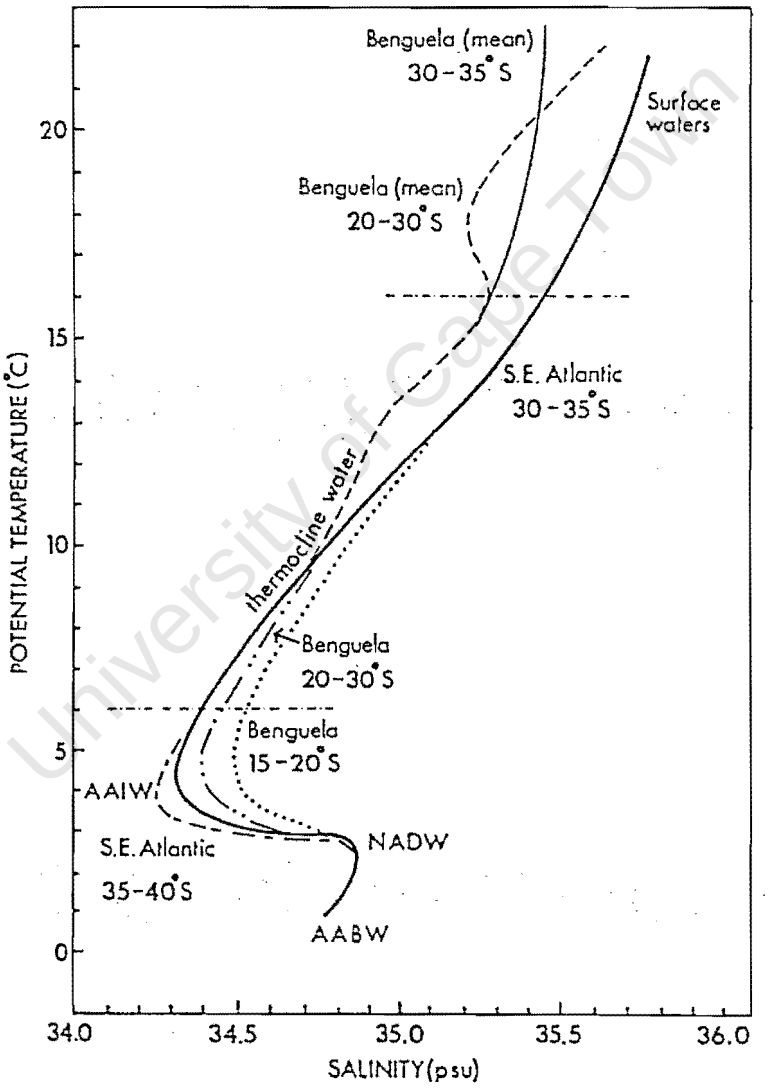

Figure 1.2: The principal water masses and potential temperature - salinity characteristics of the South East Atlantic and Benguela system. Adapted from Shannon and Nelson (1996).

Coastal Upwelling

This section of the dissertation is not meant to be a detailed analysis of the Benguela upwelling process and its variability, but to serve as a broad overview of the topic as a result of the numerous scientific papers published on the subject. It is suggested that review articles by Brink (1983) and Brink and Robinson (1998) be referred to for more information pertaining to the theoretical aspects of upwelling.

Wind induced upwelling manifests itself as a negative sea surface temperature (SST) anomaly due to cold nutrient rich water being brought to the surface to maintain continuity. The SST anomaly is mainly within 150 - 200 km from the coast (Shannon, 1985, Lutjeharms and Stockton, 1987) hours after the onset of the favourable longshore equatorward wind. Nelson and Hutchings (1983) reported that the source of upwelling water is typically from a depth of 200 - 300 m. It was shown in the preceding section that such depths coincide with the linear part of the θ-S curve described as thermocline waters such as SACW. Upwelled water has a typical temperature range between 9 - 12°C together with a rich nutrient supply (Taunton-Clark, 1985). After upwelling has introduced cold nutrient rich water into the euphotic zone, primary production is enhanced together with its subsequent biological succession. This has been illustrated using ocean colour (CZCS) satellite imagery by Shannon *et al.* (1985).

There are four main upwelling plumes present along the west coast of southern Africa between 22°S and 35°S, namely the Lüderitz cell (27°S), Hondeklip Bay/Namaqualand cell (30°S), Cape Columbine cell (33°S) and the Cape Peninsula cell (34°S) (Figure 1.3). These upwelling plumes are variable tongues of cold surface water spreading from the coast. Their presence has been related to local maxima in wind stress curl (Jury, 1988), changes in coastline orientation (Shannon and Nelson, 1996) and a narrowing of the continental shelf (Nelson and Hutchings, 1983). There are two theories that attempt to explain the location and shape of the upwelling tongues off the Cape Peninsula and Cape Columbine (1) cold water is preferentially funnelled

through a canyon off the SW Peninsula (Cape Point Valley) (Shannon *et al.*, 1981) and (2) the coastal mountains influence (possibly strengthen) the local upwelling favourable winds (Jury, 1988). It also likely that both processes are active at different times.

The semi-permanent cell is in the vicinity of Lüderitz effectively dividing the Benguela into a northern and southern section. The upwelling cell is coincident with an area that experiences highly consistent winds throughout the year, hence it semi-permanent nature. A study of satellite thermal imagery by Lutjeharms and Stockton (1987) revealed that the Lüderitz cell does not grow from a fixed point, but makes approximately the same angle with the coast at all times. Johnson and Noli-Peard (1998) estimated from an 18-year wind time series that the average volume of water upwelled along an assumed baseline of 100 km is 0.1 Sv. The offshore extent of the Lüderitz cell is about 250 km (Shannon and Nelson, 1996).

The upwelling cell at Hondeklip Bay appears to be more confined to a narrow coastal strip and Jury and Taunton-Clark (1986) suggest that the base of this plume coincides with a broadening of the continental shelf and location of a local longshore wind stress maximum. Due to the confinement of the plume to a narrow coastal strip, it appears to have a long base against the coastline from which the cell emanates.

The upwelling plumes off Cape Columbine and the Cape Peninsula are more seasonal in nature. Both have an inverted "S" shape suggesting topographic control (Shannon, 1985). The elongated shapes of the upwelling plumes extend north westward enclosing cooler water at the coast. According to Taunton-Clark (1985), the peninsula upwelling plume is present during summer months, but can be masked during periods of north westerly wind, which usually occur prior to the arrival of a cold front near the CapePeninsula.

The upwelling plume at Cape Columbine has similar characteristics to the one at the Cape Peninsula. Kamstra (1985) and Jury (1985a) have related the generation of this upwelling plume to the cyclonic wind stress curl in the vicinity of Cape Columbine. When the atmospheric marine boundary layer thickness is comparable to the topographic elevation along the coast, a shallow

south easterly wind event (Jury, 1985a) develops. During such an event, cyclonic wind curl is maximised resulting in a more pronounced plume developing. Johnson and Nelson (1999) estimated from a 34-year wind time series that, on average, approximately 1.2 x 10^{-2} Sv of water is upwelled at Cape Columbine during a 3-month window in summer. Monteiro (1996), using the same method as Johnson and Nelson (1999), showed summer upwelling rates for Cape Columbine between 1992 and 1994 to be 3.5 x 10^{-2} Sv and 4.1 x 10^{-2} Sv, respectively.

The cold nutrient rich water upwelled against the coast is separated from the offshore water by a well-defined, convoluted and highly variable front (Brundrit, 1981). A baroclinic jet, is located west of Cape Town along the upwelling front, with surface current speeds ranging from 40 - 80 cms^{-1} (Boyd and Nelson, 1998). Nelson and Hutchings (1983) showed that the jet current is typically in excess of 50 cms^{-1} offshore of Cape Columbine and has a width between 20 - 30 km. Strub *et al.* (1998) showed that the jet can be strengthened near the Cape Peninsula if warmer Agulhas water, with high steric height, is located close offshore. The jet current separates into two branches in the vicinity of Cape Columbine. The first branch flows into St Helena Bay (just to the north of Cape Columbine), whereas the second branch flows more intensely over the shelf edge until 33°S. Altimeter data showed that the jet continues for several hundred kilometers offshore in a convoluted fashion (Strub *et al.*, 1998)

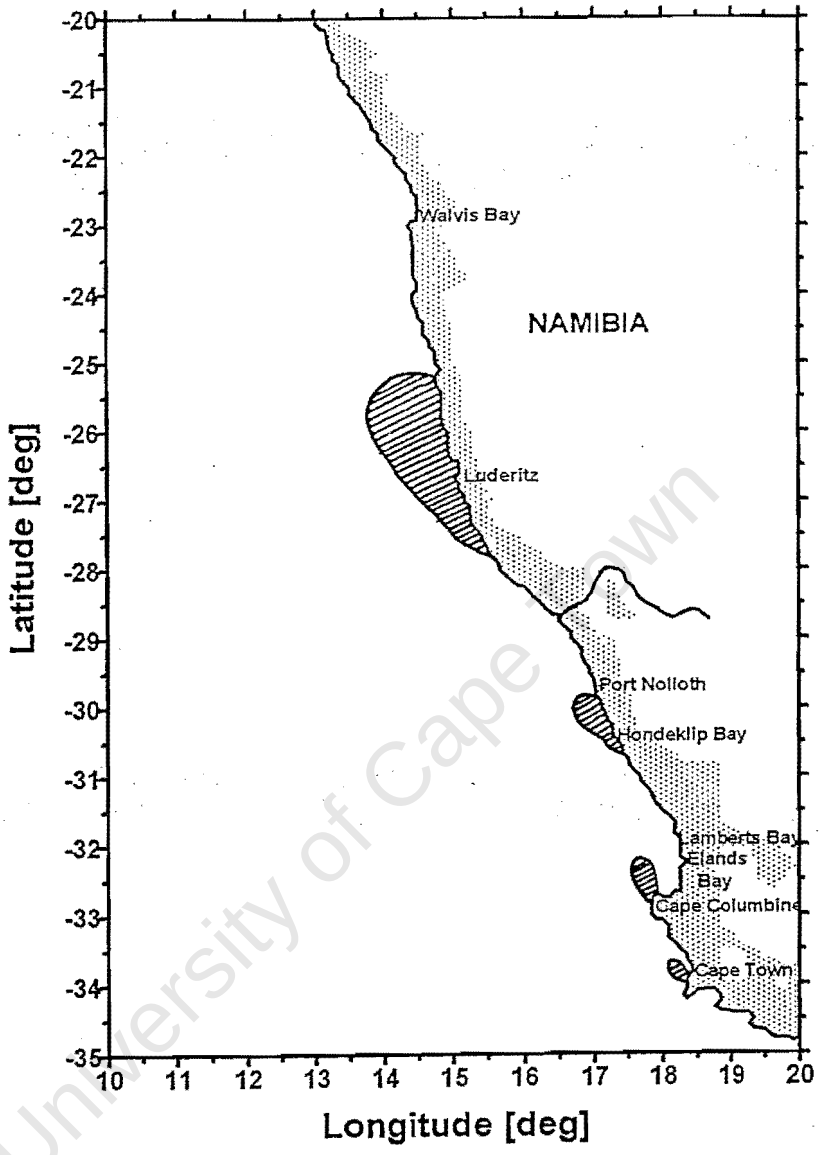

Figure 1.3: Upwelling centres along the west coast of southern Africa between latitudes 20°S and 35°S (based on Shannon, 1985). Upwelling centres, represented by the enclosed areas along the coast, from the north are Lüderitz, Hondeklip Bay, Cape Columbine and Cape Peninsula. Adapted from Chapman and Bailey (1991).

ATMOSPHERIC FORCING

The general atmospheric circulation pattern along the west coast of southern Africa has been reviewed by Preston-Whyte and Tyson (1988) and more recently by Shannon and Nelson (1996). The circulation is strongly modulated by the semi-permanent high pressure centre, with an anticlockwise air flow regime, known as the South Atlantic Anticyclone (SAA). The SAA forms part of a discontinuous belt of high pressure that encircles the subtropical southern hemisphere. It is maintained throughout the year with seasonal differences in pressure being in the order of 3 – 4 hPa, and shifts over 6° and 13° of latitude and longitude, respectively (Shannon and Nelson, 1996). The northern-most latitudinal extremity is reached in May and the southern-most, in February. The most extreme westward position is reached in August (Tyson, 1986).

The air pressure field also shows marked seasonality over the subcontinent. During summer, as a result of strong thermal heating and subsequent vertical uplift, a well-developed low pressure trough forms, which increases the horizontal pressure gradient between land and sea. And as a result of arid or desert-like conditions along the west coast (Nelson and Hutchings, 1983) a thermal barrier is formed. The combined effect is an enhancement or acceleration of southerly winds as maritime air, flowing around the SAA, is compressed. Winter is characterised by a weak high pressure system over the land as the continental trough and Inter-Tropical Convergence Zone (ITCZ) migrate northward together with the SAA.Periods of southerly wind flow are interrupted by the pathway of transient low pressure systems during both summer and winter seasons. Such low pressure cells form ahead of planetary waves in the belt of westerly winds between 35°S and 45°S (Preston-Whyte and Tyson, 1988). Associated cyclonic rotation of air around the low pressure centre can cause the wind field as far north as 30°S to be affected with an intensity that increases southwards to Cape Point (Shannon and Nelson, 1996). Depending on season, southerly winds along the coast weaken, abate or rotate clockwise. During summer, transient low pressure systems are steered south of the subcontinent and effects on wind

circulation are usually manifested as a periodic weakening of the SAA. During winter, the SAA is situated about 5° of latitude further north and the cold front is allowed to impact the wind circulation at the coast ? . Wind direction rotates clockwise from southerly to westerly or north westerly and can blow at gale force for several hours, often accompanied by rain (Jury, 1985), in cycles lasting 3 – 10 days (Shannon and Nelson, 1996).

The west to east passage of a cold front is often associated with the formation of a coastal low pressure system near Lüderitz (23°S). Coastal lows are best observed during summer, when an approaching transient low pressure system weakens the SAA. The evolution of coastal lows is from the interaction between westward moving anticyclones and the southern African escarpment (Reason and Jury, 1990). Anticyclones inducing coastal low formation are in turn driven by upper level convergence on the lee side of Rossby waves in the westerly jet stream (Jury *et al.*, 1990). Coastal lows tend to propagate at a regular rate of between 400 – 600 km.day^{-1} (Jury, 1988) and although they appear to progress in an anticlockwise sense around the escarpment, Hunter (1987) suggested that there is some uncertainty about the continuity of propagation. Schumann (1989) analysed wind and air pressure data at six stations around the coast and found that the pressure system propagated faster than the changing effect of the wind speedin the coastal low. It was concluded that the difference was as a result of differences in scale. Cyclonic air flow around coastal lows gives rise to warm, dry offshore winds at the leading edge as air blows off the escarpment and is heated adiabatically. These warm, dry offshore winds are commonly known as "Berg" winds. Misty and overcast conditions are associated with the on-shore flow. The main consequence of coastal low propagation is that it results in suppression of local upwelling during summer.

Another notable atmospheric feature of importance over the west coast of southern Africa is the surface trough of low pressure. Surface convergence and upper air divergence gives rise to general upward motion. It has long been known that the occurrence of a surface trough produces a situation conducive to widespread rains over the western part of South Africa

(Preston-Whyte and Tyson, 1988). The feature appears throughout the year, but is more frequent during summer and autumn resulting in reduced southerly wind flow along the coast.

A typical sequence of events that affects the atmospheric circulation over the Benguela is given in Figure 1.4. The transition from one synoptic cycle to the next typically occurs with a periodicity of six days (Preston-Whyte and Tyson, 1988). The cyclic pattern in atmospheric systems leads to strong variability in coastal upwelling and shelf currents in periods ranging between three and six days (Nelson and Hutchings, 1983). Jury *et al.* (1990) related the pulsing nature of the Benguela system to the resonance between shelf waves and the passage of coastal lows with an optimum resonant pulse interval of 10 days (Jury and Brundrit, 1992).

A number of small scale studies have been conducted focussing on the relationship between local wind and mesoscale upwelling structures in the Benguela (Jury, 1984, 1985a, 1985b, Jury *et al.*, 1985a, 1985b, Jury, 1988, Jury *et al.*, 1990, Jury and Brundrit, 1992, Kamstra, 1985, Taunton-Clark, 1985, 1990). As a consequence of the complex and irregular land topography, wind speed maxima were located offshore resulting in areas of cyclonic wind stress curl being identified in the lee of Cape Columbine and Cape Peninsula. Jury (1985a), using aerial radiation thermometry, showed that the topographically induced wake (and cyclonic curl) of SST in the lee of Cape Columbine intensified in "shallow" southeaster events when the inversion layer was low. During "deep" southeaster events, when the atmospheric inversion layer was high, the SST "wake" and cyclonic curl was less intense. Penven (2000) correctly, states that although the presence of cold SST in the upwelling plumes in the lee of Cape Columbine and Cape Peninsula can be related to topographically induced cyclonic wind stress curl.

The differences between wind regimes in the northern and southern parts of the Benguela are well known. The perennial centre of upwelling favourable wind lies near Lüderitz (27°S) with a secondary centre near Cape Frio (18°S). This north-south difference is enhanced during winter when there is a northward shift in the SAA. In the south, there is an increased frequency of westerly winds, which do not produce upwelling, and so the the coastal upwelling shows marked

seasonality. Andrews and Hutchings (1980) showed that upwelling in the southern Benguela is confined to the period between September to March. This temporal and spatial distribution of upwelling favourable winds, together with an irregular coastline, results in a distinctive spatial manifestation of upwelling centre distribution. It results in upwelling north of 31°S showing little seasonality compared to the southern Benguela region where there is a strong seasonal cycle.

Kamstra (1985) undertook a statistical analysis of monthly averaged wind data measured by Voluntary Observing Ships (VOS) in a parallel study,to that conducted by Nelson (1977) off California. Long-term monthly mean patterns of wind stress and wind stress curl were derived showing the difference between consistent equatorward wind in summer compared to more northerly winds in winter. Results from a Principle Component Analysis by Walker (1987) on a 23-year marine data set identified local wind forcing and sea-surface temperature (SST) associations; and that the role of remote forcing is undoubtedly critical to major SST events particularly in upwelling areas. Hutchings and Taunton-Clark (1990) examined time-series' of wind measured at the Cape Columbine and Cape Point lighthouses, stretching over 30-years and concluded that there is little spatial coherence between the two sites.

Parrish *et al.* (1983) undertook a comparative climatology of the world's four major eastern boundary current systems, including the Benguela. Bakun and Nelson (1991) extended this analysis to consider seasonal changes in wind stress and wind stress curl over sub-tropical eastern boundary current regions. During all seasons, the area of maximum wind over the Benguela was located at approximately 25°S, coincident with a coastal wedge-shaped area of strongest negative wind stress curl. According to Bakun and Nelson (1991) the wedge is approximately 200 km wide and reaches its most limited poleward extent in June and July, while from late spring to early autumn it extends past Cape Columbine and around the Cape Peninsula. Generally, the offshore area is marked by positive wind stress curl.

Together with the spatial variation in the wind field, ther is long term temporal variation. There are distinct variations at the interannual scale in the synoptic wind cycle over the Benguela.

The most reported phenomenon affecting the Benguela wind field is the Pacific El Niño – Southern Oscillation (ENSO). Preston-Whyte and Tyson (1988) describe its relationship and effects on southern African weather and rain. During the low -El Niño (high - La Niña) phase of the El Niño-Southern Oscillation the longshore, upwelling favourable winds in the extreme southern Benguela tend to weaken (strengthen) Shannon *et al.*, (1990) showed that the causative mechanisms for intra-annual and interannual variability in the marine environment along the west coast of southern Africa can be ascribed to, among others, El Niño, Benguela Niño, Agulhas intrusions and variability in the Sub-Tropical Convergence.

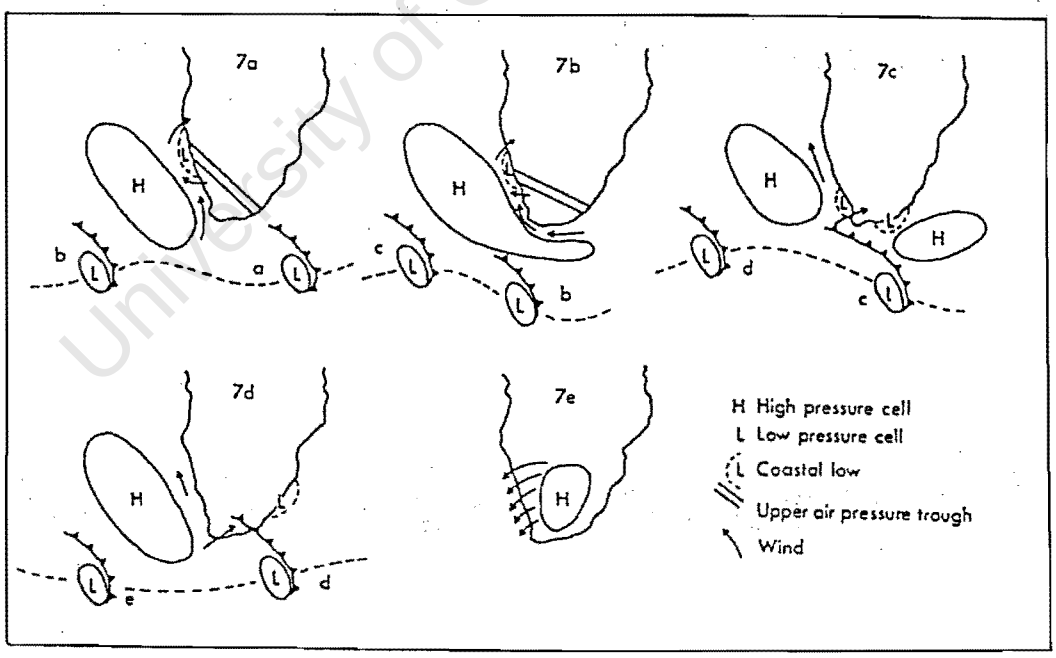

Figure 1.4: Cyclic weather pattern over the Benguela system, typical of summer conditions. (a) South Atlantic Anticyclone established - coastal low at Lüderitz - southerly winds at Cape Town. (b) South Atlantic Anticyclone ridging - gale force winds at Cape Town - coastal low moves south. (c) South Atlantic Anticyclone weakens - North West winds at Cape Town, following passage of the coastal front. (d) South Atlantic Anticyclone strengthens - southerly winds along the west coast. (e) Berg wind conditions. Adapted from Nelson and Hutchings (1983).

RED TIDES - FORMATION AND CONSEQUENCE

This section contains a brief introduction to red tide formation or harmful algal blooms off the west coast of southern Africa, but is mostly concerned with related rock lobster stranding events and their associated meteorology..

Red water or red tide are popular terms that refer to unusually high concentrations of fresh water or marine unicellular (dinoflagellate) organisms which, by virtue of their pigmentation, scattering and absorption of light, cause a reddish discolouration of the water (Brown *et al.*, 1979). Red tides have been observed throughout most of the world, but are mostly confined to coastal regions (Horstman, 1981). The majority of organisms that cause red tides are non-toxic, but can have an adverse effect on marine fauna and its environment through secondary complications such as gill clogging, hypoxia and anoxia (Horstman, 1981).

A particular consequence of oxygen depletion by red tides is mass rock lobster stranding events, which lead to high mortality. It is this aspect that is a focus of this part of the dissertation. Pitcher *et al.* (1998) present a good conceptual model of harmful algal bloom development off the west coast of southern Africa. They discuss the sequence of events that occur during the development of harmful algal blooms

Formation of Red Tides in the Southern Benguela

The west coast of South Africa is often subjected to several problems as a result of blooms of harmful and toxic algae impacting both commercial and recreational interests. Harmful algal blooms are usually attributed to migratory dinoflagellates or other flagellate species and red tides represent spectacular localised accumulations of widespread seasonal dinoflagellate blooms (Pitcher *et al.*, 1993a). There is a tendency for the occurrence of red tides to be during late summer - early autumn when there is a high degree of stratification through the water column.

Pitcher *et al.* (1998), after analysing data from several transect lines, proposed a conceptual model of red tide formation in the southern Benguela. The model suggests the following:

> dinoflagellates increase relative to diatoms as seasonal stratification increases during the upwelling season. Outside the centre of upwelling stratification is maintained by the broadening of the shelf and is responsible for a widespread distribution of dinoflagellates across the entire shelf. Here the population develops subsurface and in association with the thermocline. The inshore region is subjected to phases of active upwelling and dinoflagellates appear as a surface bloom. These blooms can be displaced further from the coast due to the active phase of upwelling. The red tides impact the coast during the phases of upwelling relaxation. As wind stress decreases during the quiescent phase of upwelling, cross-shelf currents become weaker and directed onshore. Dinoflagellates are accumulated inshore. The close proximity of cold water to the surface on the inner shelf makes the inshore environment highly responsive to upwelling by meteorological forcing.

The analysis of Pitcher *et al.* (1998) off Lambert's Bay (32.2°S) between 1995 and 1997 showed that the marine environment was highly stratified with a subsurface *in situ* fluorescence maximum associated with the thermocline. The subsurface phytoplankton assemblage was dominated by toxic dinoflagellates, whereas phytoplankton concentrations in the surface waters were very low.

Photosynthetic dinoflagellates were more common inshore where the importance of local wind events governed the inshore environment. Sea surface temperatures were sensitive to changes in the wind and exhibited an almost immediate response (Pitcher *et al.*, 1998). Southerly wind resulted in decreased water temperature as a consequence of upwelling, whereas increased water temperatures were found during episodes of northerly wind. From satellite imagery, thermal front dynamics was linked to the behaviour of the wind. The front would be located further

offshore during periods of southerly wind, due to upwelling, whereas a landward retreat would occur during northerly wind periods.

Pitcher *et al.* (1995) have identified several meteorological patterns associated with the development of red tide at the seasonal, event and interannual scales. Using meteorological composites, red tides were found to occur during late summer when surface air pressure fields were dominated by N-S low pressure at the longitudes 20-25°E or when a coastal low pressure cell initiated a quiescent wind phase. An air pressure trough links continental and marine low pressure cells, and acts to displace the South Atlantic Anticyclone westwards resulting in a relaxation of the surface pressure gradient. Consequent light onshore winds and shoreward transport between latitudes 30-35°S favour the development of a strong thermocline and spectacular dinoflagellate accumulations along the coast at locations such as Lamberts Bay and Elands Bay (Pitcher *et al.* 1995). Pitcher *et al.* (1995) also reported that during the shoreward transport of the bloom there was evidence of downwelling during an intensive 24-hour sampling period off Lamberts Bay. Each red tide event was found to be dissipated by wind induced mixing.

Rock Lobster *Jasus lalandii* Mortalities During 1997

West coast rock lobster *Jasus lalandii* are distributed from 23°S, just north of Walvis Bay in Namibia, to about 28°E on the east coast of South Africa (Cockcroft *et al.*, 1998). Greatest commercial catches are found along the west coast from 25°S in Namibia to Cape Hangklip (34°23'16"S) in South Africa (Pollock, 1986). The fishery provides employment for more than 4000 people and is currently valued in excess of R150 million per annum with an actual Total Allowable Catch (TAC) for the 1996/1997 season of 1680 tons (Cockcroft *et al.*, 1999).

Mass rock lobster mortality events (hereafter referred to mortalities), like red tides, are not uncommon along the west coast of South Africa and have been well documented since 1962. It is thought that the principle cause of such mortalities is dinoflagellate blooms or red tide. The

mortalities result from secondary effects such as oxygen depletion or anoxia during the decay of dinoflagellate blooms. The rock lobster mortality events ranged from 3 tons during March 1993 to 60 tons during March 1994 (Matthews and Pitcher, 1996) and more recently 2000 tons in 1997 (Cockcroft *et al.* 1999). Mortalities are not always linked to red tide activity (Cockcroft *et al.*, 1998), since at least one such event investigated by Pollock and Bailey (1986) was attributed to oxygen-deficient water being advected into the nearshore region by the poleward undercurrent.

During a quiescent wind phase in late summer the onshore movement of the upwelling front resulted in a dinoflagellate bloom explosion. When dissolved oxygen levels in the shallow waters close to the coast reached values lower than 2 $ml.l^{-1}$, rock lobsters responded by moving to shallower waters in an attempt to avoid the anoxia. They accumulated in extremely shallow water during high tides and were unable to retreat fast enough to avoid exposure during ebb tides. This lead to mass strandings and mortality (Pollock and Bailey, 1986).

During 14 March to 7 May 1997, South Africa experienced its worst ever low-oxygen induced rock lobster mortality, when approximately 2000 tons of *Jasus lalandii* were stranded in and around Elands Bay (~32.5°S) just to the south of Lambert's Bay (Figure 1.5), an important fishing area along the west coast. A total of six stranding events occurred in this period, but Cockcroft *et al.* (1999) states that these events should be considered collectively as a single event rather than discrete responses to low oxygen conditions. It was also reported that significant periods of reduced equatorward wind were evident preceding and during strandings (Cockcroft *et al.*, 1999).

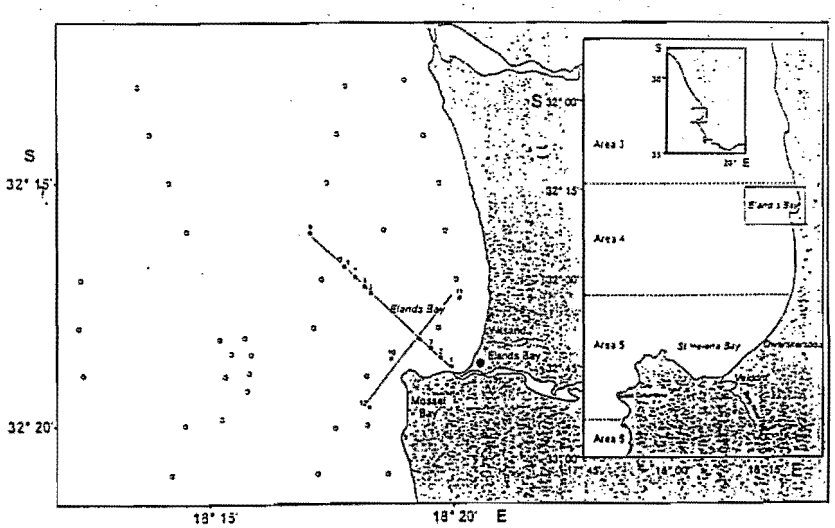

FIGURE 1.5: The study area in and around Elands Bay used by Cockcroft *et al.* (1999) to report on rock lobster stranding events during 1997. Indicated on the map are

Chapter 2

This chapter starts with an introduction to the NASA scatterometer NSCAT. NSCAT operated between September 1996 to June 1997, onboard the Japanese *Advanced Earth Observing Satellite* (ADEOS I). The introduction is followed by an explanation of the method used to gain maximum information from the satellite wind stress data set and a comparison with automatic coastal weather station wind data. A comparison of these data sets reveals how effective the coastal stations are at representing the wind over the shelf environment. By combining use of the two kinds of measurements, a powerful data set is available to gain insight into the temporal and spatial wind field dynamics.

INTRODUCTION TO THE NASA SCATTEROMETER (NSCAT)

A few decades ago, marine radar operators noticed "noise" on their radar screens, which obstructed the echo of small ships and aeroplanes. The "noise" was termed "sea scatter" and this clutter was as a result of reflection of radar pulses by the short wave length waves on the ocean surface. The idea of remote sensing of ocean surface winds was based on the belief that these surface "ripples" were in equilibrium with the local wind stress (Liu, 1997). Different empirical model functions have been developed to investigate the relationship between satellite derived radar backscatter and surface wind speed (e.g. *Seasat* and ERS-1 data).

Since the mid-1980's, wind data derived from satellite observations undoubtedly provided additional and very detailed spatial information. Satellite derived winds are in fact a sea surface wind estimation which has been reconstructed from the roughness state of the oceanic surface (Servain *et al.*, 1993). According to Willard (1989), the ocean surface roughens rapidly due to increasing wind speed, which in turn increases sigma-0 or backscatter of a microwave signal. Satellite instruments such as microwave radiometers, altimeters and scatterometers measure oceanic roughness through a measure of the returning radar cross section. Microwave radiometer and altimeter instruments only measure the modulus of the wind (i.e. the wind speed), whereas the scatterometer is able to measure both wind speed and direction. Latter data have only been available since 1991, thanks to the active microwave imager (AMI) on the ERS-1 satellite (Servain *et al.*, 1993).

More recently, onboard the National Space Development Agency of Japan's (NASDA) Advanced Earth Observing Satellite (ADEOS), a NASA-built scatterometer (NSCAT) was incorporated. The ADEOS satellite consisted of an $80m^3$ main body (bus) and three 26m solar paddles with an approximate weight of 3.5 tons (Figure 2.1). The satellite was successfully launched into a near-polar and sun-synchronous orbit in August 1996. The complete data transmission period was from 15 September 1996 to 30 June 1997. The scatterometer used an

array of six 3m long antennae radiating microwave pulses at 14 GHz, scanning two 600km wide swaths on the sea surface on each side of the instrument's orbit path separate by a 330km gap (Liu, 1998) (Figure 2.2). This made it possible for the instrument to monitor 90% of the earth's surface in two days under all weather conditions.

Each antenna measured values of sigma-0 (backscatter) from the earth's surface with a 25 km resolution. Using a Wind Retrieval Model Function, an algorithm estimates wind speed and direction for each grid cell containing sufficient number of backscatter values. Wind speed was calculated to a reference height of 10m in a neutrally stratified atmosphere. It is known that wind speed at the reference level may be different from true surface wind speed as it depends on, amongst other factors, vertical atmospheric temperature and humidity profiles. According to Liu and Tang (1996), the rationale for selecting neutral winds at a reference height to be the geophysical product of a spacebome scatterometer, lies in the physics of scatterometry and turbulent transport in the atmosphere. The assumption of neutral atmospheric stability may be tolerable based on the notion that the error introduced by wind measurements and bulk parameterisation far exceeds the error introduced by the assumption of a neutral atmosphere. Data were initially examined and then verified by the NASA Physical Oceanography Distribution Active Archive Centre (PODAAC) at the Jet Propulsion Laboratory (California Institute of Technology). Validation of observations were made using the output of the numerical weather prediction model (NWP) of the European Center for Medium-Range Weather Forecasts (ECMWF) and data collected by research vessels and buoys.

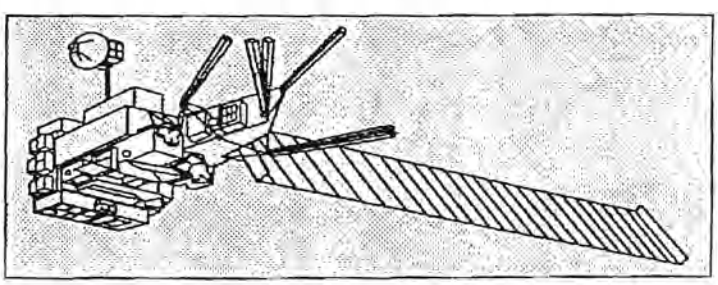

FIGURE 2.1: A schematic of the Japanese satellite *ADEOS* showing the main-body (bus) and solar paddle. The six antennae of NSCAT are in the forefront.

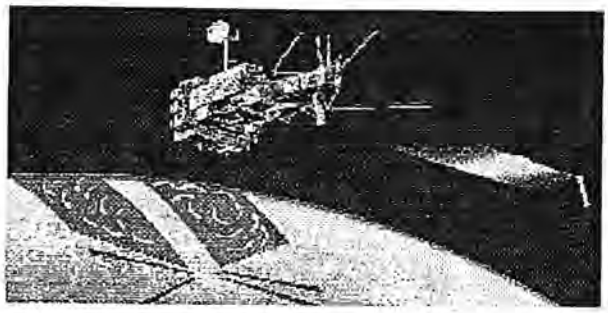

FIGURE 2.2: Diagram to show the two swath-paths of NSCAT. The paths are each 600 km wide and separated by a 330 km gap.

Expected global design accuracy for NSCAT wind speed and direction were 2 ms^{-1} and 20°, respectively (Liu, 1998). A study conducted by Bourassa *et al.* (1997) compared NSCAT data with scientific observations made from research ships. The correlation of speed and direction were 0.882 and 0.985, respectively. Such correlation values allowed for the supplementation of ship measurements with NSCAT synoptic wind data to improve analyses.

The exact satellite repeat time was 41 days and it took approximately 101 minutes to complete one revolution and 525 revolutions were repeated in one repeat cycle (Bourassa *et al.*, 1997).

NASA SCATTEROMETER DATA

Satellite wind data referenced to 10m height from the sea surface, were received from the Physical Oceanography Distributed Active Archive Centre, at the Jet Propulsion Laboratory, California Institute of Technology as daily averages. The data contained wind vector components measured along satellite swaths that crossed the Benguela Current in a particular day. Where consecutive swaths coincided, data were averaged. Along the swaths, data were placed in half-degree squares. The final product received contained wind vector components at fixed half-degree squares as shown in Figure 2.3. Using the data in this form will give insight into the synoptic

behaviour of the wind field over the continental shelf. A drawback of using the data in this form is apparent from Figure 2.3, ie. there are many areas containing no data.

It was found that when reaveraging three consecutive daily data sets, the Benguela study region would be extremely well sampled except for very small blank data areas consisting of not more than two missing values. Missing values were filled by simple linear spatial interpolation. This gave rise to the second NSCAT data set, namely three day running mean values, where the date refers to the middle day. Superimposing three consecutive days results in a variable data distribution, depending on satellite swaths for the time under consideration. When overlaying the three maps of daily averaged wind data along satellite swaths, certain grid points of the study area would contain three daily data points. Other grid points would only contain two daily averaged data points during the same period and a few would only have single daily value. For grid points having more than one data point, the arithmetic average was calculated to produce a single mean value over the three-day segment. Where there was only one daily averaged value over the three-day segment, the value retained without further statistical manipulation.

Advantages of smoothing the data over three days are that: (1) there is better coverage of the area and (2) the number of segments per week are seven therefore retaining the daily temporal sampling. An obvious disadvantage is that the smoothing will result in the loss of some detail within the wind field compared to the original daily averaged data. In the three-day running mean data sets, missing values along the coast were spatially interpolated from surrounding points. An example of the three-day running mean data, including interpolated points, is given in Figure 2.4.

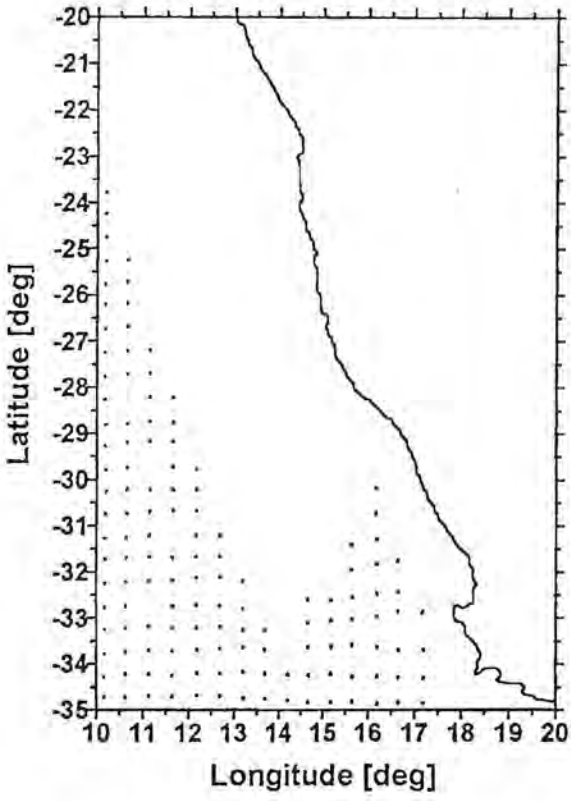

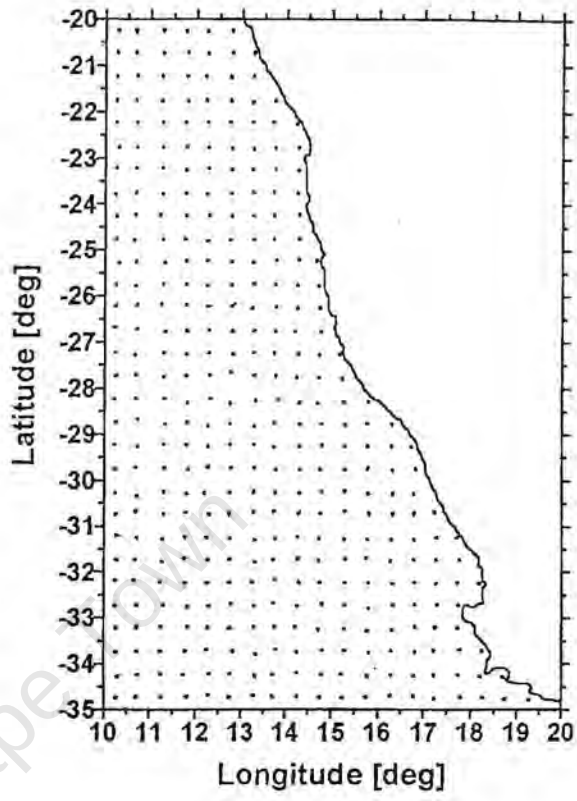

Figure 2.3 (LEFT): An example of spatial coverage from daily NSCAT data received from PODAAC. Each point represents the position of a single data record.

Figure 2.4 (RIGHT): An example of spatial coverage after applying the three day running mean filter to daily NSCAT data as well as the linear interpolation along the coast as described in the text.

AUTOMATIC COASTAL WEATHER STATION DATA

Automatic coastal weather stations in operation during the lifetime of NSCAT, were located along the west coast of the Cape Peninsula as well as Cape Columbine. Wind speed and direction, together with atmospheric pressure were sampled at 10 minute intervals at both weather stations and averaged over 60 minutes. The weather stations use a rotating cup anemometer measuring winds in meter per second (ms^{-1}), a wind vane to measure wind direction in degrees from true north and a barometer measuring atmospheric pressure in hectoPascals (hPa). A third weather station was operational at Port Nolloth (~29.2°S), near the border between South Africa and Namibia, but only hourly air pressure data was available. In order for coastal weather station data to have the same daily time interval as NSCAT, all data were re-averaged over 24 hours.

DATA PROCESSING

Importance of surface winds on eastern boundary continental shelf seas and their proximate oceans have become well known. As a result, wind stress, which is the energy transferred by the wind to the sea surface, and its spatial variation is recognised as a fundamental forcing in coastal current circulation. The stress at the sea surface can be expressed in terms of wind speed ($|u_w|$), and the vector wind velocity (u_w), atmospheric density (ϱ_a=1.204 $kg.m^{-3}$) and the drag coefficient (C_d=0.0013):

$$\tau = \varrho_a C_d u_w |u_w|.$$

The coordinate system has the y axis (north), x axis (east) and the z axis positive upward. The corresponding velocity components are v, u and w. The surface transfers horizontal momentum vertically down the water column as a body force throughout the surface boundary layer. This is known as the *Ekman layer*. The subsurface horizontal flow, the balance between the Coriolis force and friction is called *Ekman flow*.

In order to highlight the relationship between wind stress and local Ekman divergence in the surface mixed (upper) layer, it is useful to express the relative vorticity relation (Jury, 1984):

$$\underbrace{\frac{\partial}{\partial t}\left(\frac{\partial v}{\partial x}-\frac{\partial u}{\partial y}\right)}_{\text{current vorticity}} = \underbrace{\frac{1}{H\rho_0}\left(\frac{\partial \tau_y}{\partial x}-\frac{\partial \tau_x}{\partial y}\right)}_{\text{wind stress curl}} - \underbrace{f\left(\frac{\partial u}{\partial x}+\frac{\partial v}{\partial y}\right)}_{\text{surface oceanic divergence}}$$

In this expression H is the thickness of the upper mixed layer, and the curl of the wind generates vorticity. It also shows how surface oceanic divergence is compensated by a reduction in the thickness of surface mixed layer H and thus by upward vertical motion. Vertically integrating the initial equations governing particle fluid over depth H, will yield a horizontal mass transport to the left of the wind (Ekman, 1905).

In order to calculate the wind stress curl from the synoptic NSCAT wind stress data set, central differencing was applied to all points, except those located over land. Points, over land, were assigned a zero value contribution to vorticity resulting in a one-sided central differencing. The equation used to calculate the wind stress curl component about the local vertical is:

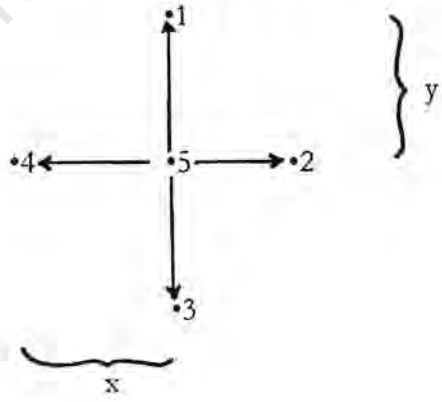

$$(\nabla \times \tau) = \tau_{curl} = \frac{\partial \tau_y}{\partial x} - \frac{\partial \tau_x}{\partial y} = \frac{\tau_{y2} - \tau_{y4}}{2x} - \frac{\tau_{x1} - \tau_{x3}}{2y}$$

The convention for the southern hemisphere was adopted in the calculation of wind stress curl, where anticyclonic curl yields positive values (downwelling producing) and cyclonic curl yields negative values (upwelling producing) (Figure 2.5).

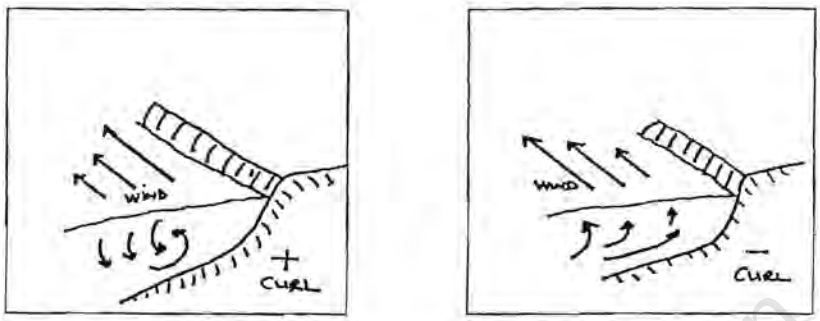

FIGURE 2.5: Schematic showing the relationship between positive/negative wind stress and downwelling/upwelling (After Jury, 1985).

EKMAN UPWELLING THEORY USED FOR ESTIMATING VERTICAL VELOCITIES

Ekman (1905) showed that for a horizontally unbounded, homogenous, infinitely deep, rotating ocean, wind forcing produced a mass transport to the left of the wind stress (southern hemisphere) in the surface layer. When a boundary is placed on one side of a longshore wind, continuity of mass requires that the surface layer mass flux towards/away from the boundary be compensated for by a vertical flux downwards/upwards. This will produce a corresponding offshore/onshore flow below the surface "Ekman" layer (McClean-Padman and Padman, 1991). The effect of imposing this boundary is assumed to be felt over a distance of approximately one baroclinic Rossby radius, R, from the boundary (Charney, 1955):

$$R = HN_0 f^{-1}$$

where H is the upper layer depth, N_0 is the ambient buoyancy frequency and f is the local Coriolis frequency. A typical value for R is between 10 - 20 km in mid-latitude coastal oceans (Pedlosky,

1979). Beyond this coastal boundary layer, the circulation approximates the unbounded case. The surface Ekman flow is compensated by an onshore bottom boundary layer flow.

The simplest Ekman coastal upwelling system is obtained when the surface and bottom layers are independent of each other, which occurs when the sum of the thicknesses of the surface and bottom layers is smaller than the overall water depth. It is customary to assume that the surface Ekman layer is equal to the surface mixed layer whose thickness, h_s can be estimated from Pollard *et al.* (1973) as

$$h_s = 1.7 u_* (|f| N_0)^{-0.5}$$

where $u_* = (\tau_s/\varrho_0)^{0.5}$ is the frictional velocity given in terms of surface wind stress, τ_s, and the fluid density, ϱ_0.

Since the sum of surface and benthic layer thicknesses is less than the continental shelf depth where NSCAT data are present, it is reasonable to use Ekman's elementary current model for decoupled boundary layers. As a result, for an equatorward coast-parallel wind stress the offshore volume flux in the surface Ekman layer is (eg. Pond and Pickard, 1986)

$$Q_{xE} = \tau_y/\varrho_0 f$$

where ϱ_0 is the typical fluid density and the upwelling velocity, w, at the base of the surface layer is

$$w \approx -\tau_y/\varrho_0 f R.$$

Similarly, the vertical velocity due to Ekman pumping (w_{Ekman}) arising from wind stress curl or vorticity (Pedlosky, 1979) is as follows:

$$w_{Ekman} \approx \tau_{curl}/\varrho_0 f.$$

The equations for both vertical velocities, based on the **z** axis pointing upward, will have positive values for Ekman divergence during upwelling and when vorticity is upwelling favourable (clockwise). The synoptic scatterometer data will use these two expressions as exploratory tools in order to help interpret the complex dynamics and coupling between the coastal ocean and atmosphere.

COMPARING NSCAT AND WEATHER STATION DATA

In order to proceed with a more detailed analysis of scatterometer data, it was imperative to compare it to available automatic weather station data. This comparison would help validate the measurements made by NSCAT, as well as give some insight into how well coastal weather stations represent the wind dynamics over the shelf. Only two complete time series were available from coastal weather stations, namely at Witsand on the Cape Peninsula and another station at Cape Columbine. Data from these two coastal weather stations were compared to two fixed NSCAT locations closest to the weather station locations. The coordinates for the two satellite grid points are (32.75°S;17.25°E) and (34.25°S;17.75°E), located directly offshore of the weather stations at Cape Columbine and Cape Peninsula, respectively (Figure 2.6).

The longshore component of wind measured by NSCAT and the weather station at Cape Columbine was extracted and presented as a time series in Figure 2.7*a*. In Figure 2.7*b*, the difference between the two time series is plotted against time. Figure 2.7*b* shows that offshore wind speed measured by NSCAT tends to be higher than that measured on the coast. The difference could be an artifact as a result of the distance separating the points considered or alternatively, airflow undergoes greater resistance along the coastal topography. The only way in which to evaluate or ground-truth satellite measurements would be to have wind measuring devices far enough offshore to eliminate topographical effects.

Figure 2.7*c* shows the correlation between NSCAT and the coastal weather station at Cape Columbine (cc). The correlation coefficient is 0.69 and the trend in the data is

NSCAT=0.867 * cc + 2.158.

The same analysis as above was done for the satellite point and coastal weather station data along Cape Peninsula. The time series of extracted longshore wind components are shown in Figure 2.8*a* as well as the component difference (Figure 2.8*b*). There appears to be a better agreement for this location compared to Cape Columbine when considering peaks within the time

series. Troughs in the time series are more accentuated with the weather station showing more wind reversals in the first half. The second half of the data shows somewhat less coherence in peaks and troughs leading to greater differences.

Figure 2.8*c* shows the correlation between NSCAT and the coastal weather station along Cape Peninsula (cp). The correlation equals 0.70 and the trend in the data is

NSCAT = 0.634 * cp + 3.249.

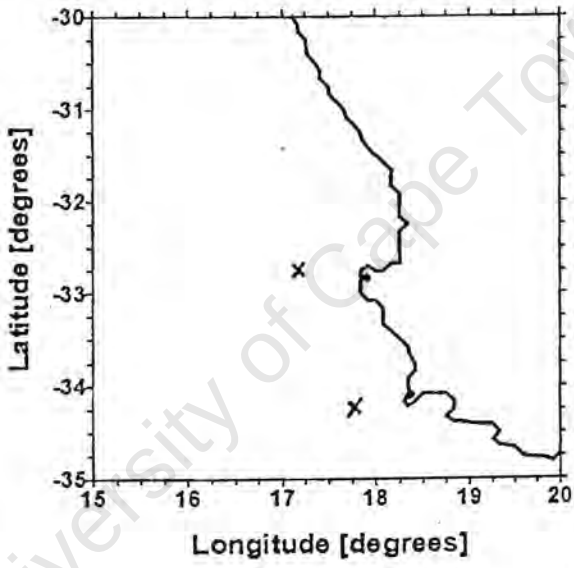

FIGURE 2.6: The relative positions of coastal weather stations (•) and NSCAT points (x) used for comparison is given here. The northern point and cross represents Cape Columbine and the southern point, Cape Peninsula, as referred to in the text.

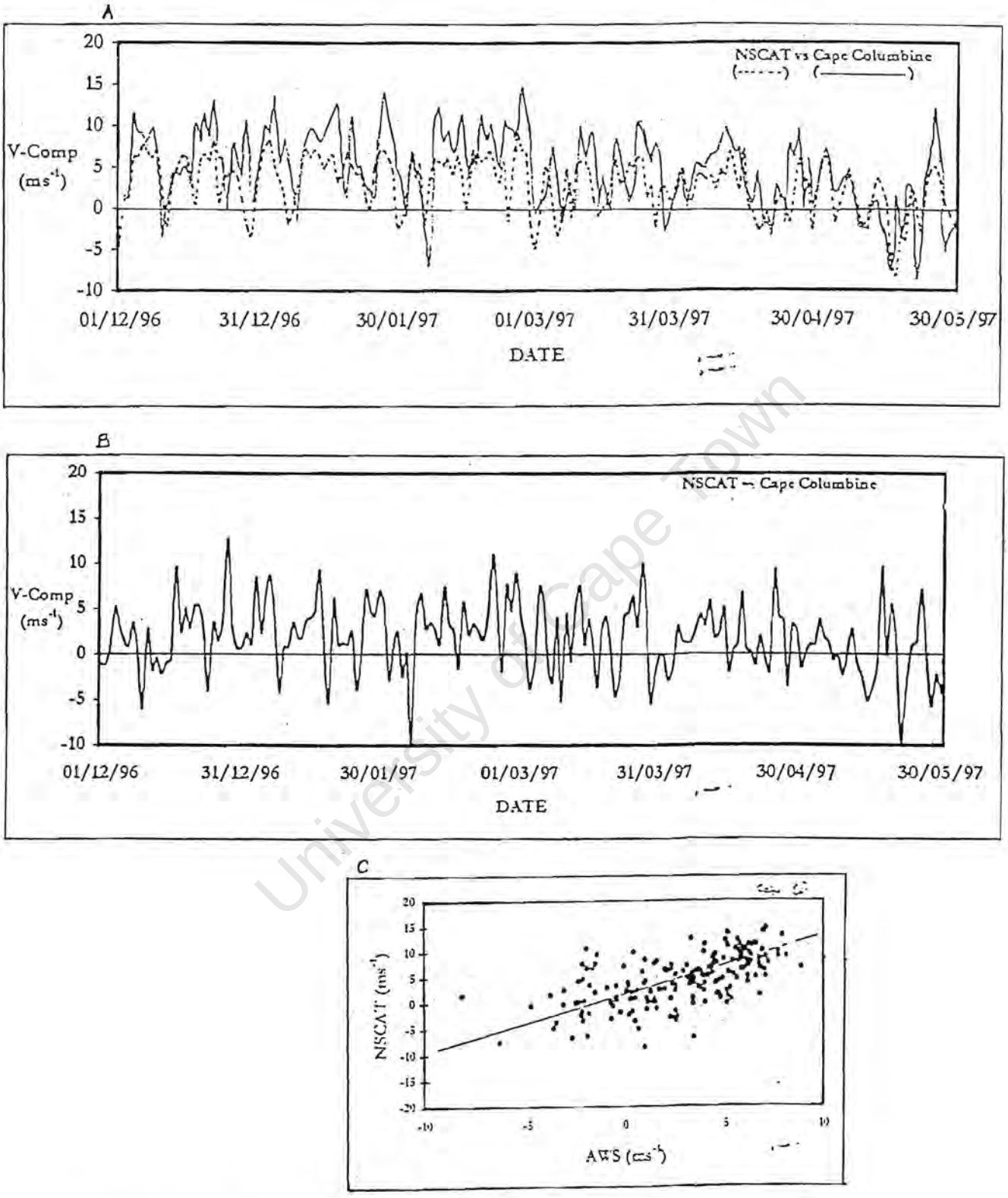

Figure 2.7: Daily NSCAT and automatic weather station data located in the vicinity of Cape Columbine between 1 December 1996 and 30 May 1997. (a) Longshore component as a time series, (b) NSCAT minus automatic weather station longshore components and (c) the correlation between NSCAT and weather station longshore components.

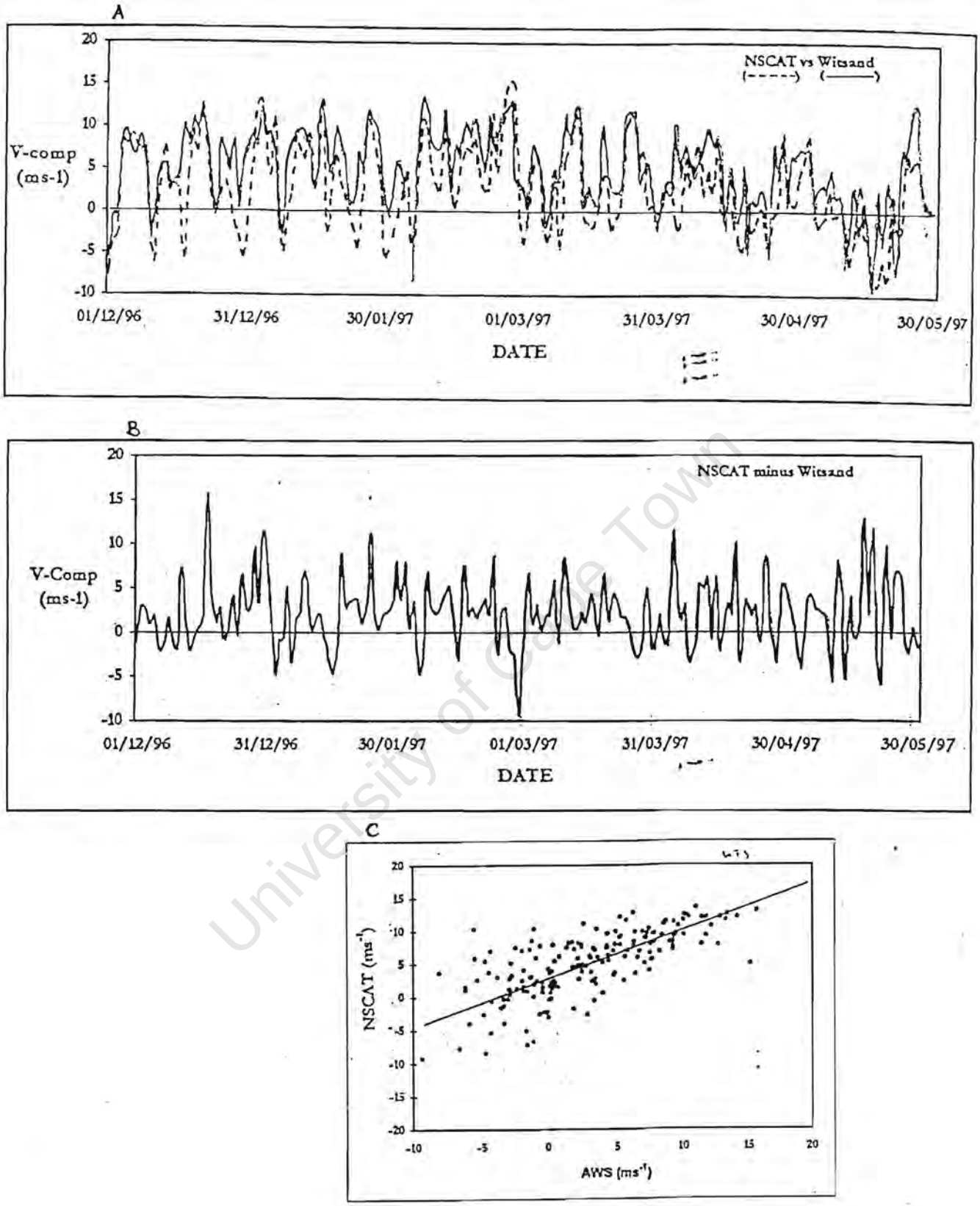

FIGURE 2.8: The same as Figure 2.7, but for longshore components measured in the vicinity of Cape Peninsula.

Both longshore time series show a change in wind behaviour from March 1997. Separating the time series into two parts, namely 1 December 1996 to 28 February 1997 (period 1) and 1 March to 31 May 1997 (period 2), average statistics were calculated and is shown in Table 2.1.

SITE	Cape Columbine Average V-component (ms^{-1})	Cape Peninsula Average V-component (ms^{-1})
Period 1 (1/12/96 - 28/2/97)		
Coastal Weather Station	4.02	4.21
Scatterometer	6.52	6.57
Period 2 (1/12/96 - 28/2/97)		
Coastal Weather Station	1.65	1.45
Scatterometer	2.73	3.55
Percentage Decrease		
Coastal Weather Station	58.9%	65.5%
Scatterometer	58.1%	50.0%

TABLE 2.1: Averaged longshore or V-component statistics and percentage decrease for Period 1 (1/12/96-28/2/97) and Period 2 (1/3-31/5/97). Components are expressed in meters per second (ms^{-1}).

Using the above tabulated statistics, it is noted that there is an accompanying change in longshore wind components at Cape Columbine between the coastal weather station and NSCAT. Between periods 1 and 2, the average longshore wind component from the coastal weather station was reduced from 4.02 to 1.65 ms^{-1}, a reduction of 58.9%. For the NSCAT data located to the west of Cape Columbine, the average longshore wind component is reduced from 6.52 to 2.73 ms^{-1} from period 1 to 2, a reduction of 58.1%. Eventhough NSCAT wind speeds, on average, were higher than that at the coastal weather station, the percentage decrease experienced by both data sets show good coherence. The absolute difference between measurements can be interpreted in terms of frictional flow. Air flow along the coast is subjected to greater friction, and subsequent reduction in speed, due to topographical features and an uneven coastline compared to air flow

over the shelf sea area. The accompanying reduction in longshore components in both data sets show that measurements taken by satellite and weather stations recorded the same synoptic wind regime changes, adding value to both data sets.

Along Cape Peninsula, the longshore wind component reductions for the weather station and scatterometer are 65.5% and 50%, respectively. The higher reduction along the coast could be ascribed to much greater topographical steering by steeper, higher and rougher terrain compared to Cape Columbine thus increasing the frictional force exerted on air flow.

Based on this simple analysis, it is assumed that coastal weather stations appear to be good indicators of the shelf environment in terms of wind flow. It also shows that scatterometer data, can be used in conjunction with the wind measurements collected along the coast. The satellite derived wind data has the advantage of greater spatial coverage compared to only two automatic weather stations a long distance apart on the coast. The remainder of the dissertation uses NSCAT wind data exclusively, unless otherwise stated.

Four scatterometer grid points coincident with known centres of upwelling were selected for further analysis. The points have the co-ordinates (33.75°S; 18.25°E), (32.75°S; 17.75°E), (30.75°S; 17.25°E) and (26.25°S; 14.75°E) corresponding to upwelling centres located at the Cape Peninsula, Cape Columbine, Hondeklip Bay and Lüderitz, respectively. These grid points can serve as a proxy for coastal weather station data. The scatterometer grid points are all located within 15 nmiles from the shore, thus being a fair representation of the near-coastal environment.

Scalar speeds at the four sites are displayed as time series' in Figure 2.9. There appears to be good agreement between peak and trough distribution at Cape Peninsula and Cape Columbine with a correlation of 87.3%, although there is a non-consistent lag (1-2 days) that switches from one station to the next. The temporal coherence between the two stations is stronger during summer and appears to weaken with the approach of winter. During periods when the Cape Columbine time series leads the Cape Peninsula, it is often as a result of a west coast low pressure

trough forming and propagating southward. Alternatively, when the Cape Columbine time series lags the Cape Peninsula it is due to an eastward ridging SAA south of the sub-continent.

The good overall coherence between Cape Columbine and the Cape Peninsula within the NSCAT data set contradicts findings of Hutchings and Taunton-Clark (1990). The authors concluded that mesoscale effects such as topography play an important role in the longshore wind. Although this is not disputed, Hutchings and Taunton-Clark did not consider the critical point of measurement at the Cape Point lighthouse. The weather station is situated on a south facing, sharply convex slope at the southern-most extremity of the peninsula about a hundred meters above sea level. In such a scenario, slight perturbations in wind direction could result in an exaggerated or disproportionate bifurcation of air flow around the topographic configuration leading to a bias in the measured wind vector components.

Correlation between Hondeklip Bay and Cape Columbine, and between Hondeklip Bay and the Cape Peninsula, yield coefficients of 0.842 and 0.698, respectively. Hondeklip Bay's weaker correlation with the Cape Peninsula should be viewed as a culmination of (1) greater topographical steering by the high mountains of the peninsula and (2) the distance of approximately four degrees of latitude separating the two sites. Hondeklip Bay has a stronger correlation with Cape Columbine partially explained by weaker topographic steering at the latter site, compared to Cape Peninsula, and the shorter distance between the two sites. Based upon correlation statistics only, it can be suggested that the Cape Peninsula and Hondeklip Bay regions experience similar synoptic scale forcing at most times, but not necessarily always identical. This means that the two areas can, at any given time, display completely different wind fields. This becomes important when considering atmospheric systems propagating from the north. Cape Columbine appears to be an intermediate point being influenced by systems to the south of it as well as propagating systems from the north, hence the good correlation with both Hondeklip Bay and the Cape Peninsula.

The wind speed time series for Lüderitz shows different variability from that of the southern Benguela. Correlation coefficients between the central and southern Benguela are generally below 0.50, for example, the correlation coefficient is 0.432 between Cape Columbine and Lüderitz. Descriptive speed (ms^{-1}) statistics for the four stations are tabulated below calculated from 90 daily values:

STATISTIC	Cape Peninsula	Cape Columbine	Hondeklip Bay	Lüderitz
Mean	6.02	5.53	4.92	7.39
Std Error	0.22	0.22	0.18	0.20
Std Deviation	2.87	2.82	2.35	2.65
Minimum	0.43	0.78	0.16	0.61
Maximum	12.72	12.64	10.13	11.98

TABLE 2.2: Descriptive wind speed statistics (ms^{-1}) for the four coastal NSCAT points calculated from daily values for the period 1 December 1996 to 28 February 1997.

Highest wind speed was recorded at Cape Peninsula, but the mean value is higher at Lüderitz. This emphasises that wind at Lüderitz is more consistent in speed and direction with time. The maximum wind speed in the south can be ascribed to the pulsing nature of winds under influence of the SAA (Jury, 1985). The average wind speed over the entire study area considering all NSCAT points from 1 December 1996 to 31 May 1997 is 5.96 ms^{-1} corresponding to a standard error of 0.20 ms^{-1}. The error is equivalent to 3.35%, which is statistically insignificant. NSCAT data proves to be a valuable data set for studying synoptic scale variation of wind stress and other derived products on the Benguela shelf region and adjacent seas.

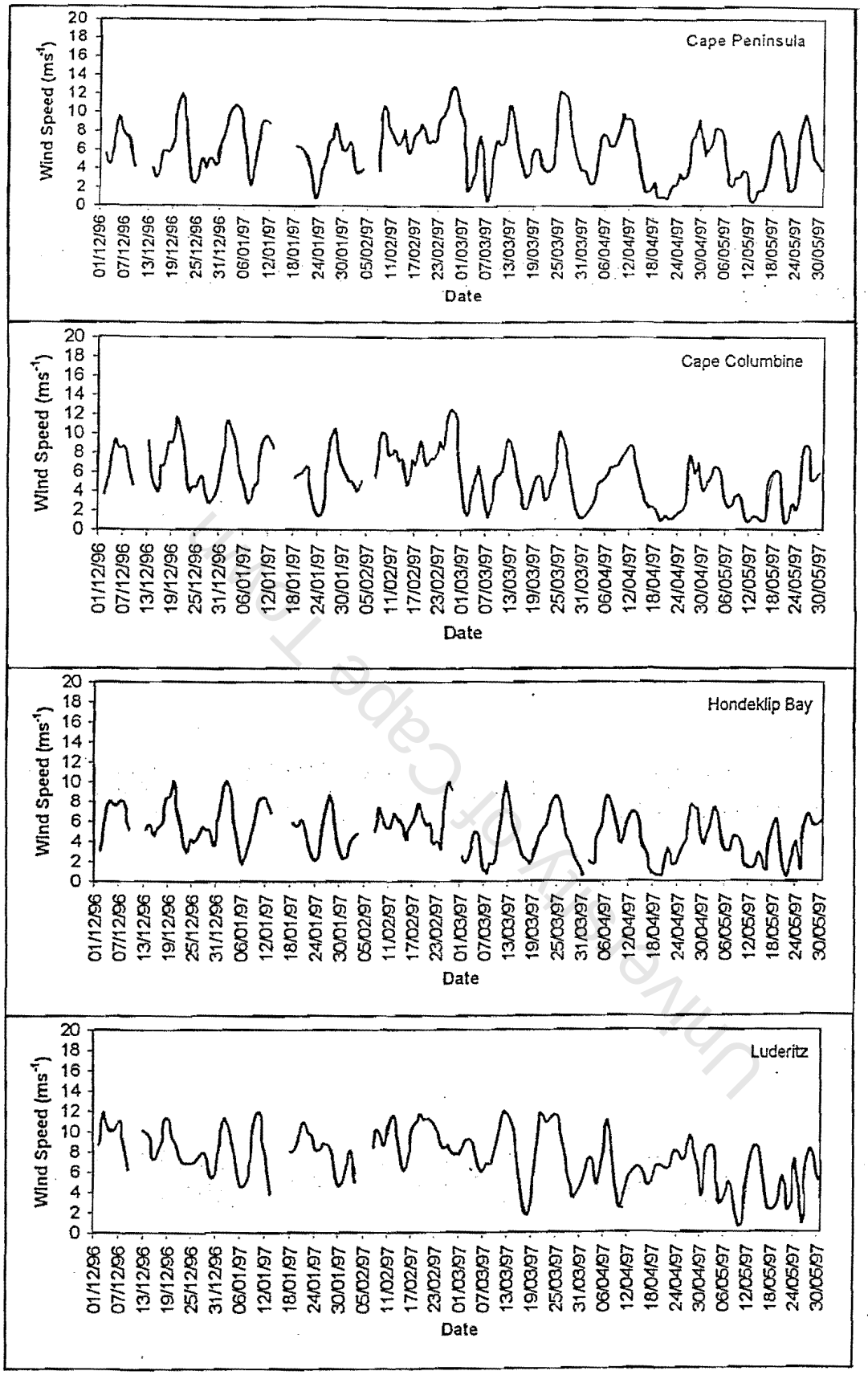

Figure 2.9: Daily-averaged wind speed measured by four NSCAT points selected to coincide with four major upwelling centres along the west coast of southern Africa. Wind speed is in meters per second and the time series extend from 1 December 1996 to 30 May 1997. Each location of measurement is displayed in the upper right-hand corner of the time series.

Using the equation described earlier, Ekman divergence estimates yield a mass transport in kilograms per second per meter of coastline (Q_{xE}). Dividing by density of seawater and then multiplying by total length of coastline over which upwelling occurs, a total volume transport perpendicular to the coast is obtained. This value is expressed in Sverdrup (Sv = 10^6 m^3s^{-1}). The length of coincident upwelling coastline was gauged using several satellite thermal images from the NOAA series as well as from published imagery contained in the collective work on the *South African Ocean Colour and Upwelling Experiment* (1985) edited by L.V. Shannon. A schematic diagram for the Lüderitz upwelling centre is given in Figure 2.10 to illustrate the application of the simple Ekman two-layer model. Lengths of coincident upwelling coastline for Cape Peninsula, Cape Columbine, Hondeklip Bay and Lüderitz are 10 km, 30 km, 15km and 100 km, respectively. Calculated upwelling volumes for the four sites are displayed in Figure 2.11. It is recognised that the dynamics around Cape Peninsula and Cape Columbine are different compared to Lüderitz due to "tongue" formation at the capes, but the same model was applied for consistency.

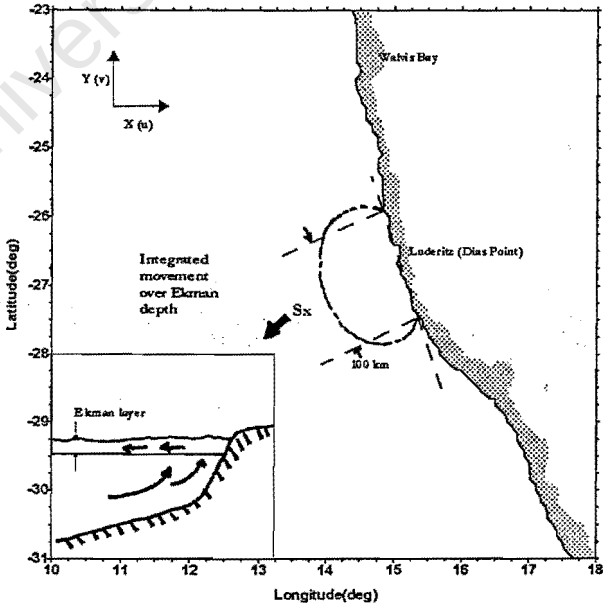

Figure 2.10: A schematic of the Ekman model for the Luderitz upwelling centre resulting from coastal divergence under the action of longshore wind. The schematic was derived from the mean thermal distribution for January (1987 to 1993) from NOAA Pathfinder data set.

The descriptive statistics, for upwelling indices displayed in Figure 2.11, are tabulated below.

STATISTIC	Cape Peninsula (10 km)	Cape Columbine (30 km)	Hondeklip Bay (15 km)	Lüderitz (100 km)
Mean	0.97	1.98	0.81	13.59
Std Error	0.07	0.15	0.06	0.67
Std Deviation	0.85	1.94	0.77	8.78
Minimum	-0.29	-1.11	-0.93	-12.06
Maximum	3.78	8.20	3.14	32.37

TABLE 2.3: Descriptive statistics for Ekman divergence estimates measured at the four NSCAT coastal points. Data are in units of 10^{-3} Sv and derived from daily values. Length of coincident coastline is given in brackets below each name, therefore minima and maxima occur for short time.

The Lüderitz upwelling volumes are an order of magnitude larger compared to all other sites. On average it contributes 3.61 times the collective sum of the other three sites and 6.86 times more than Cape Columbine. A maximum value at Lüderitz of 3.24×10^{-2} Sv is reached at the start of the time series, but other secondary maxima are visible throughout. These values are in agreement with Ekman estimates for the same upwelling site using long-term coastal weather station data presented by Johnson and Noli-Peard (1997).

Using the above statistics, it is possible to theoretically calculate a total volume contribution for the main upwelling period 1 December 1996 to 28 February 1997 as well as the remaining three months. These theoretically derived totals are given below, where bracketed numbers indicate values for 1 March to 31 May 1997:

Cape Peninsula **0.12 Sv (0.05 Sv)** *Cape Columbine* **0.25 Sv (0.11 Sv)**

Hondeklip Bay **0.09 Sv (0.04 Sv)** *Lüderitz* **1.23 Sv (1.22 Sv)**

TOTAL MASS FLUX = **1.69 Sv (3.12 Sv)**

Seasonal upwelling cells contribute the bulk of their mass flux during summer compared to autumn, but this is not surprising. During summer, seasonal cells contributed in excess of 65% of its total mass flux. Lüderitz upwelled 50% during summer, which reinforces the perennial nature of upwelling winds here.

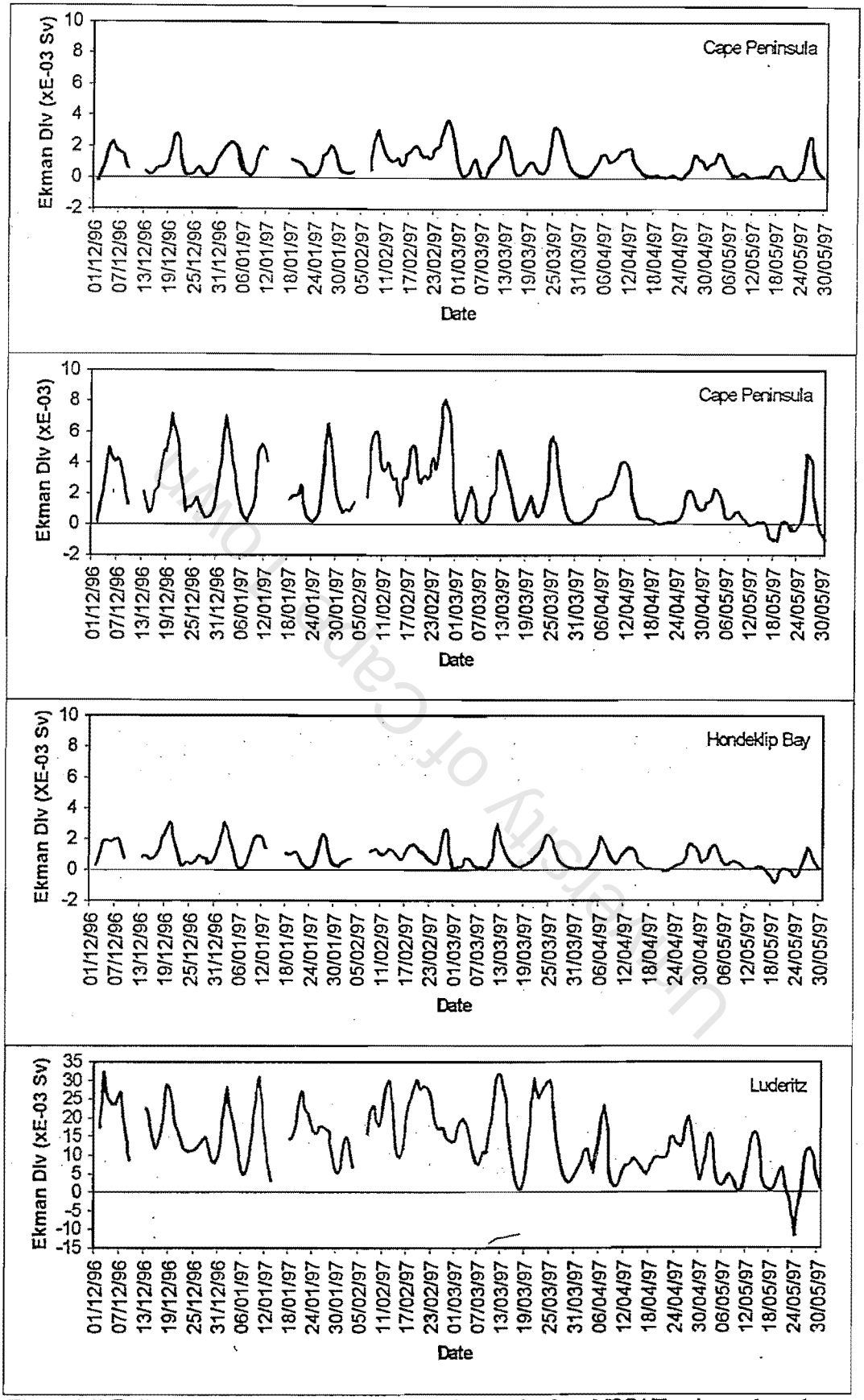

Figure 2.11 Daily-averaged Ekman divergence estimates for four NSCAT points selected to coincide with four major upwelling centres along the west coast of southern Africa. Ekman divergence in units of 10^{-3} Sv and the time series extend from 1 December 1996 to 30 May 1997. Each location of measurement is displayed in the upper right-hand corner of the time series.

Chapter 3

This chapter concentrates on the two different temporal scales of the NASA scatterometer, namely (1) daily averaged data along swaths and (2) a reconstructed average based on a three-day running mean filter. The swath and running mean data will be used concurrently in order to describe wind field dynamics related to specific synoptic systems in the atmosphere. For any specified synoptic system, swath data are used to identify some detail within the flow field, ie. small scale features. Swath data becomes inadequate when calculating vorticity due to blank data areas and therefore 3-day running mean data are used. As a consequence of the full coverage of the study region, central differencing can be applied to calculate vorticity or wind stress curl.

WIND FIELD VARIABILITY MEASURED BY SATELLITE SCATTEROMETER

In Figure 1.4 a typical summer sequence of atmospheric synoptic weather events propagating from west to east over the Cape Peninsula, was shown. Using the daily NSCAT data four typical synoptic systems are investigated with respect to the evolution of the wind fields. Associated with each synoptic system is a very distinct geostrophic flow regime. The synoptic systems are (1) an established South Atlantic Anticyclone along the west coast of southern Africa slowly ridging to the south of the subcontinent, (2) transient mid-latitude cyclone or cold front, (3) poleward propagating coastal low pressure system and (4) west coast trough of low pressure. In all cases wind vectors and speed isotachs are used in conjunction in order to gain maximum information from satellite data.

South Atlantic Anticyclone (1 - 4 January 1997)

During the period 1 - 4 January 1997, the South Atlantic Anticyclone (SAA) was located to the west of South Africa and slowly ridged south of the country. Synoptic weather maps from the South African Weather Bureau (SAWB) (Figure 3.1) shows isobaric surfaces and wind vectors from a network of weather stations and ships of opportunity. Associated with an established SAA (1 - 2 January), are upwelling favourable south easterly winds along the west coast of South Africa. This system occurs primarily during spring and summer. As the SAA ridges south of the country (2 - 4 January), the air pressure gradient over the continental shelf is increased, due to interaction with the terrestrial escarpment. This produces stronger and more intense coastal south easterly winds that lead to the intensification of coastal upwelling.

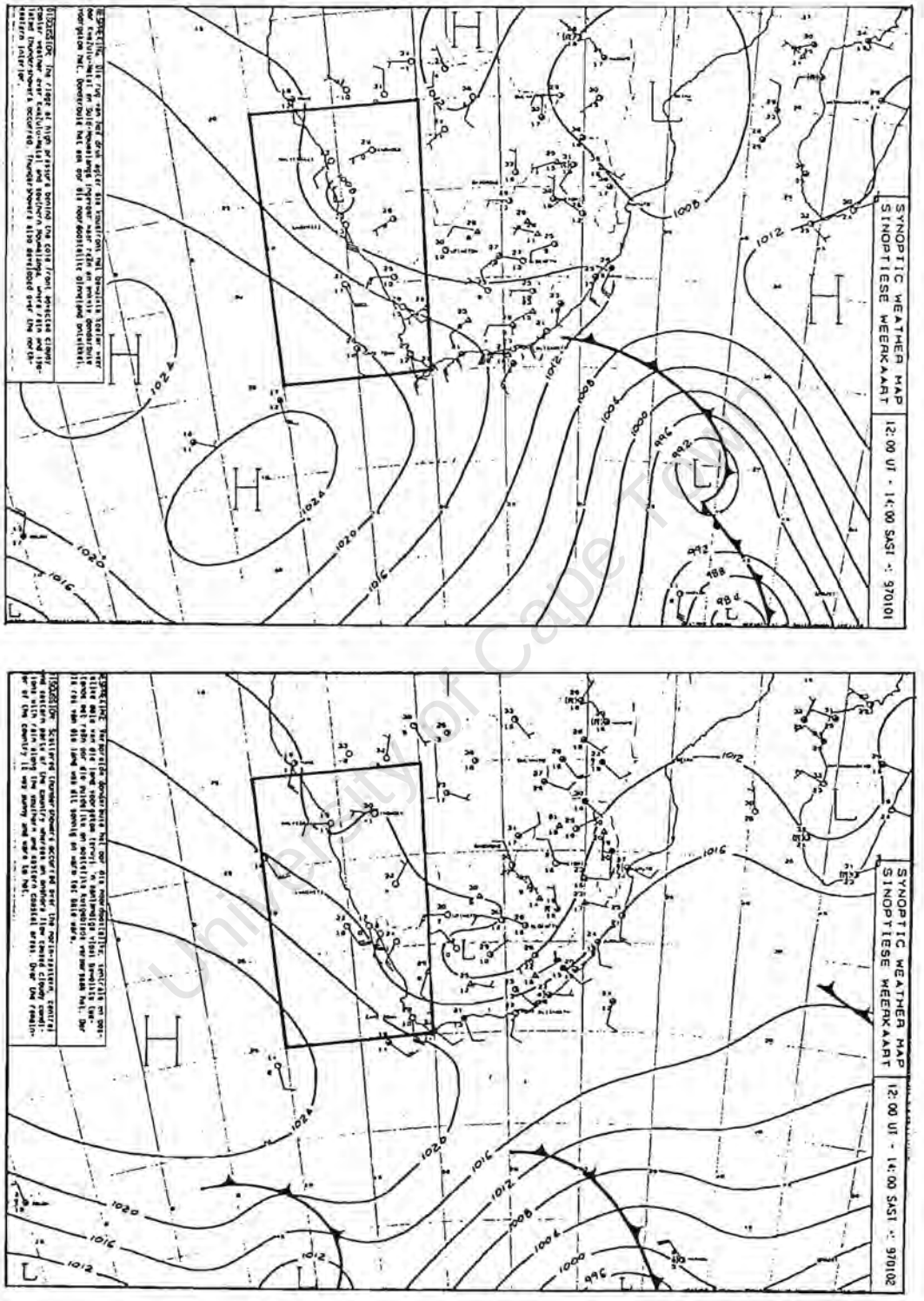

Figure 3.1: Daily synoptic weather maps produced by the South African Weather Bureau for the period 1 - 4 January 1997. The period coincides with the South Atlantic Anticyclone moving from an established phase west of the subcontinent to a regime of eastward ridging.

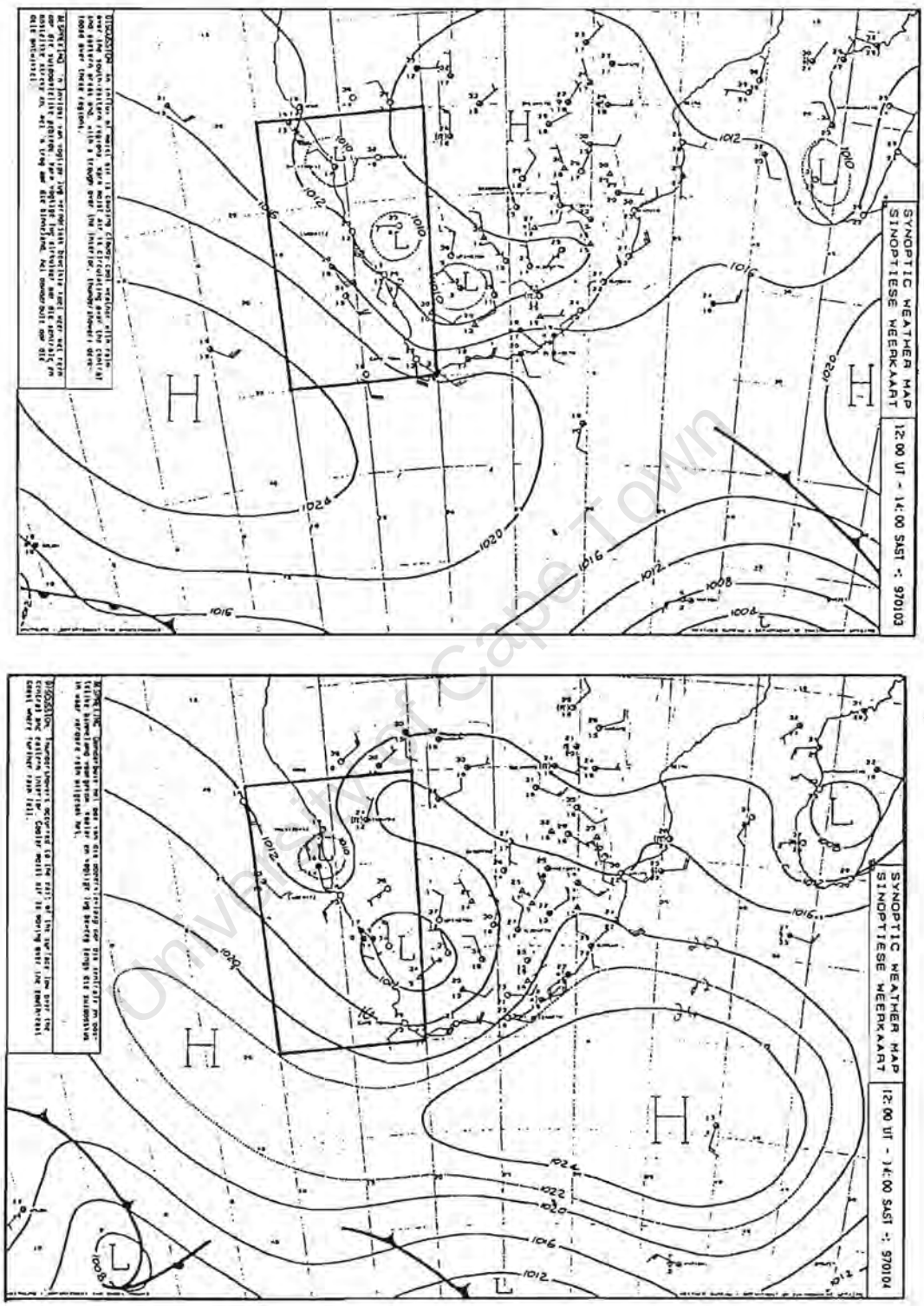

Figure 3.1: Daily synoptic weather maps produced by the South African Weather Bureau for the period 1 - 4 January 1997. The period coincides with the South Atlantic Anticyclone moving from an established phase west of the subcontinent to a regime of eastward ridging.

Daily Averaged NSCAT data

Averaged NSCAT wind vectors, derived from individual satellite passes in a single day, for the period 1 -4 January 1997 are shown in Figure 3.2. Figure 3.3 has corresponding wind speed isotachs. In general, vector alignment is parallel to the coast and consistently from the south. Winds closest to the coast are altered by local topography, especially in the vicinity of the Cape Peninsula-Cape Columbine area and the prominent bulge in the Namibian coastline between 29°S and 23°S. Along, but more so in the lee of these two areas, the effect of topography is to alter wind direction from predominantly alongshore to more onshore wind flow. The effect of topographical steering is evident up to a distance of approximately 120 nautical miles (nmiles) (~220 km) from the coast based on NSCAT vectors (Figure 3.2). Offshore wind vectors become more southerly in direction with time as the SAA becomes more established and starts to ridge south of the country. The reason for the small area of quasi-convergent flow located around (34°S; 12°E) in Figure 3.2 (1 Jan) is not known, but is assumed to be an artifact due to a data averaging process of consecutive satellite swaths that are separated by several hours.

From 1 - 3 January 1997 highest wind speeds are coupled with areas of irregular coastline (Figure 3.3). On 1 January offshore of Lüderitz (~26.5°S) and Cape Columbine (~33°S) wind speeds (in isolated cells) are in excess of 12 ms^{-1} and 10 ms^{-1}, respectively. The deceleration of winds due to onshore rotation is seen to the north of Lüderitz, where isotachs perpendicular to the coastline decrease northward. Decelerating southerly winds in the lee of Cape Columbine can not be seen due to two possible reasons: (1) the spatial scale over which the deceleration occurs is small and is contained within the area with no data along the coast or (2) when a deep southeasterly wind blows (as defined by Jury, 1984) the inversion layer is high and air is allowed to flow over the topography leading to no wake in the lee of Cape Columbine.

On 2 January, at the start of the SAA ridging south of the subcontinent, there is a widespread intensification of wind speeds, and vector alignment is almost uniform except in the

lee of Cape Columbine due to topographic steering. The lack of data in the lee of Lüderitz does not allow for a similar interpretation. A large area of wind speed exceeding 11 ms^{-1} occupies the Namibian coast from ~30°S extending to 22.5°S, with a smaller cell located to the west of Cape Columbine.

As the SAA moves further to the south on 3 January, lower wind speeds of 8 ms^{-1} appear along the north coast of Namibia between 23°S and 20°S. Isolated areas of maximum wind speed are found on 3 January, but at this time strongest winds (>13 ms^{-1}) are located offshore of Cape Columbine centred around coordinates (32.5°S; 16.5°E). A second cell of high wind speed (>12 ms^{-1}) can be found just to the south of Lüderitz.

Finally on 4 January, when the SAA has ridged to the south of South Africa, lower winds appear over the offshore area ranging from 7 - 9 ms^{-1}. There is a steep decreasing wind speed gradient to the north of Cape Columbine showing the deceleration of wind as it rotates around the cape towards the coast. The wind speed maximum (>12 ms^{-1}) that was located near Cape Columbine has now moved further poleward and is offshore of Cape Point.

When comparing coastal and offshore winds around prominent coastline irregularities, onshore wind rotation due to topographic steering produces flow divergence.

It can be suggested from the daily NSCAT data that the established SAA (1 - 2 January) favours southerly winds over the entire continental shelf and therefore results in strong upwelling. As the SAA ridges poleward around southern Africa, wind speed decreases from the north but increases over the Cape Columbine-Cape Peninsula area due to an increased isobaric gradient.

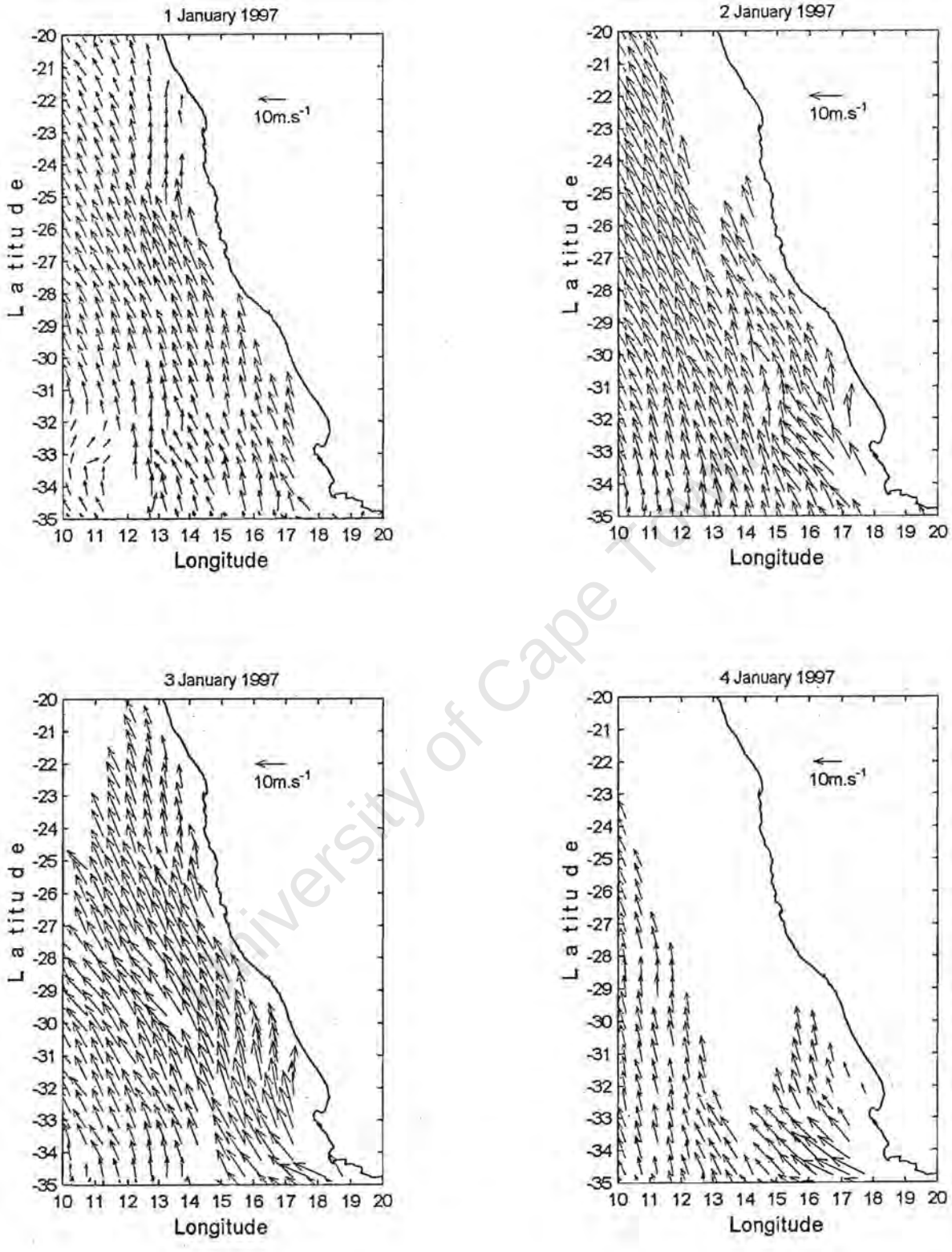

Figure 3.2: Daily-averaged NSCAT wind vectors for the period 1 - 4 January 1997. The vectors scale is near the upper right-hand corner of the figure.

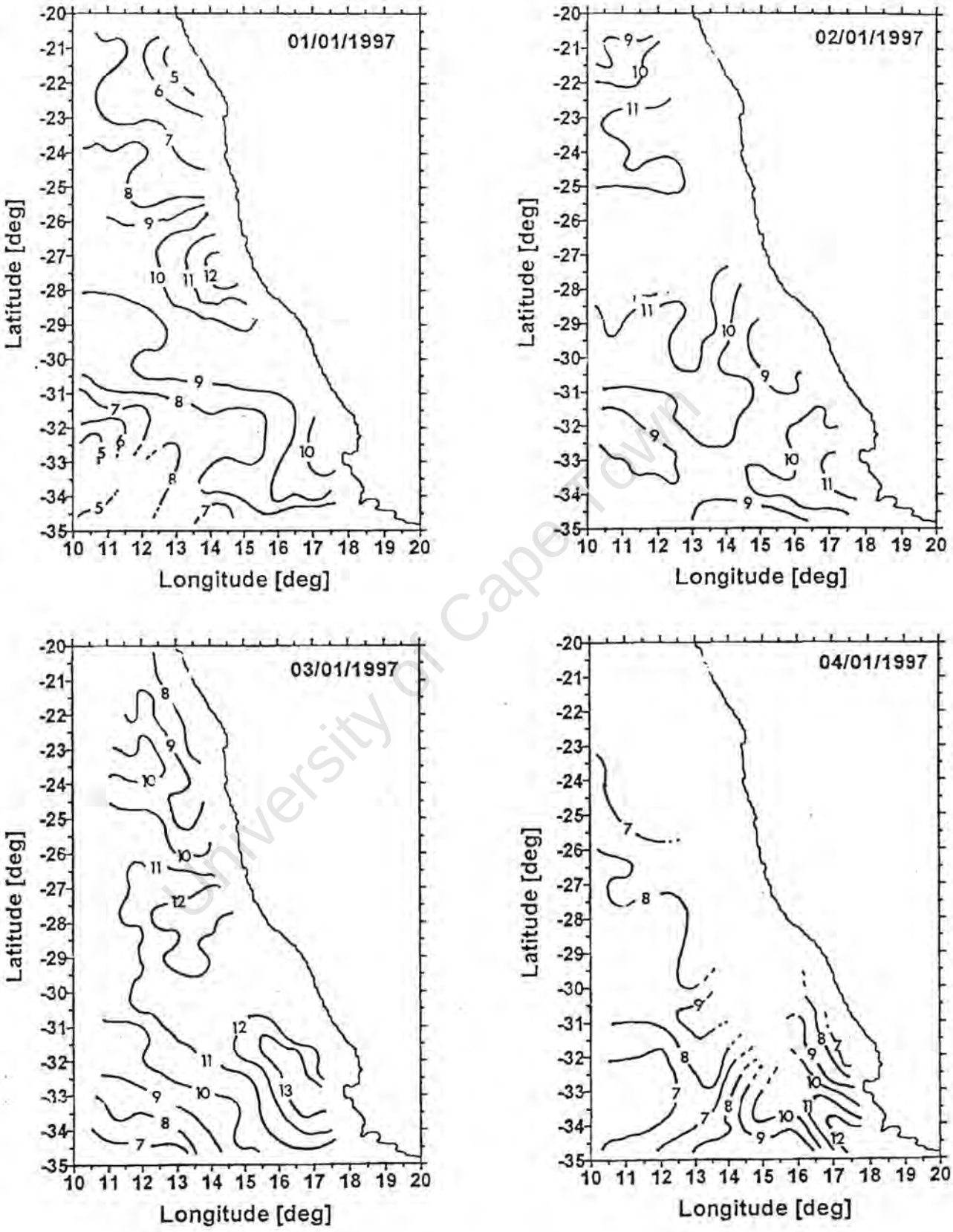

FIGURE 3.3: Daily averaged NSCAT wind speed isotachs ($m.s^{-1}$) from 1 to 4 January 1997 collected along satellite swaths. The contour interval is 1 $m.s^{-1}$. Where contours become dashed signifies areas with no data.

Three-Day Running Mean NSCAT Data

In the previous chapter the reason for the use of a three-day running mean was explained, but in essence it was used to achieve full spatial wind vector coverage over the study region. To reiterate, the nomenclature used to identify each three day segment can be explained as follows: for 1 January 1997 - it consists of the average values for 31 December 1996-1 January 1997-2 January 1997. In the same way 2 January 1997 would consist of 1-2-3 January 1997.

Figure 3.4 shows wind vectors and Figure 3.5 contains wind speed contours (isotachs) for three-day running mean segments from 1 to 4 January 1997.

In general, wind vectors from these three day composites are much more consistent in direction than those in the daily NSCAT data shown in the preceding section. Eventhough wind vectors cover the entire study region, the filtering process has removed spatial variability in the daily data vector pattern. There is, however, good agreement when comparing the wind flow around the Cape Columbine-Cape Peninsula area where the wind direction becomes more easterly with a ridging SAA. There is also some indication that winds decelerate and rotate onshore in the lee of coastline irregularities as was the case for daily NSCAT data.

Wind speed isotachs in Figure 3.5 show less detailed spatial features compared to isotachs of daily NSCAT data (Figure 3.3) due to the three-day running mean filter. Overall, filtered wind speeds are reduced compared to daily data, but highest wind speeds are still associated with the Cape Columbine-Cape Peninsula area and along the Namibian coast as before. On 1 January an extensive area of wind >9 ms^{-1}, compared to >12 ms^{-1} in daily data, is located to the west of Lüderitz with no local second wind speed maximum in the south. The second area of highest wind appears in the south on 2 January (>11 ms^{-1}) connected to Cape Columbine. The area adjacent to Lüderitz has an increase of 1 ms^{-1} resulting in a local maximum of >11 ms^{-1} along the coast between latitudes 26°S and 28°S. The two centres of local wind maxima (>11 ms^{-1}) are

separated from each other along the coast by an area of wind speeds <10 ms^{-1}. Both the maxima mentioned above are enclosed by a 10 ms^{-1} isotach running from 25°S to ~34°S.

On 3 January, due to the ridging of the SAA, winds are stronger in the south. The area enclosed by the 11 ms^{-1} isotach separates from the coast and moves offshore located 30 nmiles from the Cape Columbine-Cape Peninsula area. The 10 ms^{-1} isotach, that previously enclosed the two areas of highest wind speed (2 January), has separated becoming (1) an enclosed local maximum in wind speed along the Lüderitz coast and (2) an area surrounding the Cape Columbine-Cape Peninsula maximum, but protruding northwestward.

On 4 January when the SAA ridged around the south of the country, the study area is almost completely covered by winds ranging between 8 - 9 ms^{-1}. Winds along the west coast of South Africa between Cape Columbine and 29°S are reduced to below 7 ms^{-1}. The 11 ms^{-1} isotach has moved somewhat further south, simultaneously reducing and moving the area covered by the previously protruding 10 ms^{-1} isotach, poleward. The isotach structure south of 31oS is similar on 3, 4 January with the 9 ms^{-1} contour now in the same position as the 10 ms^{-1}. Except for a very small area along the Cape Columbine-Cape Peninsula coast, the wind speed is reduced over the rest of the study area after the SAA has ridged to the south of South Africa.

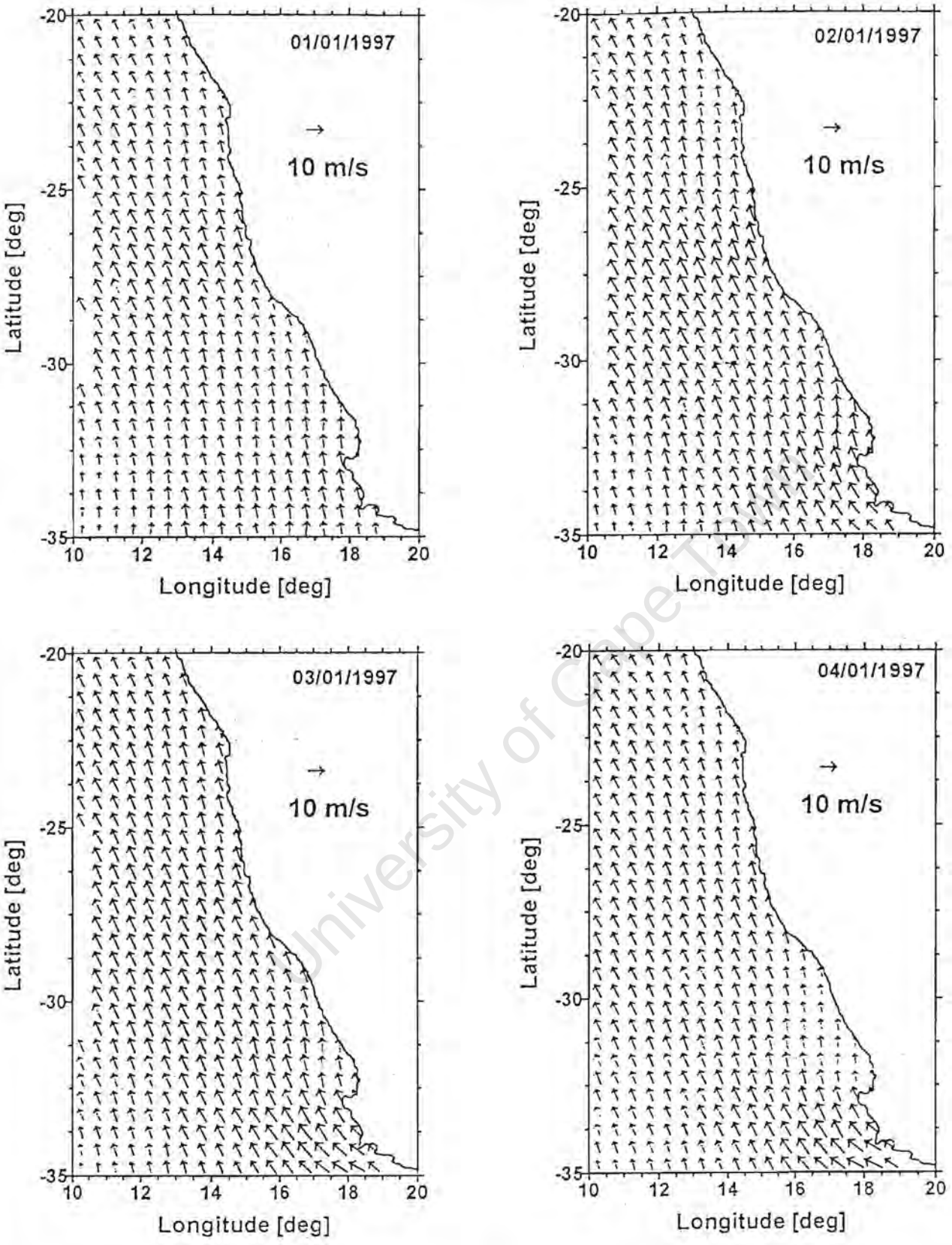

FIGURE 3.4: Wind vectors from three day running mean data constructed from daily averaged NSCAT wind vectors for the period 1 to 4 January 1997 as explained in the text. The reference vector over land represents 10 $m.s^{-1}$.

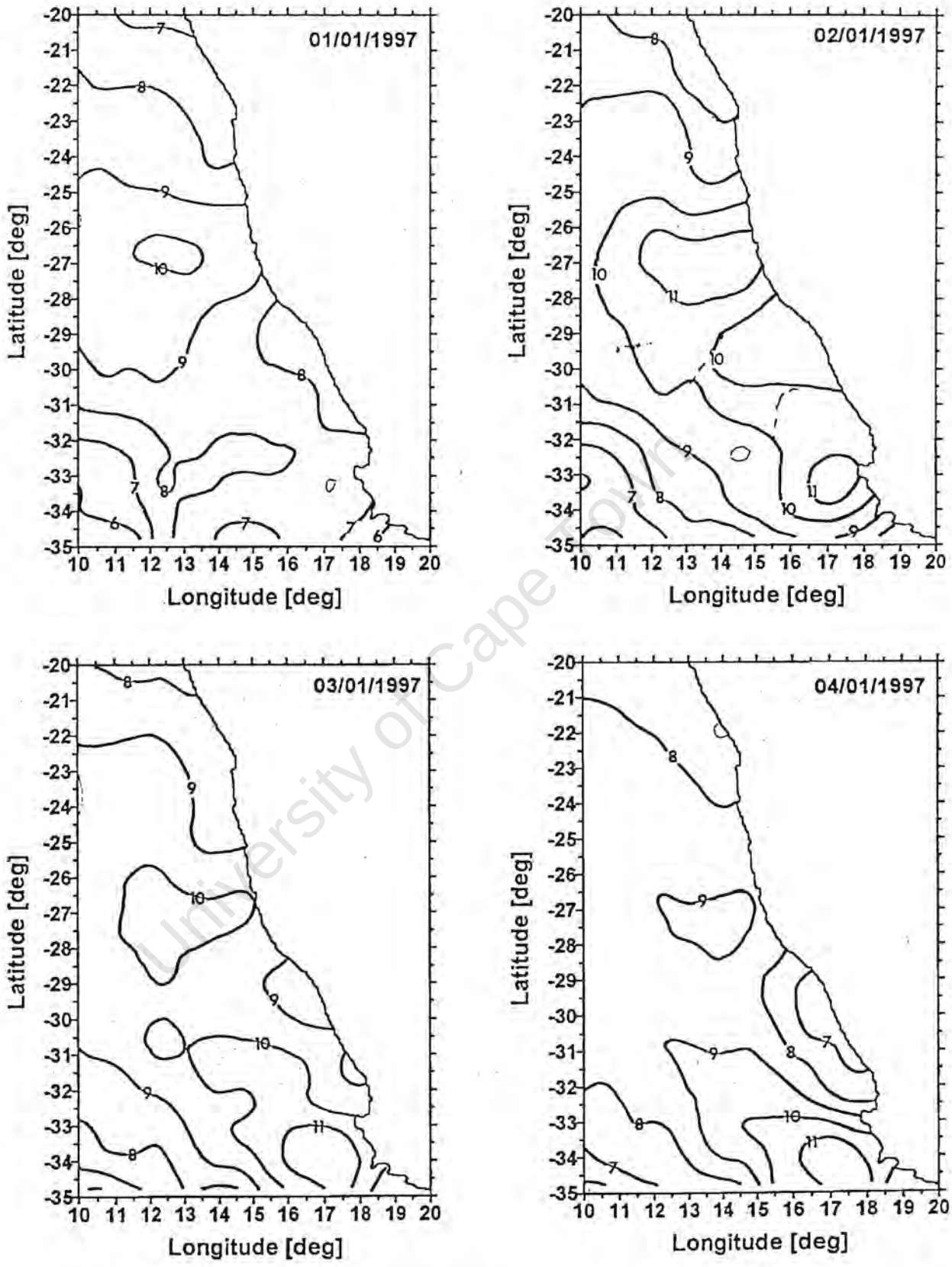

FIGURE 3.5: Wind speed isotachs for three day running mean data constructed from daily averaged NSCAT wind vectors for the period 1 to 4 January 1997 as explained in the text. The contour interval is 1 $m.s^{-1}$.

Vorticity or Wind Stress Curl

Vorticity was calculated from the interpolated three-day running mean NSCAT data using the formula shown in a preceding chapter. Figure 3.6 shows vorticity fields for the period 1 to 4 January 1997. Shaded areas indicate negative, cyclonic (clockwise) vorticity as opposed to unshaded areas indicating positive, anticyclonic (anticlockwise) vorticity. On 1 January, with an established SAA situated west of southern Africa, negative values occur all along the coast with only small areas of slightly positive vorticity intermittently interrupting its attachment to the coast. A localised negative vorticity maximum is located at Lüderitz with a value of $-4x10^{-7}$ Nm^{-3}.

As the ridging of the SAA commences on 2 January, causing the formation of two areas of high wind speeds (>11 ms^{-1}) as seen in Figure 3.5, a split in the negative vorticity field is observed. The vorticity field separates in a similar way as wind speed shown earlier with a second centre of maximum located along the coast between 31°S and 34°S. Due to the greater degree of topographic steering induced by mountains in the Cape Columbine-Cape Peninsula area, vorticity values exceed that along the Namibian coast. A maximum negative vorticity value of $-8x10^{-7}$ Nm^{-3} is found overlying Cape Columbine. Seaward of zero vorticity there is indication of positive vorticity values ~$4x10^{-7}$ Nm^{-3} in the south.

On 3 January as the SAA ridges further around the coast, negative vorticity intensifies along the capes with a new maximum of $-12x10^{-7}$ Nm^{-3} becoming separated from the coast. The $-4x10^{-7}$ Nm^{-3} and $-8x10^{-7}$ Nm^{-3} contours appear to have a more accentuated northwestward protuberance, north of Cape Columbine, compared to the previous day. These protuberances appear to roughly coincide with the 10 ms^{-1} isotach drawn from Cape Columbine and shown in Figure 3.5. The high vorticity values shown in the south is a direct consequence of the ridging action of the SAA causing a high degree of shear in air flow around the topography of the capes. The topography results in offshore southerly winds accelerating and curling towards the coast,

hence inducing clockwise/negative vorticity. The separated negative vorticity areas have fused again to form a continuous zone semi-detached from the coast.

On 4 January the intensification of negative vorticity, in the south, continues with the centre of maximum ($-16x10^{-7}$ Nm^{-3}) still located to the west of the capes. To the north of 31°S vorticity values are slightly negative and it appears that the continuous zone of negative curl is becoming smaller, especially in the far north beyond Lüderitz where detachment from the coast is far greater than in the south.

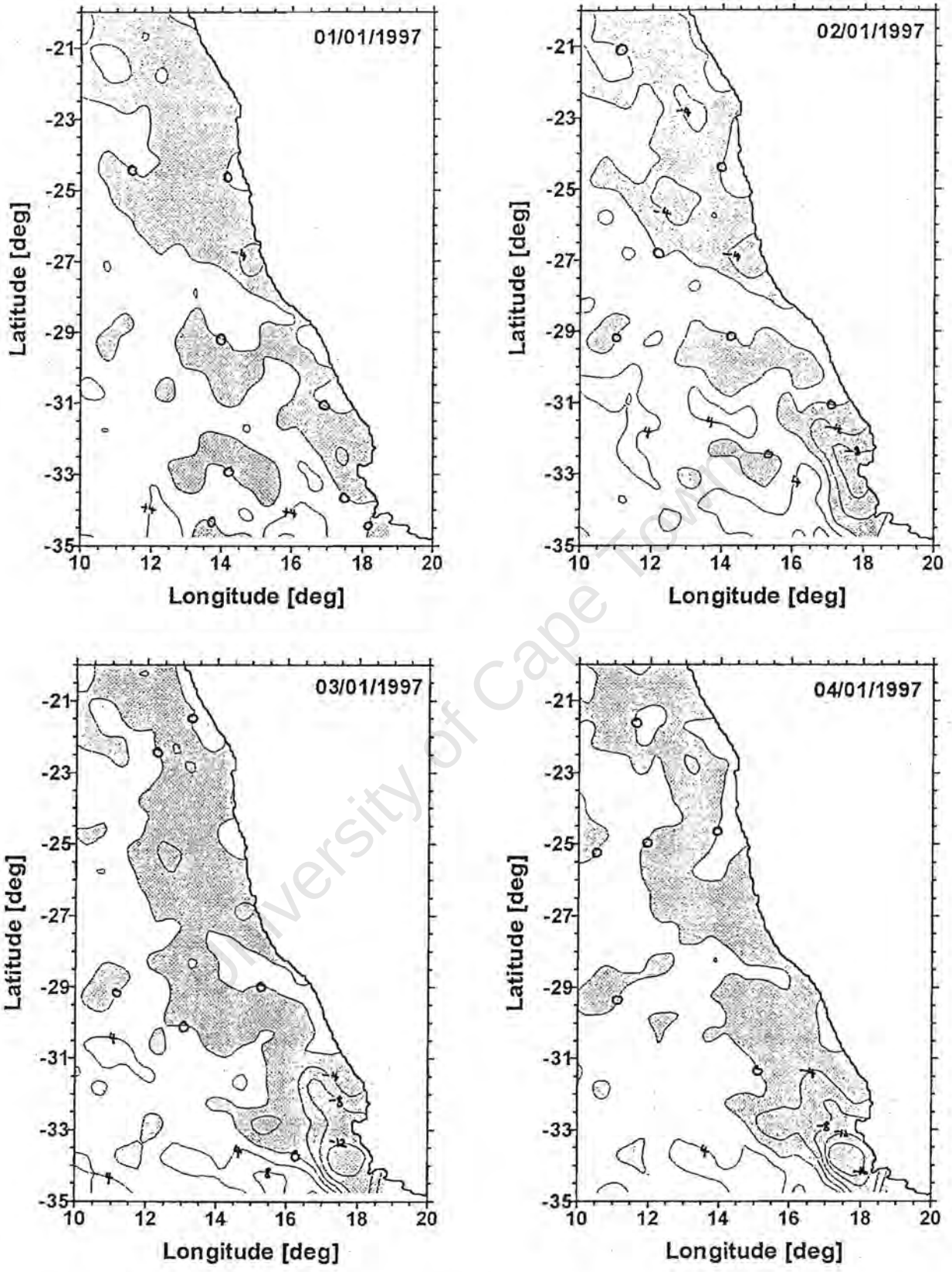

FIGURE 3.6: The vorticity or wind stress curl field (Nm^{-3}) constructed from three-day running mean NSCAT composites for the period 1 - 4 January 1997. Shaded areas are for negative, cyclonic values and unshaded areas are for positive values. The contour interval is 4×10^{-7} Nm^{-3}.

Vertical Velocities (w and w_{Ekman})

Under the conditions of an established and ridging SAA, the strong coastal upwelling will be due to strong southerly winds. Vertical velocities can be calculated using the formulae given in Chapter 2. Due to the reasonable agreement between NSCAT and coastal weather station data at Cape Peninsula and Cape Columbine, satellite data closest to the coast will be used to "simulate" a result for Ekman divergence. The coastal upwelling velocity w, can be calculated from NSCAT data points closest to the coast and the Ekman pumping velocity w_{Ekman}, will be calculated from a corresponding vorticity. Negative wind stress curl and consequently w_{Ekman} should be interpreted as a "priming" of the base of the Ekman layer. "Priming" describes the upward movement of the Ekman layer base towards the surface, thus making it shallower. As a consequence, coastal Ekman divergence requires less time (and energy) to allow the base of the Ekman layer to broach the surface. Results from the upwelling and Ekman pumping velocities calculated for Cape Columbine and Cape Peninsula during the established and ridging SAA are tabulated below in Table 3.1.

SITE	DATE	Upwelling Velocity (w) m.day^{-1}	Ekman Pumping (w_{ekman}) m.day^{-1}
Cape Peninsula	1 January 1997	56.04	0.01
	2 January 1997	67.48	0.62
	3 January 1997	73.72	1.14
	4 January 1997	67.76	1.56
Cape Columbine	1 January 1997	65.07	0.17
	2 January 1997	98.82	0.29
	3 January 1997	75.43	0.65
	4 January 1997	56.89	0.75

TABLE 3.1: Upwelling (w) and Ekman pumping (w_{Ekman}) velocities from 1 - 4 January 1997 at Cape Columbine and Cape Peninsula derived from NSCAT wind data.

The tabulated values above give some initial insight into the behaviour of the base of the Ekman layer, rate of upwelling and relative importance of vorticity or wind stress curl compared to upwelling. The vertical velocity rates do not take into account the length of coastline subjected to upwelling, but it should be noted that the baseline at Cape Columbine (~30 km, after Johnson and Nelson, 1999) is approximately two to three times that at Cape Peninsula based on high resolution AVHRR thermal imagery. Eventhough the vertical velocities are comparable the total volume of water brought to the surface by upwelling will be two or three larger along Cape Columbine than at Cape Peninsula. Upwelling rates are comparable to that suggested by Gill () when considering that it manifests at the sea surface within inertial period, which is roughly 12 hours for the southern Benguela system. When considering a mixed-layer depth of 50 m, a typical vertical upwelling velocity would be ~100 m.day^{-1}.

On 1 January 1997 the upwelling velocity (w) is 65.07 m.day^{-1} with a corresponding Ekman pumping velocity (w_{Ekman}) of 0.17 m.day^{-1} at Cape Columbine. It effectively means that the base of the Ekman layer (or mixed layer) is raised by only 17 cm in one day due to wind stress curl. This is very small when considering that the average mixed layer depth is approximately 50 m along the west coast of southern Africa (Shannon and Nelson, 1996). The system at this time is therefore predominantly driven by coastal Ekman divergence with little help from wind stress curl. A similar scenario is present at Cape Peninsula where the values are 56.04 m.day^{-1} and 0.01 m.day^{-1} for w and w_{Ekman}, respectively although the raising of the mixed layer base is much smaller.

The upwelling velocity at Cape Columbine shows the highest rate on 2 January (98.82 m.day^{-1}) marking the start of the ridging SAA process. At this time there is an equivalent 60% increase in the Ekman pumping velocity (0.29 m.day^{-1}). Along Cape Peninsula the upwelling velocity increase is not as dramatic, but there is an increase in Ekman pumping velocity to a value of 0.62 m.day^{-1} brought about by an increase in vorticity.

With the increased wind velocities brought about a continuously ridging SAA on 3 and 4 January, upwelling rates at Cape Columbine decrease to below that calculated for 1 January. Over

the same period Ekman pumping velocities increase to attain a value of 0.75 $m.day^{-1}$ on 4 January. This translates to the lifting of the mixed layer base by 75 cm, which is not very large for the priming process. The system is therefore still driven by mainly Ekman divergence at the coast during this period at Cape Columbine.

Along Cape Peninsula upwelling velocities change to 73.72 and 67.76 $m.day^{-1}$ from 3 to 4 January, respectively. Over the same period Ekman pumping velocities increase to 1.14 and 1.56 $m.day^{-1}$, which equates to the mixed layer thickness decreasing by these depths in a day. The priming of the mixed layer base is therefore more effective along Cape Peninsula due to possibly stronger topographic steering leading to higher vorticity during the ridging of the South Atlantic Anticyclone.

Summary

From the above analysis of NSCAT data over the Benguela coinciding with a period when the South Atlantic Anticyclone (SAA) (1 - 4 January 1997) moves from being established to ridging, wind field dynamics change most dramatically along the coast south of 30°S. With the established SAA wind vectors were consistently from the south over the entire region except along the coast in the vicinity of Cape Columbine-Cape Peninsula and Lüderitz. The topography influences air flow by creating shear causing a cyclonic curvature of southerly winds. As a consequence winds attain a larger onshore component in the lee of the capes and Lüderitz.

As the SAA ridges to the south of the subcontinent, wind vectors in the vicinity of Cape Peninsula become more easterly whereas between Cape Columbine and Cape Peninsula clockwise curvature increases, resulting in higher vorticity values in this region.

At the start of the study period upwelling at Cape Columbine and Cape Peninsula was purely driven by coastal Ekman divergence due to equatorward longshore winds. As the ridging process commenced, vorticity or wind stress curl became increasingly important as it had the potential to lift the mixed layer depth by up to 1.5m in one day at Cape Peninsula. It appears that vorticity and subsequent open-ocean upwelling is much less than coastal Ekman divergence.

West Coast Trough of Low Pressure (11 - 14 January 1997)

During the period 11 to 14 January 1997, a trough of low pressure developed along the west coast of southern Africa. SAWB synoptic weather maps for this period are given in Figure 3.7. On 11 January a small centre of low pressure (1008 hPa) is located in the vicinity of Walvis Bay. Wind speeds measured at Walvis Bay and Lüderitz are 20 and 40 knots, respectively and blowing towards the centre of the low pressure. Other coastal wind speeds measured to the south of Lüderitz show values ≥ 20 knots. On the same day, a second low pressure is situated over central Namibia and wind vectors suggest surface convergence. The SAA is situated well to the west, but there appears to be some ridging to the south of the subcontinent.

On 12 January the low pressure cell along the coast extends further south to approximately 32°S drawing moist tropical air from the Inter-Tropical Convergence Zone poleward. It results in almost the entire west coast being under the influence of the low pressure trough. The area underlying the 1012 hPa isobar, which appears to be defining the trough, has a reduction in wind speed compared to the previous day. At Lüderitz the wind speed decreases from 40 knots to 5 knots and the wind direction changes from westerly (12/01/97) compared to southerly (11/01/97). The wind speed at Walvis Bay remains constant from 11 to 12 January, but the wind direction changes to onshore instead of northerly.

On 13 January the 1012 hPa isobar encloses a small area, similar to a coastal low, with winds converging toward the centre in a clockwise manner. The 1016 hPa isobar assumes a similar aerial coverage and position along the west coast, but extends further poleward to beyond the Cape Peninsula. Winds along the west coast have moderate wind speeds between 5 and 20 knots and the direction is mostly onshore. On the following day the situation remains almost the same except that the wind direction is more southerly and longshore at Walvis Bay.

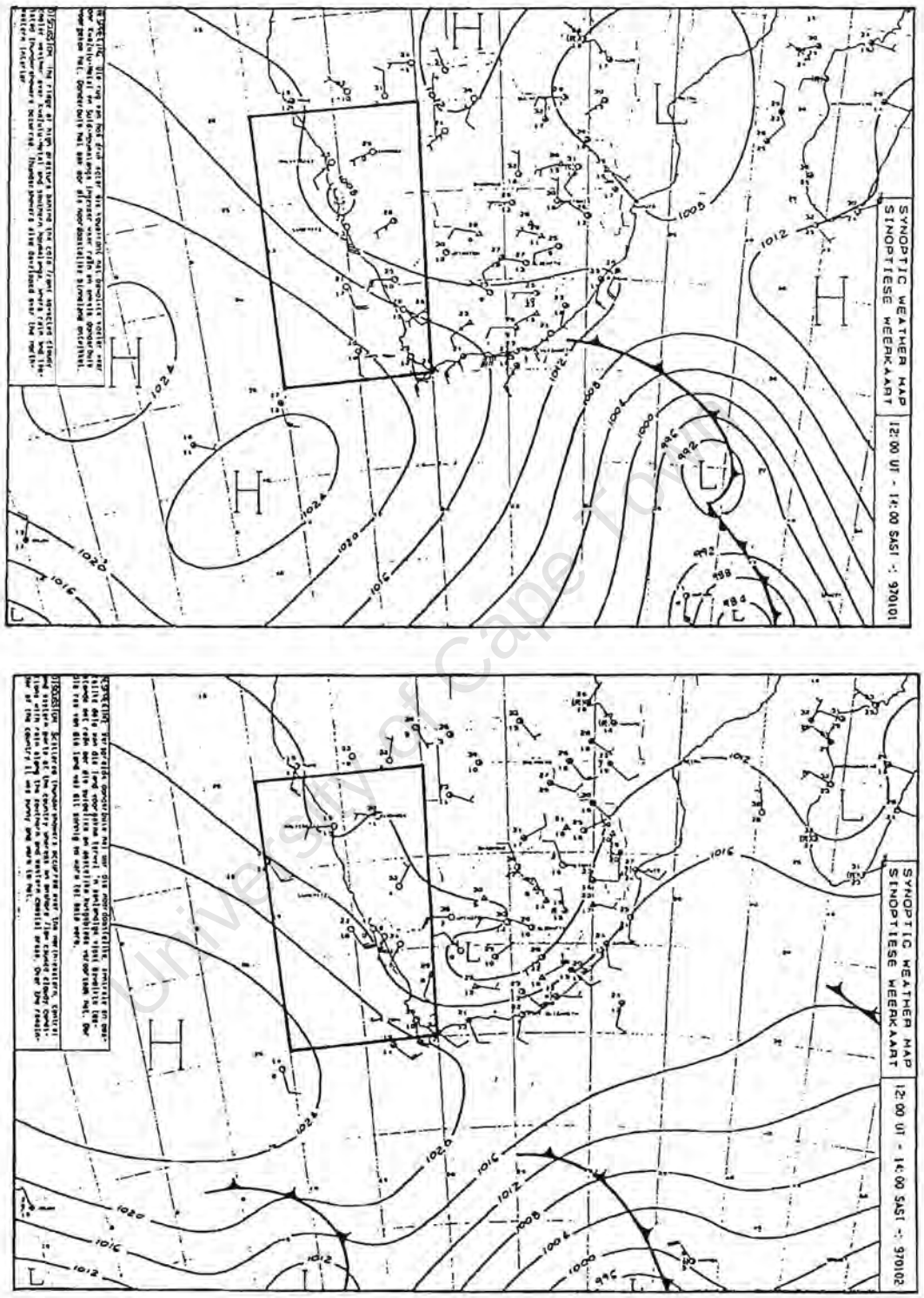

FIGURE 3.7: Daily synoptic weather maps produced by the South African Weather Bureau for the period 1 - 4 January 1997. The study area is highlighted and covering the west coast of southern Africa. The development of a low pressure trough is shown during this period along the west coast.

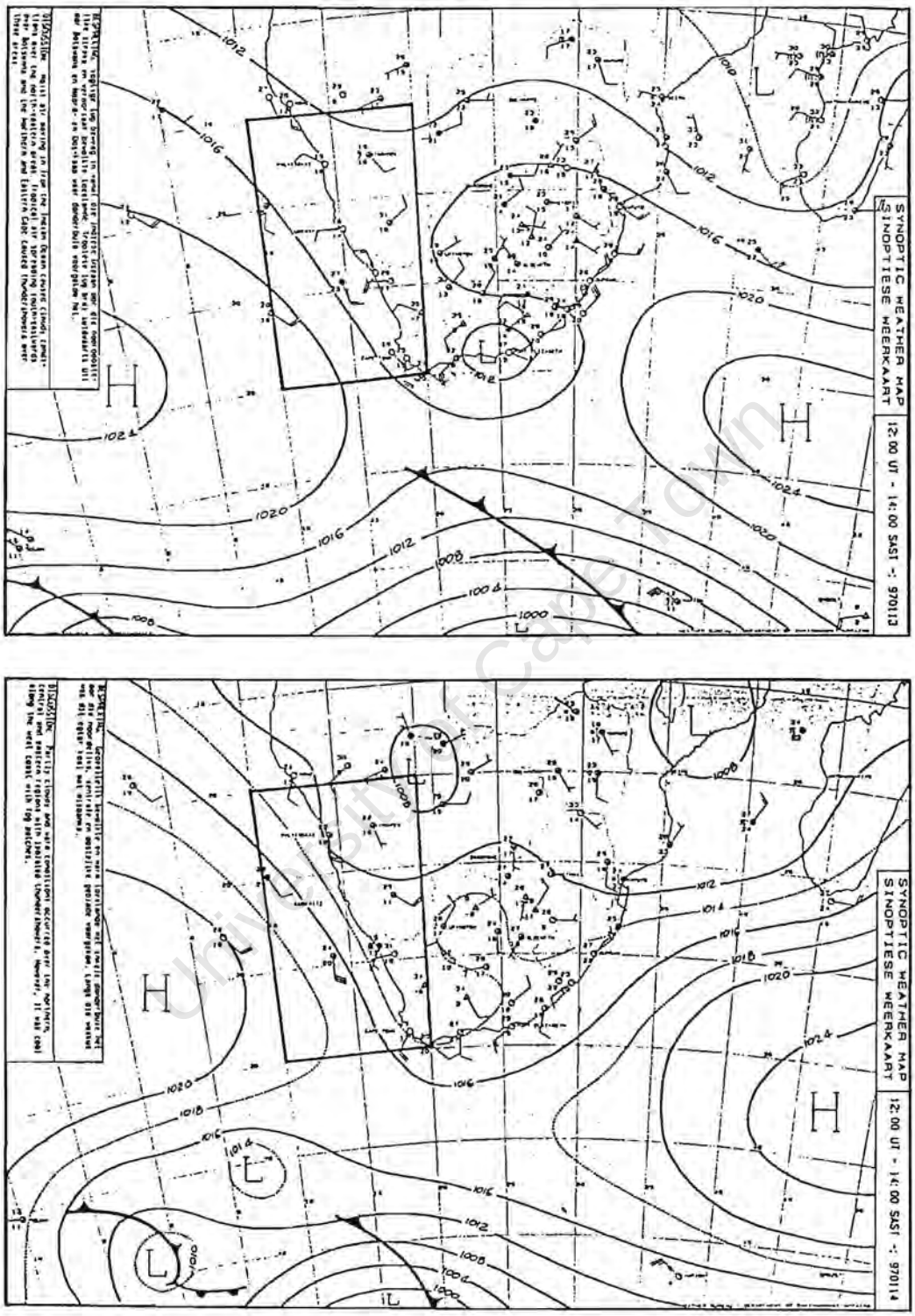

Figure 3.7: Continued....

Daily Averaged NSCAT data

Daily averaged NSCAT wind vector data derived from all satellite passes covering the area of research in a single day for the period 11 - 14 January 1997, are presented in Figure 3.8. Corresponding wind speed isotachs, in meters per second, are given in Figure 3.9. On 11 January the highest wind speed isotach is 13 ms^{-1} located between 28°S and 29°S and values steadily decrease poleward. Along the coast from Cape Columbine to the Cape Peninsula isotach values reduce from 11 to 7 ms^{-1}, respectively (Figure 3.9) and the vectors show longshore equatorward wind direction. This acceleration would result in wind driven surface divergence off Cape Columbine and subsequently enhance upwelling. The principal vector orientation over the west coast shelf is south easterly and there appears to be very little steering around prominent coastal topography. If synoptic wind data existed close to the coast and it corroborated a situation where winds blow uninhibited by topography, it could be as a result of a deep south easterly wind regime as described by Jury (1984).

On 12 January the SAWB charts (Figure 3.7) show the southward extension of the low pressure trough and its influence on coastal winds. The daily averaged winds measured by NSCAT on this day were fairly extensive and covered the entire study area except for the narrow strip along the coast. The wind vectors (Figure 3.8) for 12 January show a pronounced difference between two rather distinct zones of air flow. The first region is over the shelf extending diagonally to the northwest from the coast (at 29°S) to approximately 22°S along the western border of the study region. Wind vectors contained in this wedge are not in consistent alignment and wind speeds recorded by NSCAT are less than 6 ms^{-1}. The 6 ms^{-1} isotach roughly coincides with the 1012 hPa isobar shown in Figure 3.7. This suggests that on 12 January the wedge of low inconsistent winds along the coast marks the zone under the influence of the west coast trough of low pressure. The area to the south and south west of the 6 ms^{-1} isotach shows a rapid increase in wind speed, and wind direction is much more consistent. Highest wind speeds are contained in a

fairly narrow strip in a NW-SE coast-parallel orientation surrounded by the 10 ms^{-1} isotach. Contained within this elongated strip are two smaller wind speed maxima of 11 ms^{-1} centred on the coordinates (30.5°S; 12.5°E) and (32°S; 15.25°E). The high winds offshore are due to an intensified isobaric gradient between the trough of low pressure and the SAA as the anticyclone moves closer to the coast. Between the 10 ms^{-1} isotach and the south western corner of the map wind speed decreases, but increases again around the capes to values of 10 and 11 ms^{-1}. The winds around the Cape Peninsula and Cape Columbine area show a large degree of topographic steering as expressed by the clockwise rotation of vectors here. The higher winds around the capes are also due to a steeper pressure gradient, but this time it is the SAA squeezing the isobaric surfaces (and subsequently the air flow) against the high mountains.

On 13 January the trough of low pressure extends further south. The available wind vector data along the satellite swaths (Figure 3.8) suggest that the low wind over the shelf is contained within a narrow coastal strip only 120 nmiles wide between the latitudes 23 - 32°S. The narrow coastal strip of low wind is co-incident with the overlying trough and contains wind speeds ranging from 1 - 8 ms^{-1}. On the other hand, wind speed isotachs (Figure 3.9) show that low winds extend far offshore to the west of Namibia with values ranging from 3 - 7 ms^{-1} appearing along the western border of the study region between latitudes 22 - 26°S. As a result, the wedge-like shape of the area containing low winds is maintained. This shape is not as evident within the vector map (Figure 3.8) due to the data gap between swaths on 13 January. Once again wind vectors on the seaward side of the area of low winds are more consistent in direction and generally stronger.

On 13 January the highest isotach gradient (3 to 8 ms^{-1}) is found over the shelf between 27 - 32°S, within a distance of 120 nmiles from the coast. This is as a consequence of the SAA moving closer to the coast causing an increase in pressure gradient between itself and the low pressure trough. The sharp pressure gradient also gives rise to a very abrupt change in vector alignment and wind speed between the two synoptic atmospheric systems (SAA and trough).

Offshore of the high isotach gradient there is a large, elongated, coast parallel area containing wind speed ≥ 9 ms^{-1} centred on the coordinates (30.5°S; 14.5°E). This area of wind speed exceeding 9 ms^{-1} appears to be separated from smaller areas containing similar values in the vicinity of the capes and another smaller area inbetween (33°S; 16°E). This configuration could be an artifact of the contouring process, whereas in reality it could very well have been a single connected area.

On 14 January the influence of the low pressure trough seems to abate and there is only a smaller region of low wind speed along the coast to the north of 25°S. The wind field structure appears to be very similar to that on 12 January, with low winds in a small area along the coast and consistent, stronger winds in a broad band stretching from around the capes to beyond the confines of the study region.

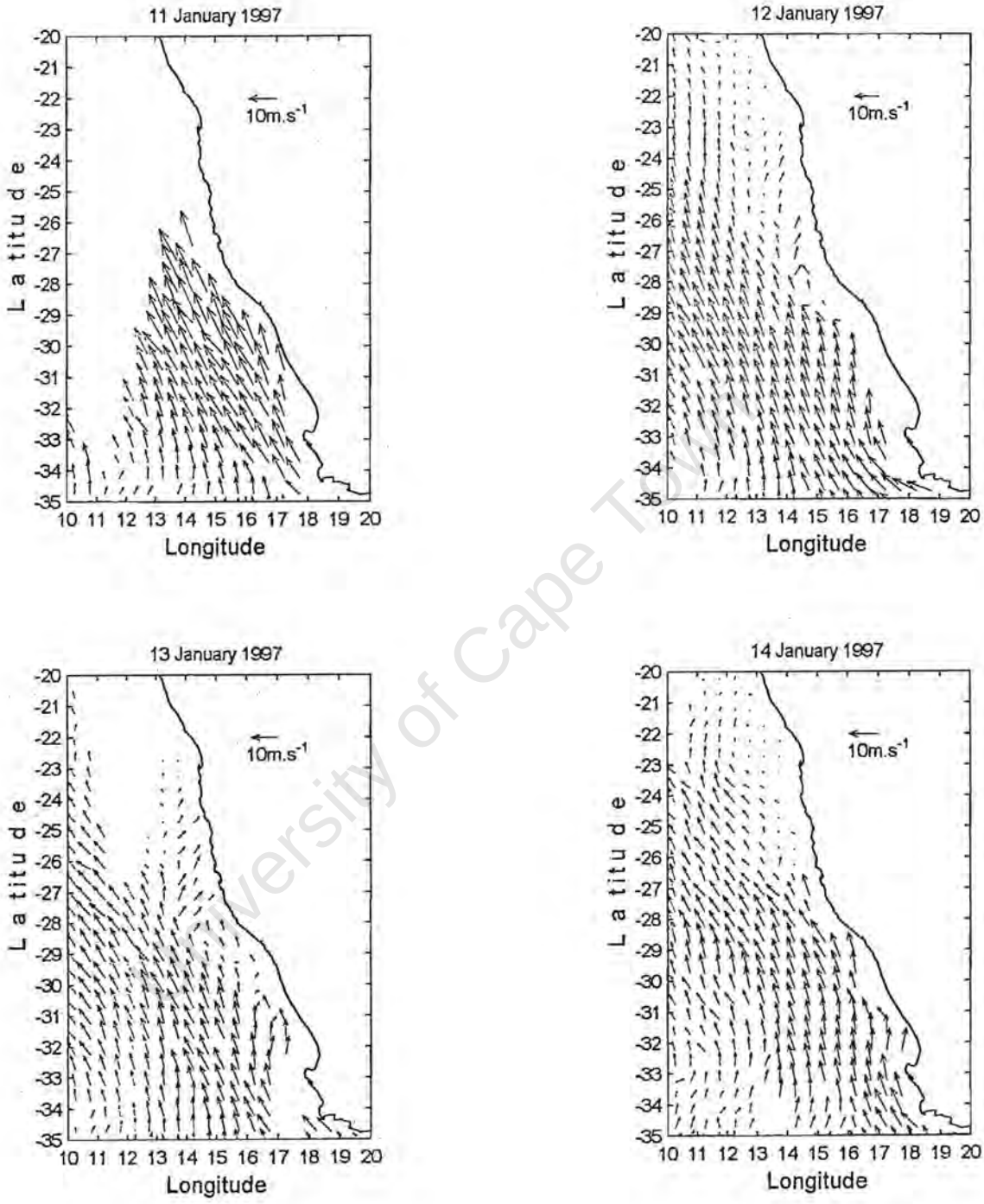

Figure 3.8: Daily-averaged NSCAT wind vectors for the period 11 - 14 Jan. 1997. The vector reference is given in the upper right-hand part of the figure.

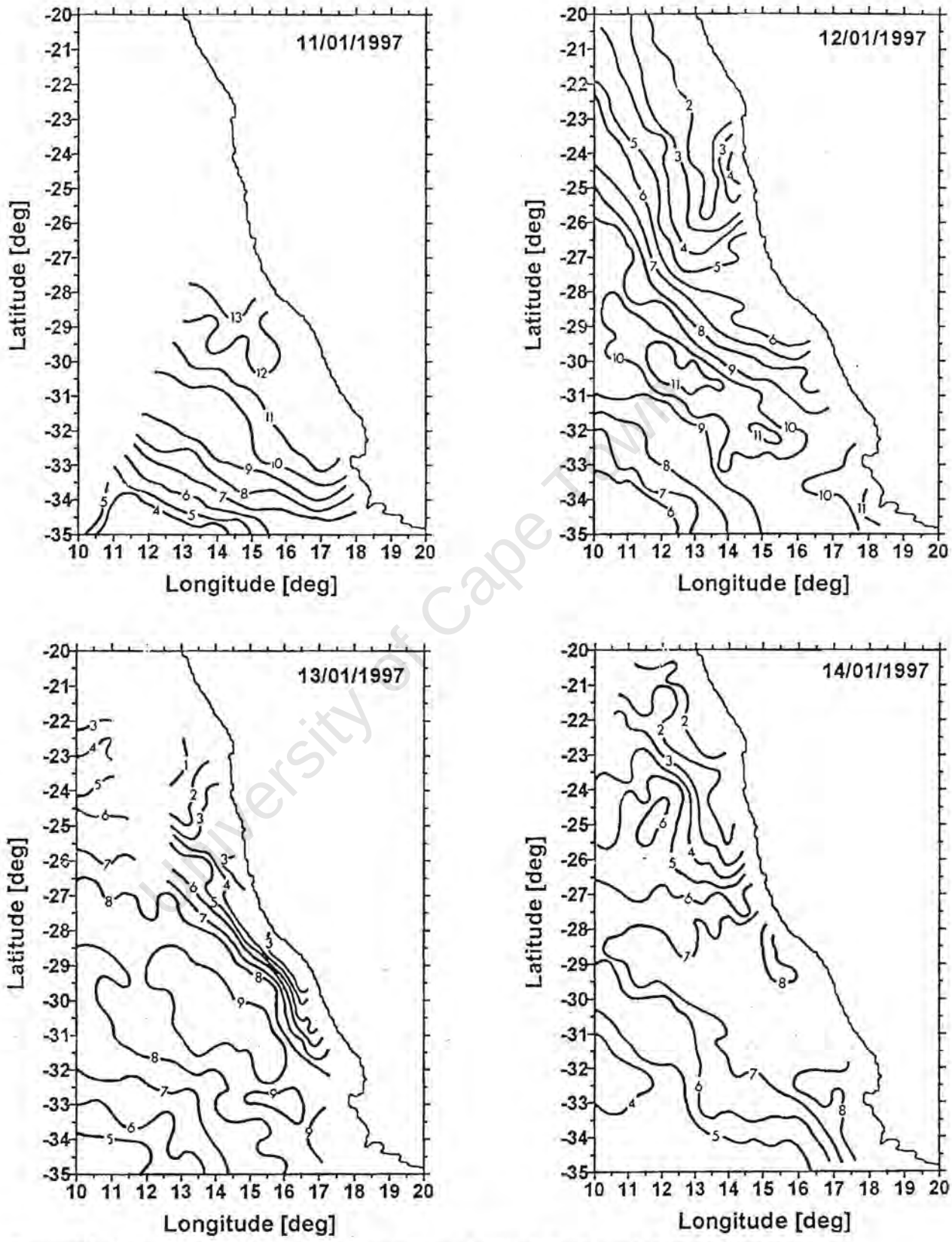

Figure 3.8: Daily-averaged NSCAT wind speed isotachs (ms^{-1}) for the period 11 - 14 Jan. 1997. The contour interval is 1 ms^{-1}.

Three-Day Running Mean NSCAT Data

The three-day running mean winds constructed for the period 11 - 13 January 1997 is presented in Figure 3.10 and corresponding wind speed isotachs in Figure 3.11. As a result of missing daily averaged data on 15 January 1997, it was not possible to construct a three-day running mean wind field for 14 January. There is some evidence in Figure 3.10 that a clear differentiation is developing between the offshore coast-parallel area of higher winds and the wedge of lower winds along the coast as discussed in the preceding section. The isotachs in Figure 3.11 enhances this view. In terms of a developing west coast trough of low pressure, based on the preceding section of daily weather maps produced by the SAWB and NSCAT wind vectors, a southward propagating system causing low wind speeds over the shelf can be seen in the three-day running means. On 11 January, to the north of 26°S, isotachs range from 6 - 9 ms^{-1} with a smaller isolated area of 9 ms^{-1} pinned against the coast between 28 - 31°S. Although vectors are fairly consistent in this area, the vector magnitudes are somewhat smaller compared to a large area located on its seaward side.

Isotachs in the area of reduced wind, to the north of 26°S, show signs of a poleward protrusion developing over the shelf as they assume a more accentuated concave shape against the coast. These poleward protrusions become much greater in extent on 12 January as was seen in the previous analysis. The 9 ms^{-1} isotach that was located between latitudes 24 - 26°S on 11 January appear to fuse with the 9 ms^{-1} isotach (pinned against the coast between 28 - 31°S on 11 January) on 12 January. The large, elongated, coast parallel area enclosed by the 9 ms^{-1} isotach corresponds to that enclosed by the 10 ms^{-1} isotach in the daily averaged data seen earlier. The poleward advancement of isotachs $\leq$9 ms^{-1} along the coast increases the cross shelf-directed gradient of wind speed over the shelf, but to some lesser degree than in the daily NSCAT data.

On 13 January there is clear indication that a zone of reduced wind exists in a wedge-like shape along the coast north of the latitude 32°S in the wind vector plots (Figure 3.10) and isotach

plots (Figure 3.11). Eventhough the three-day running mean wind vectors are much smoother than the daily averaged data collected by NSCAT, their agreement on this day is fair. The coherence between isotachs, in general, is good when comparing the three-day running mean (Figure 3.11) and daily averaged wind data (Figure 3.9). The intensification of the west coast trough of low pressure results in a further increase in cross shelf wind speed gradient eventhough the degree of intensification is less than that shown for 13 January in the daily averaged data (Figure 3.8). The three-day running mean data suggest that wind speeds underlying the trough of low pressure range from 1 - 8 ms^{-1}. This is similar to the data range in the daily averaged NSCAT analysis for 13 January. This indicates that compiling a synoptic three-day running mean wind data set from NSCAT can provide good source of wind information eventhough there is loss of spatial detail in the wind field.

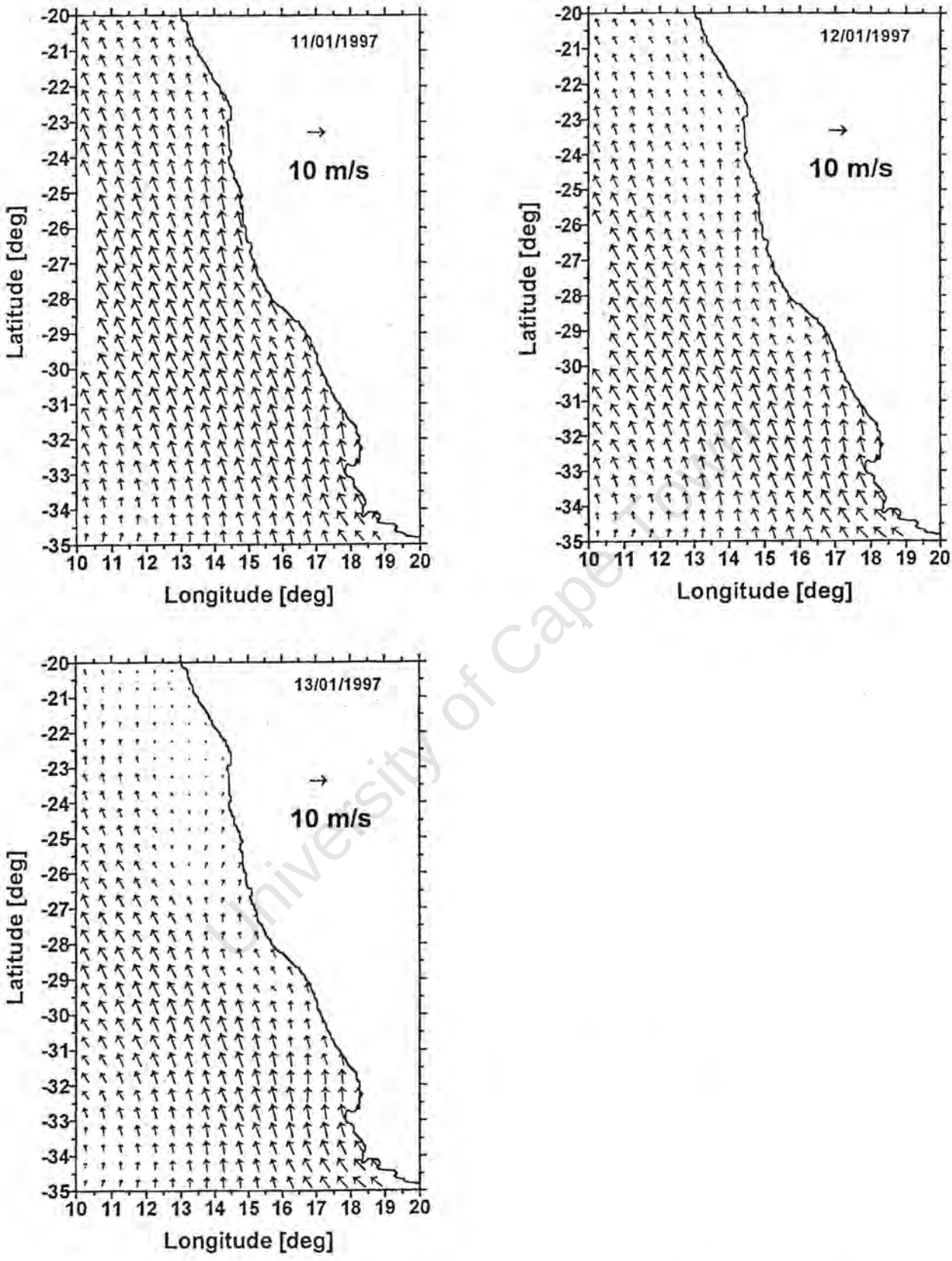

FIGURE 3.11: Three-day running mean NSCAT wind vectors for the period 11 - 13 January 1997. The reference vector is given in the upper right-hand part of the figure.

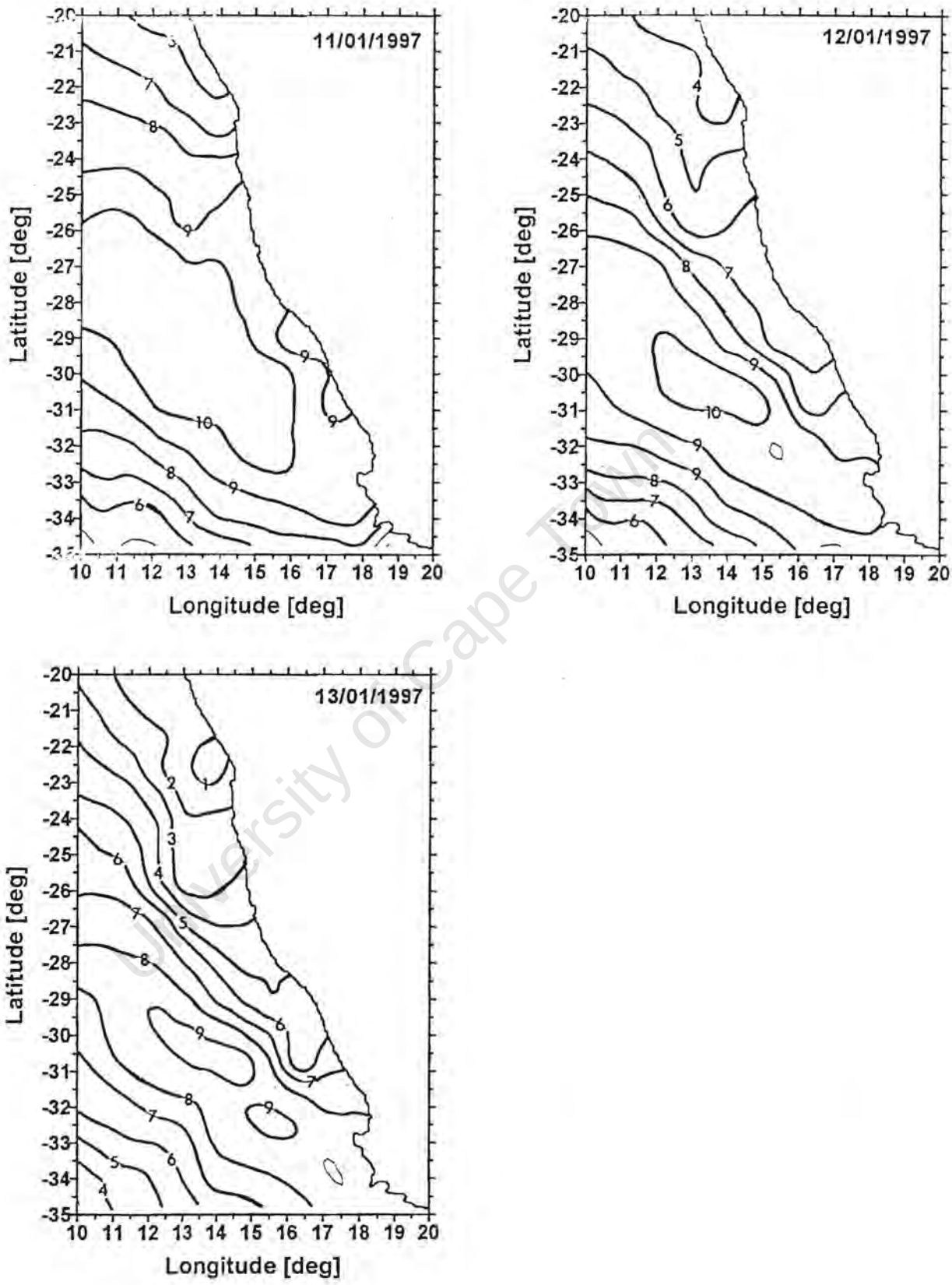

FIGURE 3.11: Three-day running mean NSCAT wind speed isotachs (ms^{-1}) for the period 11 - 13 January 1997. The contour interval is 1 ms^{-1}.

Vorticity or Wind Stress Curl

Figure 3.12 shows wind stress curl contours for the period 11 - 13 January 1997, based on the three-day running mean data (Figures 3.10 and 3.11). On 11 January a centre of wind curl maximum appears along the coast between latitudes 29 - 31°S with values of $-4x10^{-7}$ enclosing two smaller centres of $-8x10^{-7}$ Nm^{-3}. The wind stress curl differs very much from an analysis done by Jury (1984) where he showed negative curl values being confined to the capes, but this could be ascribed to a difference in the scale of measurements between the two studies. Negative or cyclonic curl coincides with the area where the steepest cross shelf wind speed gradients occur, resulting in cyclonic curl extending from the capes (in the south) to beyond the study region in the north. This negative curl configuration is similar to that found by Parrish *et al.*(1983) and Bakun (1987) who used climatological, one-degree COADS ship derived wind data.

With the southward propagation of the west coast trough of low pressure on 12 and 13 January, the pressure gradient between the trough and SAA is increased and hence the cross shelf wind speed. At this time there is a general decrease in curl values together with a concomitant offshore movement of the entire negative curl area that coincides with the steepest, coast parallel wind speed gradient. As a result, on 13 January the contours enclosing $-4x10^{-7}$ Nm^{-3} are found in a coast parallel alignment, but much further offshore (~180 nmiles from the coast).

It appears that with the southward propagation of the west coast trough of low pressure, the negative curl area and its maximum values are shifted offshore.

Summary

The analysis of the west coast trough of low pressure shows that with its development there is a decrease in wind speeds over the shelf and along the coast. The poleward movement of the trough appears in a wedge-like shape resulting in a particular wind field configuration. There is

a clear line distinguishing the area influenced by the trough and that beyond it. Wind vectors under the trough show low wind speeds and are non consistent, whereas the area beyond the trough show higher wind speeds and much greater vector flow cohesion.

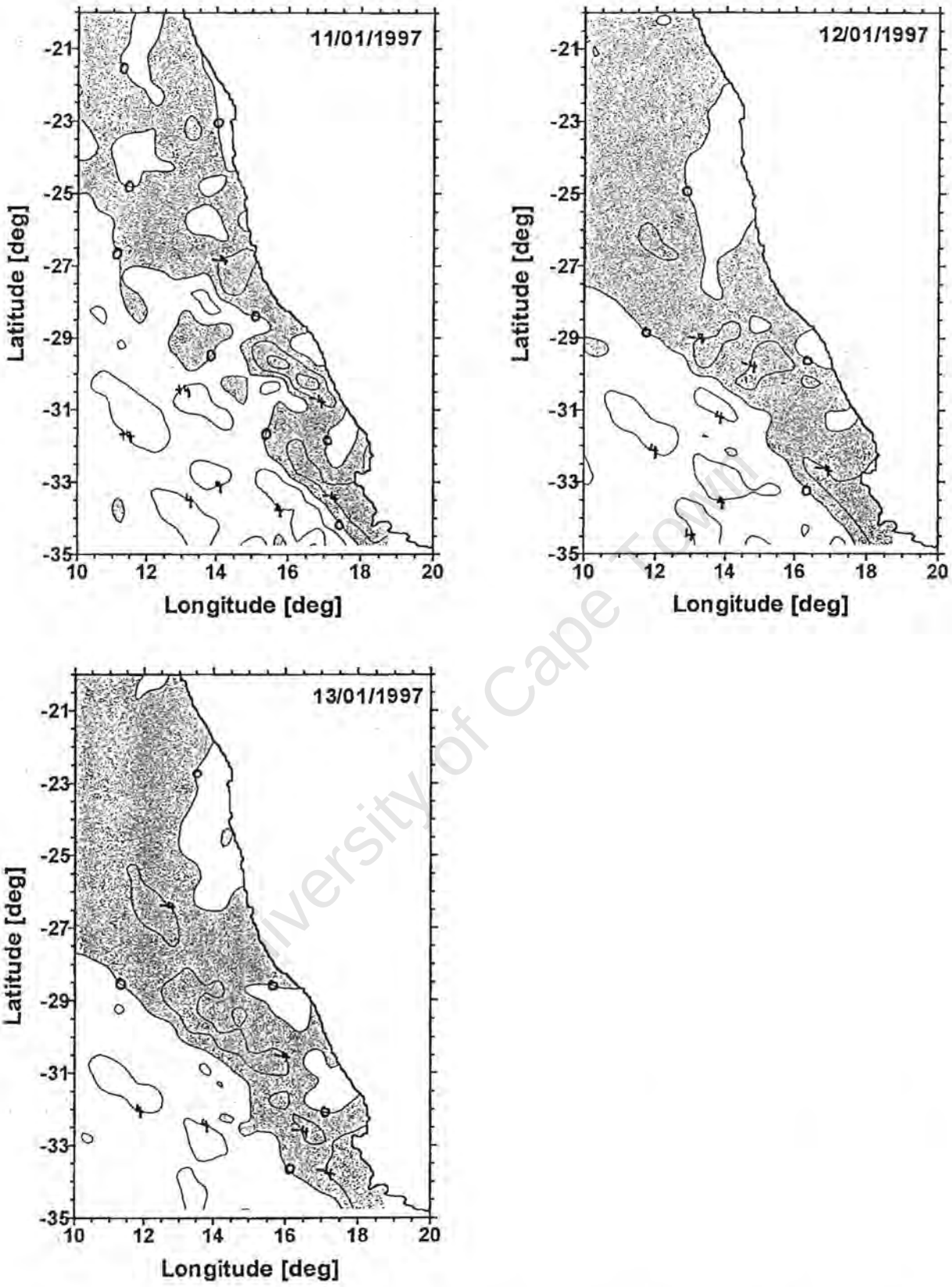

FIGURE 3.12: Three-day running mean NSCAT wind stress curl contours (Nm^{-3}) for the period 11 - 13 January 1997. The contour interval is 4×10^{-7} Nm^{-3}.

Mid-Latitudinal Cyclone or Cold Front (20 - 22 April 1997)

Figure 3.13 shows the eastward advection of a mid-latitude cyclone or what is commonly termed a cold front, as based on the daily weather charts of SAWB from 20 - 22 April 1997. On 20 April the central pressure, which was approximately 888hPa, of the cold front is situated well to the south west of the continent. Winds along the west coast of southern Africa are weak with speeds ranging from 5 - 20 knots. To the north of 30°S, wind direction is southerly, but to the south of this latitude the direction is more northerly to westerly. These are typical wind conditions associated with an approaching cold front due to the clockwise rotation of air around the central low pressure. Over the land, a low pressure is dominating to the north of 30°S.

On 21 April the front moves much further to the north showing two low pressure centres. The northern low pressure centre is now only 5° of longitude away from Cape Town, whereas the second centre is located much further to the south. Winds south of 30°S continues to blow from the north, but north of this latitude coastal winds have changed their direction to more easterly.

On 22 April the low pressure system appears to become a "cut-off" low and the cold front reaches the west coast of southern Africa. There is still strong clockwise rotation of winds around the central low pressure. Winds north of 30°S still blow from the north, but at Cape Town the wind direction has backed from north westerly to south westerly. The wind alignment at Cape Town is now similar to that of post-frontal air flow, or south westerly, when the SAA ridges in behind the transient cold front. A low pressure centre is still dominating the circulation over the central interior.

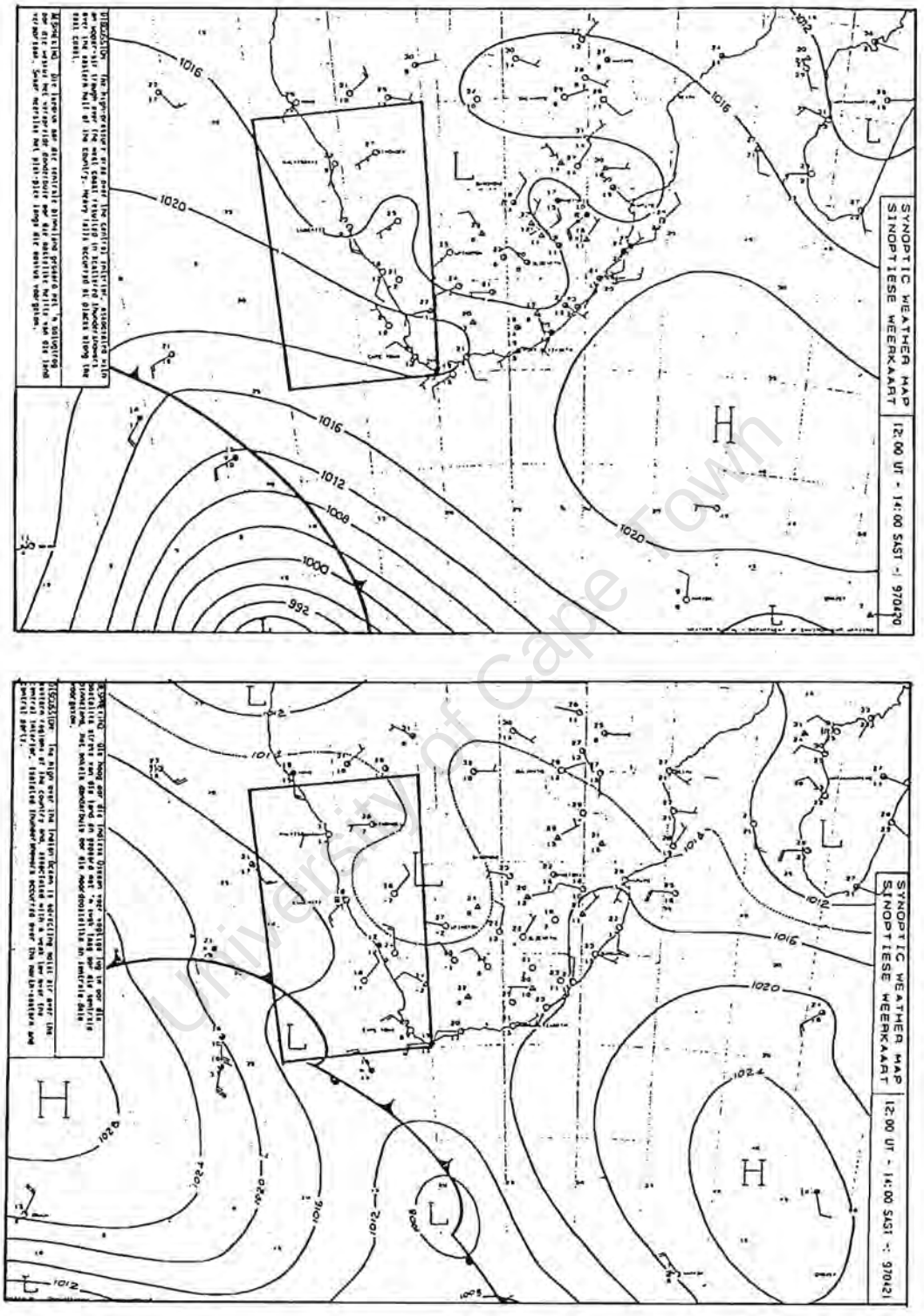

Figure 3.13: Daily synoptic weather maps produced by the South African Weather Bureau for the period 20 - 22 April 1997. The research area is highlighted and during the period a cold front passed over the subcontinent from west to east.

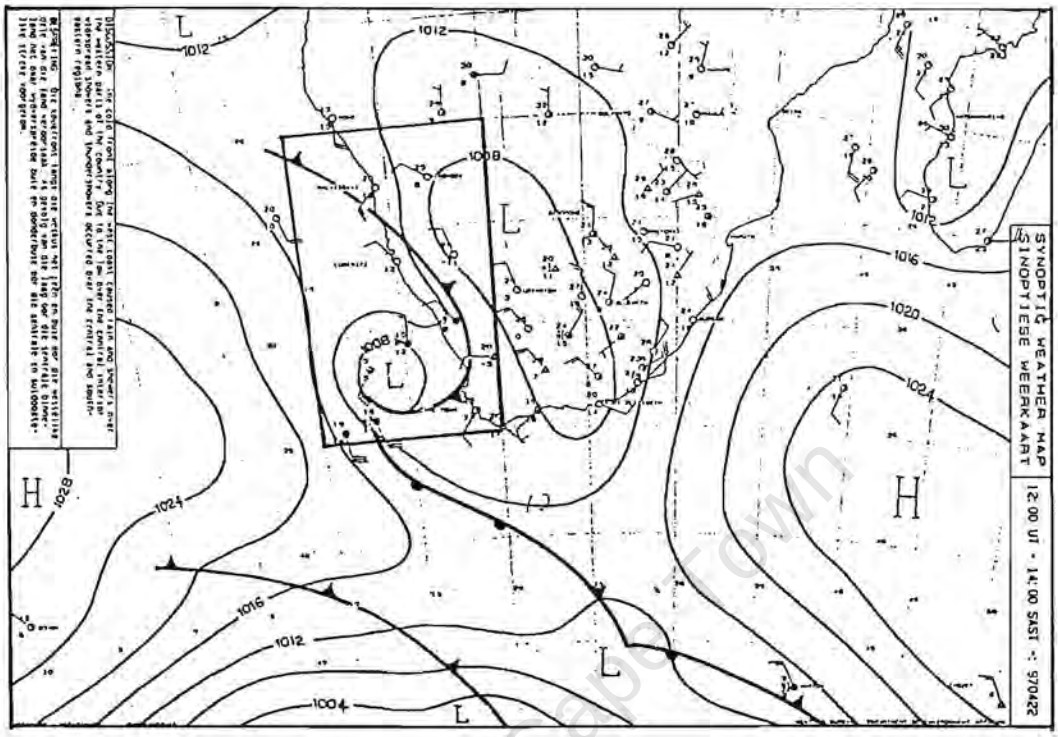

Figure 3.13: Continued .....

Daily Averaged NSCAT Data

Figure 3.14 and 3.15 show the daily averaged wind vectors and wind speed isotachs, respectively derived from NSCAT data for the period 20 - 22 April 1997. On 20 April the wind vectors south of approximately 28°S are very irregular in direction and speed except for a narrow strip along the western boundary of the study region. In the square from 28 - 35°S and 12 - 20°E, wind vectors have a predominant northerly direction which is consistent with the single offshore SAWB measurement (north west of Cape Columbine) for 20 April (Figure 3.13). This sub-square of the study region is dominated by light wind speeds of 1 - 2 ms^{-1}. Located to the west of the square are winds that are more consistently from the north and wind speeds are between 4 - 7 ms^{-1}. This is due to the approaching cold front. To the north of 28°S, winds are southerly with speeds ranging from 4 - 10 ms^{-1}. It appears that the 28°S line of latitude demarcates the area influenced by the cold front on this day.

On 21 April there is a slight northward intrusion of calm winds to approximately 25°S compared to the previous day, although this is only applicable in the region beyond the shelf edge. This northward intrusion is clearly seen in Figure 3.15 (for 21 April) where the 2 ms^{-1} isotach extends to about 26°S eventhough its overall aerial coverage has diminished compared to the previous day. The area pinned between the shelf edge and coastline to the north of 28°S maintains a southerly wind direction and the speeds are between 3 - 8 ms^{-1}.

To the south of 28°S there is strong indication of onshore flow within 4° of longitude from the coast. Wind speeds increase from 1 ms^{-1} at the coast to approximately 6 ms^{-1} at 240 nmiles from the coast. Further offshore the wind vectors appear to be from the north west and forms a large sinusoidal wave-like structure. This sinusoidal form could be some surface manifestation of the upper-air Rossby wave that controls the pathway of cold fronts, but this is highly speculative at this stage and need much greater analysis. The highest horizontal wind speed gradient is found between longitudes 14 - 15°E and latitudes 32 - 35°S where values increase from

5 ms^{-1} to 13ms^{-1}. This area is also marked by a sharp spatial gradient in direction from southerly to north westerly. The directional change, when considering the daily weather map, appears to indicate the front. This high gradient for 21 April (Figure 3.15) and convergent vector flow, indicated for the same day in Figure 3.14, indicate the possible position of the central low pressure for this cold front. This is in good agreement with the SAWB daily synoptic map for the same day.

On 22 April there are not many data points measured by the satellite due to the orbital configuration. The available data indicate that there is a region of north westerly winds along the satellite swath north of Cape Columbine. This is typical air flow prior to the actual cold front reaching the coast. Wind speeds are shown by isotachs in Figure 3.15 and values, along the coastal satellite swath north of Cape Columbine, range from 4 to 12 ms^{-1}. Vectors between longitudes 13 - 17°E and south of 33°S show strong easterly flow with speeds ranging from 6 - 12 ms^{-1}. It appears that the 33°S latitude is a zone of convergent flow separating the north westerly from the easterly flow. Collectively, the opposing flows along the swath show some cyclonic circulation typical around the central low pressure of a cold front. Offshore of the 13°E longitude winds are southerly wind speeds between 8 - 11 ms^{-1}. This completely different air flow compared to that closer to the coast could be as a result of the different times when the satellite passed. The region of very coherent wind far offshore was measured approximately 10 - 12 hours than the data east of 13°E.

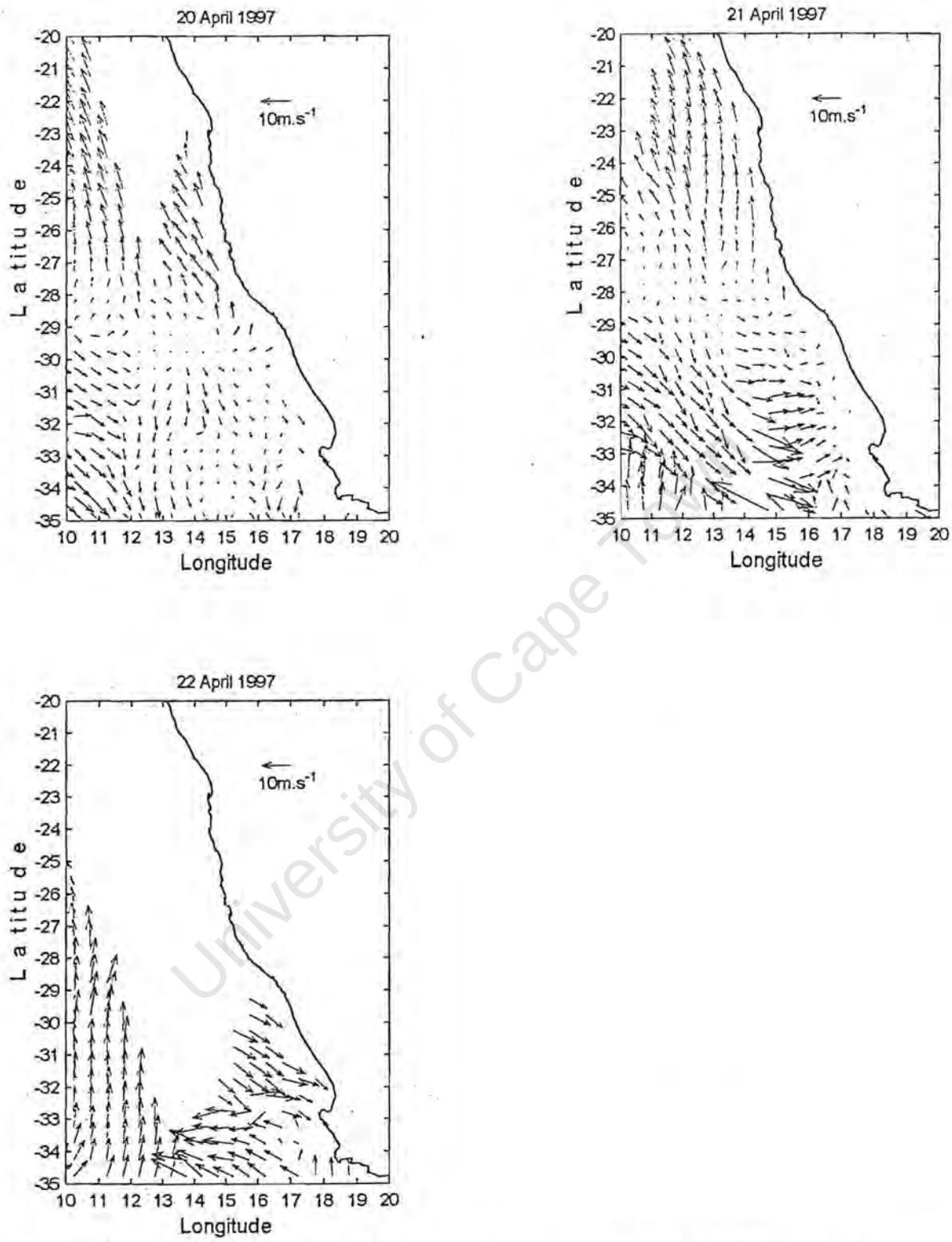

FIGURE 3.14: Daily-averaged NSCAT wind vectors for the period 20 - 22 April 1997. The vector reference is given in the upper right-hand side of the figure.

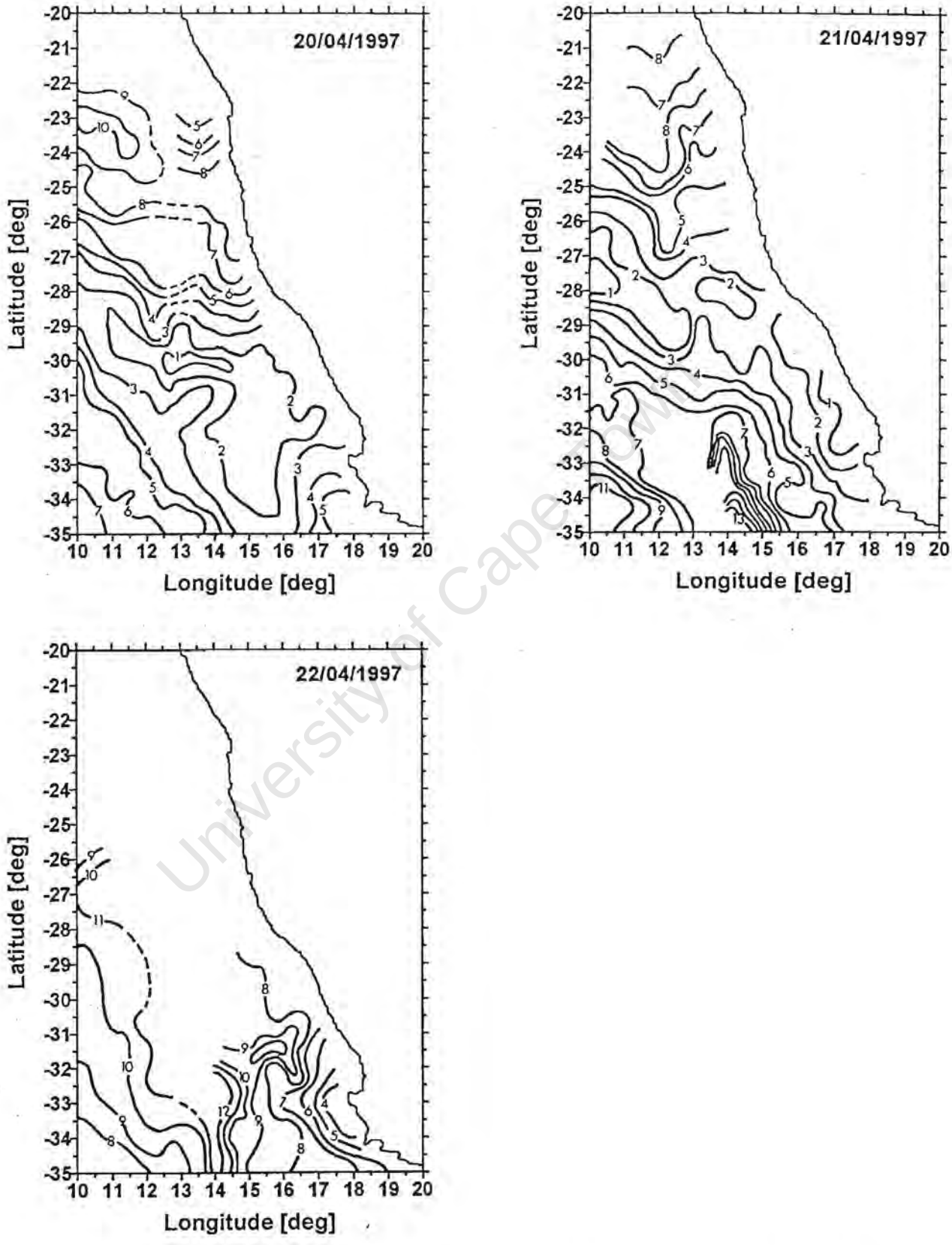

FIGURE 3.15: Daily-averaged NSCAT wind speed isotachs (ms^{-1}) for the period 20 - 22 April 1997. The contour interval is 1 ms^{-1}.

Three-Day Running Mean NSCAT Data

Figures 3.16 and 3.17 show the three-day running mean wind vectors and corresponding wind speed isotachs measured by NSCAT between 20 - 22 April 1997. The overall impression gained from the vectors in Figure 3.16 is the coherence in flow during the whole period along the coast of Namibia (north of ~28°S). The consistent southerly wind flow in this area is in agreement with the daily NSCAT data (Figure 3.14), but there are differences in absolute wind speed values. On 20 April wind speeds north of 28°S are between 4 - 7 ms^{-1}, whereas the maximum speed for this day from daily data is 10ms^{-1} located around the coordinates (23°S; 11°E). For the three-day running mean data the maximum wind speed is along the coast, in the vicinity of Lüderitz, between 24.5 - 28.5°S. South of 28°S, winds are somewhat variable in direction with speeds being dominantly between 2 - 3 ms^{-1} and either westerly or northerly in direction along the coast. This is not very different from the daily NSCAT data scenario although the isotachs are much smoother and lower in value for three-day running mean data. An example is the area around Cape Columbine where wind speeds are below 2ms^{-1}, whereas in the daily data it is ~3ms^{-1}.

On 21 April, the spatial structure of the wind has changed little, but winds along the coast between Cape Columbine and the latitude 28°S have increased in speed and the direction is more north westerly (pre-frontal). Wind speeds in the area have more than doubled and the isotachs show a much stronger gradient than the day before. Between latitudes 29°S and 35°S, wind speed values range from 3 - 14 ms^{-1}. The overall vector flow is consistent with cyclonic rotation around the central low pressure of the cold front.

On 22 April there is even stronger evidence of cyclonic flow around a central low pressure around the coordinates (33.5°S, 14°E). The assumed position of the low pressure centre in the three-day running mean data concurs with that in the daily NSCAT data (Figure 3.15) as well as the synoptic weather charts of the SAWB (Figure 3.14). Highest wind speeds (>11 ms^{-1}) are shown to occur in this area on this day. Confining the discussion to the area south of 28°S, wind

vectors between the coast and 14°E show pre-frontal north westerly winds. Between 10°E and 14°E winds are south westerly or post-frontal.

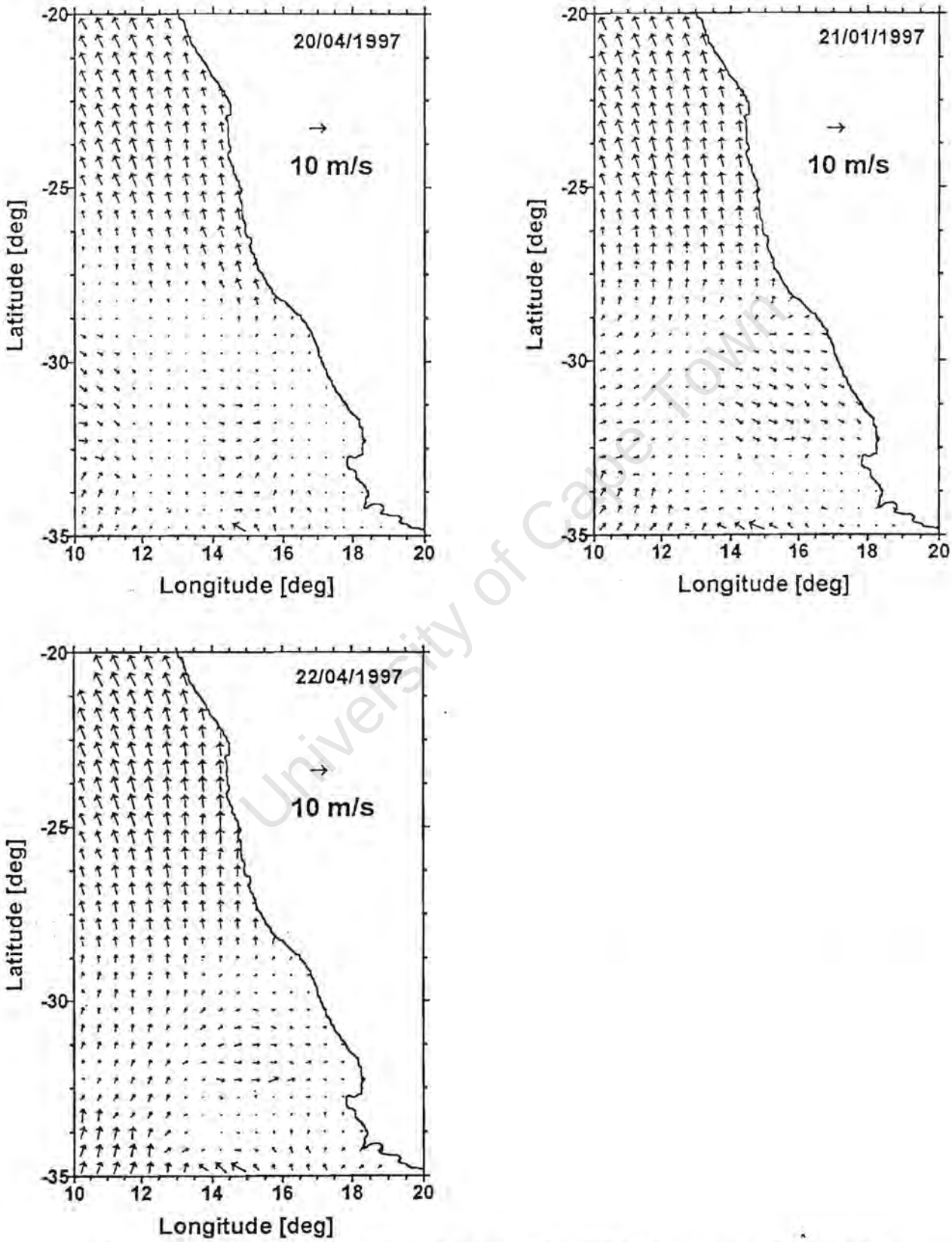

Figure 3.16: Three-day running mean NSCAT wind vectors for the period 20 - 22 April 1997. The reference vector is given in the upper right-hand part of the figure.

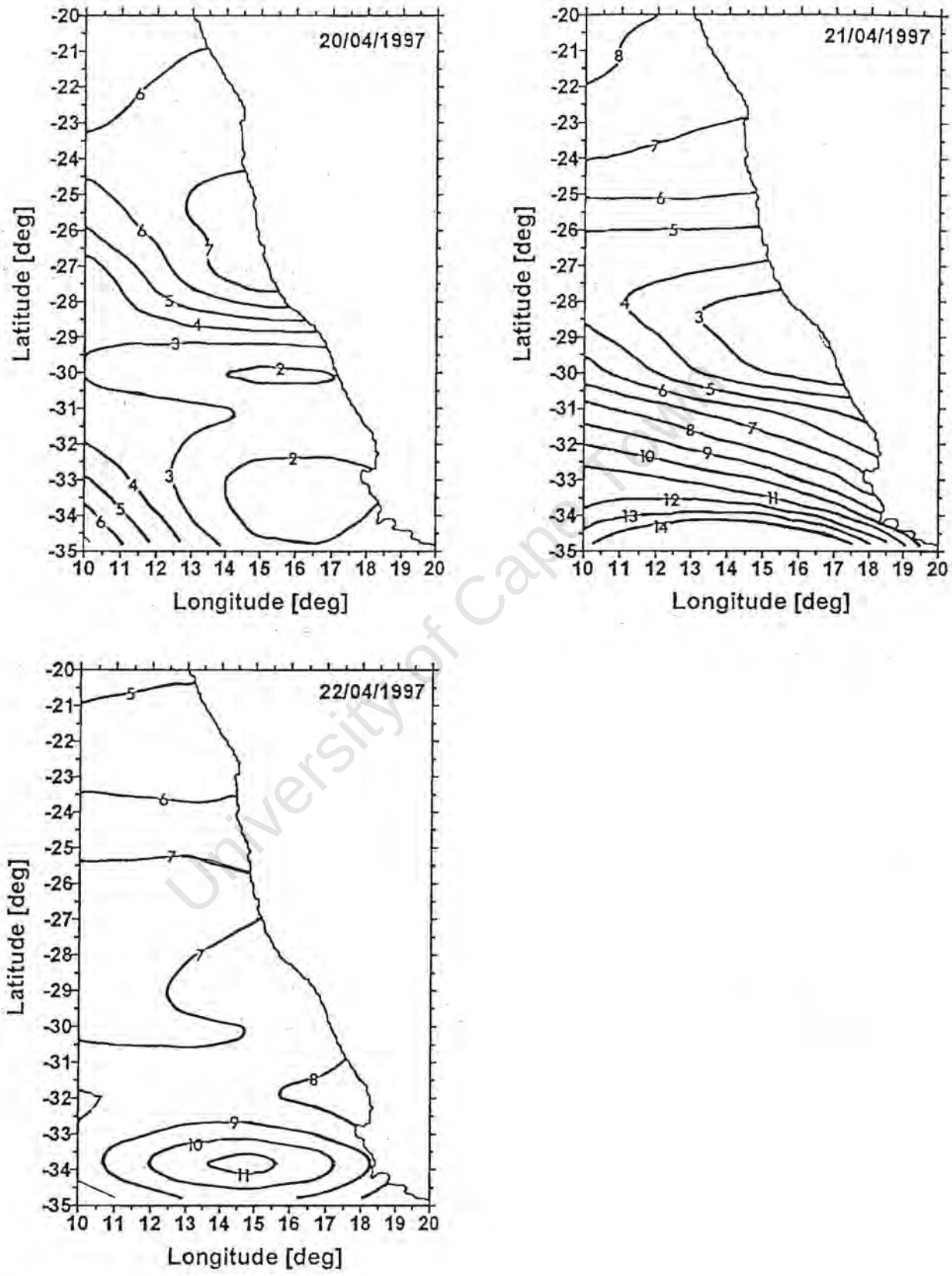

Figure 3.17: Three-day running mean NSCAT wind speed isotachs (ms^{-1}) for the period 20 - 22 April 1997. The contour interval is 1 ms^{-1}.

Vorticity or Wind Stress Curl

Figure 3.18 shows wind stress curl contours constructed from the three-day running mean data between 20 and 22 April 1997. The regions of negative curl (shaded area) are of interest and the curl configuration is the same as in previous sections. On 20 April curl values are slightly negative over the west coast shelf area and this does not change dramatically over the next two days. The only difference, in terms of negative curl, from 20 to 22 April is the equatorward retraction of the area it occupies along, and it separation from, the coastline.

On 20 April, the highest negative curl values are located in a small square between latitudes 34 - 35°S and longitudes 14 - 16°E. The curl value at the centre of this square exceeds $-1x10^{-5}$ Nm^{-3} and appears to be aligned with the central low pressure of the cold front. Using the simple formula, introduced in a preceding chapter, for calculating vertical velocity from wind stress curl yields a result between 10 - 11 $m.day^{-1}$. The vertical velocity, brought about by the strong negative wind stress curl, is much greater than that expressed for a ridging SAA discussed earlier. According to the three-day running mean data, this high negative curl value remains within the study region from 20 - 22 April. This could partially explain the reason for thermocline erosion over the continental shelf associated with a cold front.

Summary

NSCAT data, on both daily and three-day running mean time scales, show good agreement with daily weather maps. The data show that the region along the Namibian coast, north of 28°S, remains unaffected by the passing cold front as winds remain fairly strong and southerly. South of 28°S the wind field showed clockwise rotation around the central low pressure of the cold front. This wind field configuration resulted in north westerly winds over the continental shelf along the west coast of South Africa prior to the arrival of the front. After the

front has passed the wind direction rotated in an anticlockwise manner, termed "backing", to south westerly.

The vorticity analysis done showed that values of wind stress curl are slightly negative along the coast, but not particularly strong. The highest negative curl values were at the centre of the low pressure would produce an upward vertical velocity, at the base of the Ekman layer, of 10 - 11 $m.day^{-1}$. Although this value is well below that of coastal Ekman Divergence (upwelling) it is significant when considering:

(1) the wind field prior to a cold front (northerly) will tend to decrease upwelling at the coast;

(2) Ekman layer depth over the shelf is ~50m and an upward vertical velocity of 10 $m.day^{-1}$, as calculated above for the cold front, would require only five days to completely erode the thermocline;

(3) the highest value for Ekman pumping velocity (1.56 $m.day^{-1}$) associated with a ridging SAA is several orders-of-magnitude lower than that quoted above for a cold front.

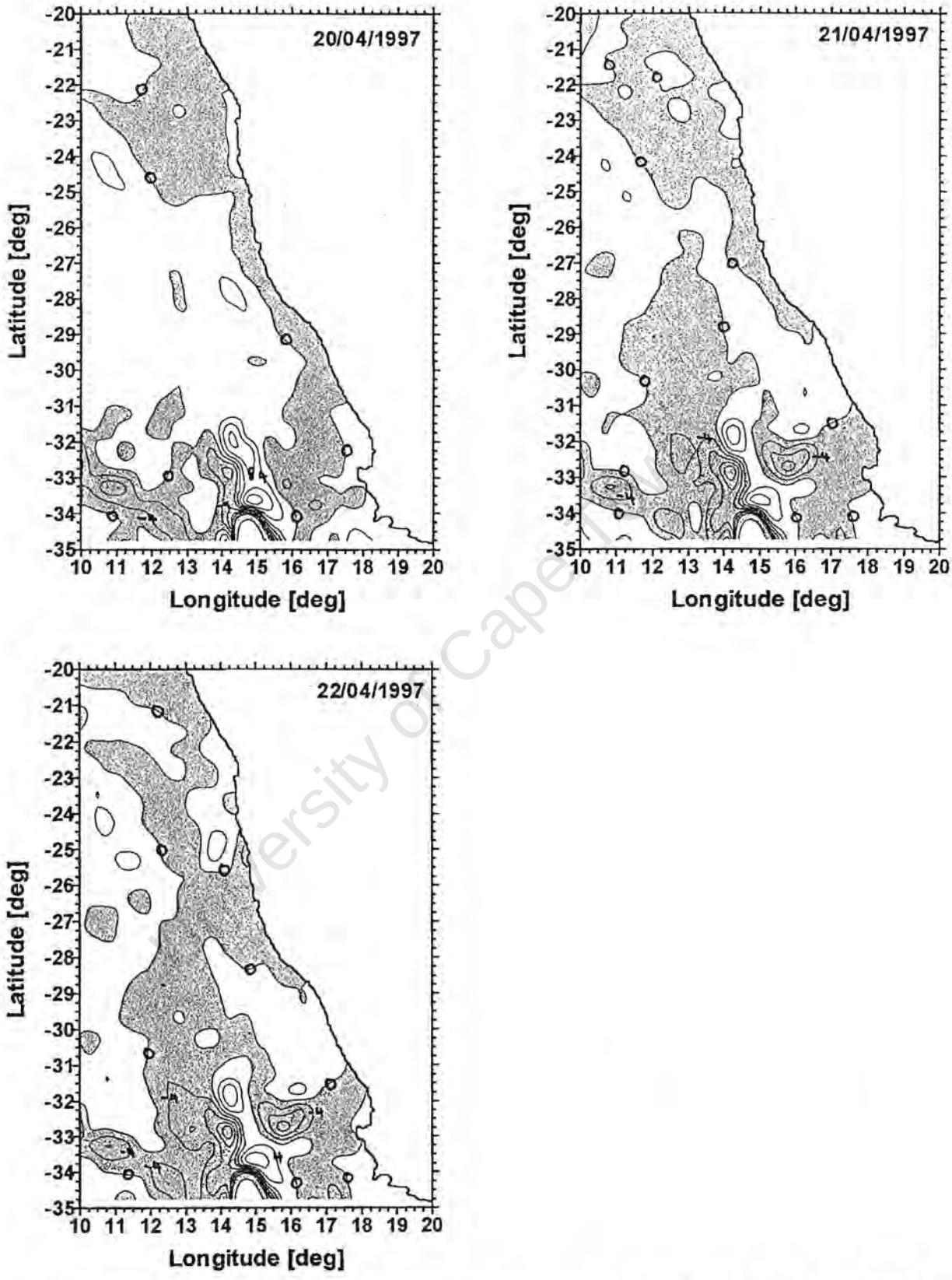

FIGURE 3.18: Three-day running mean NSCAT wind stress curl contours (Nm^{-3}) for the period 20 - 22 April 1997. The contour interval is 4×10^{-7} Nm^{-3} and the shaded area signifies negative or clockwise rotation.

Coastal Low Generation (18 - 20 December 1996, 12 - 14 April 1997)

In this section only daily averaged NSCAT data is analysed, because data averaged over a longer period smooths the wind field, thus obscuring small spatial scales. Coastal lows are transient coastal trapped systems that move at several meters per second (Reason and Jury, 1990) polewards along the west coast. Their spatial extent is much smaller than other synoptic systems found in the Benguela.

Synoptic Weather Maps (SAWB)

Figures 3.19 and 3.20 are daily weather maps produced by the SAWB for the periods 18 - 20 December 1996 and 12 - 14 April 1997, respectively. Both figures depict the development of coastal lows in the vicinity of Lüderitz (26.5°S) and/or Walvis Bay (23°S) along the coast of Namibia. Figure 3.19 shows that after the passage of a cold front on 18 December, there is a low pressure (1012 hPa) intrusion from the north along the coast of Namibia. At this time the SAA ridges behind the cold front resulting in southerly winds over the continental shelf. The highest wind speed of 50 knots was recorded at Lüderitz, which appears to be an anomaly in the area. This could possibly be due to some local enhancement. On 19 December a well-defined coastal low pressure system has formed along the coast at latitude 25°S. When considering the general alignment of vectors around the area of coastal low formation, there appears to be a tendency for winds to rotate clockwise, converging towards the centre. The only exception is the wind direction at Lüderitz, where the speed is 25 knots and direction is southerly, whereas an offshore flow is expected ahead of the coastal low. This On 20 December the 1012 hPa isobar (located at (27.5°S; 13°E)) is somewhat separated from the coast, but there is strong evidence of clockwise wind flow around the central low pressure. On this day a new cold front develops in the SE corner of the daily weather map.

Figure 3.20 shows rapid generation of coastal lows along the Namibian coast. On 12 April a large coastal low is formed between latitudes 18 - 24°S overlying a large area north and inclusive of Walvis Bay, whereas another smaller system is in the vicinity of Cape Town around the latitude-longitude coordinates (34°S, 20°E). The cyclonic wind circulation is more evident with the system around Cape Town than the one being formed at Walvis Bay. South of the country a cold front is passing followed by a ridging SAA.

On 13 April both coastal lows have propagated around the coast of southern Africa. The coastal low that was situated along the Namibian coast has moved poleward by approximately 10° of latitude and is now centred on the 32°S line of latitude. This movement implies a translation of 11 ms^{-1}, which is greater than that suggested by Jury (1988), but concurs with the statistical results of Preston-Whyte and Tyson (1973) and numerical results of Ngoc Anh and Gill (1981). The low near Cape Town propagated at a similar speed along the southern Cape coast towards Port Elizabeth.

On 14 April there is evidence of three such coastal low systems around the southern African coast. A new system has "spawned" near Walvis Bay showing clear skies before and cloudy weather behind it, illustrating the offshore and onshore flows before and after the low pressure. The system that was located along the west coast on the previous day is now situated just to the north of Cape Town, which shows some decrease in propagation speed from 11 ms^{-1} to 2.7 ms^{-1}.

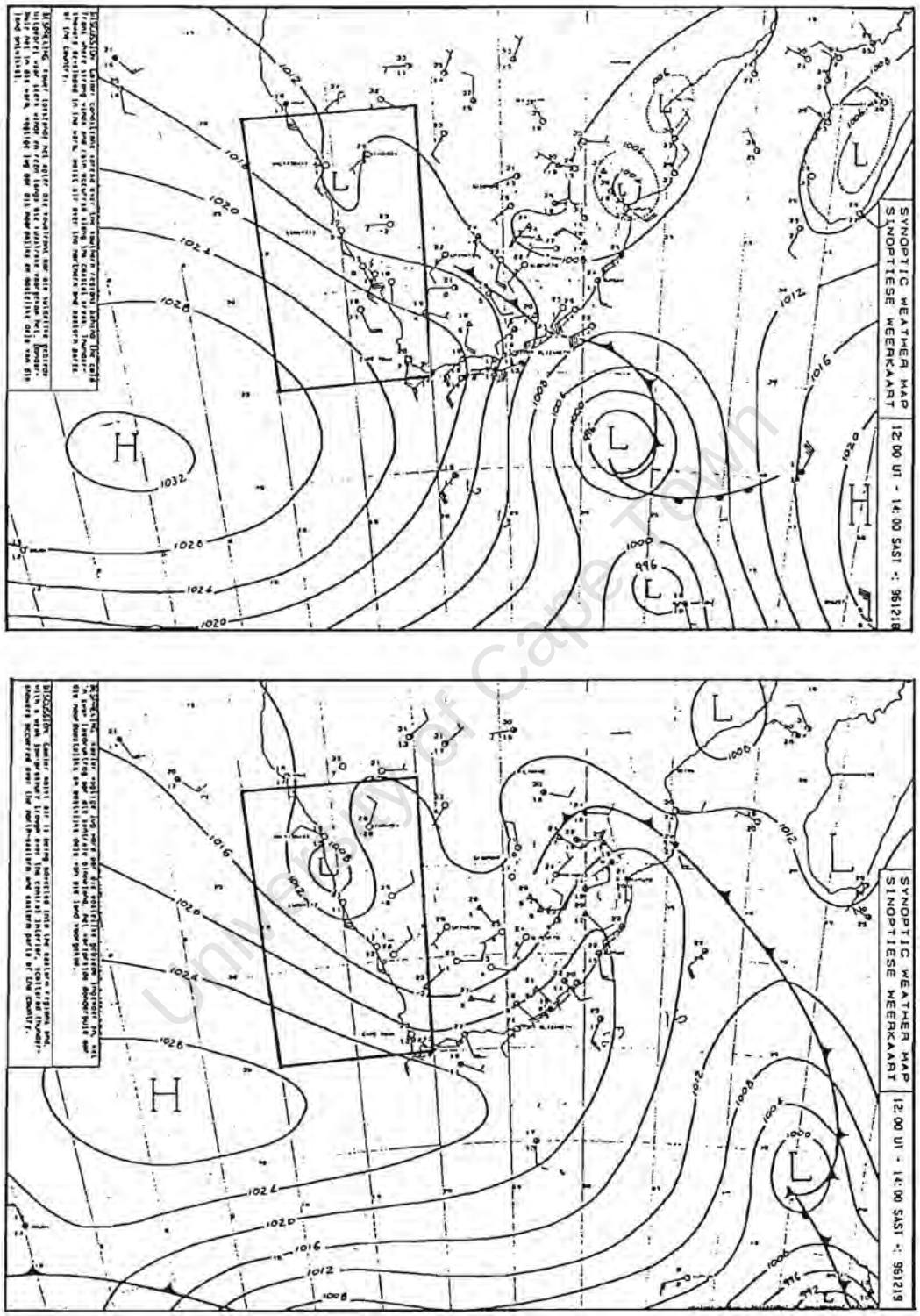

Figure 3.19: Daily synoptic weather maps produced by the South African Weather Bureau for the period 18 - 20 December 1996. During this period a coastal low formed in the vicinity of Lüderitz and propagated down the coast.

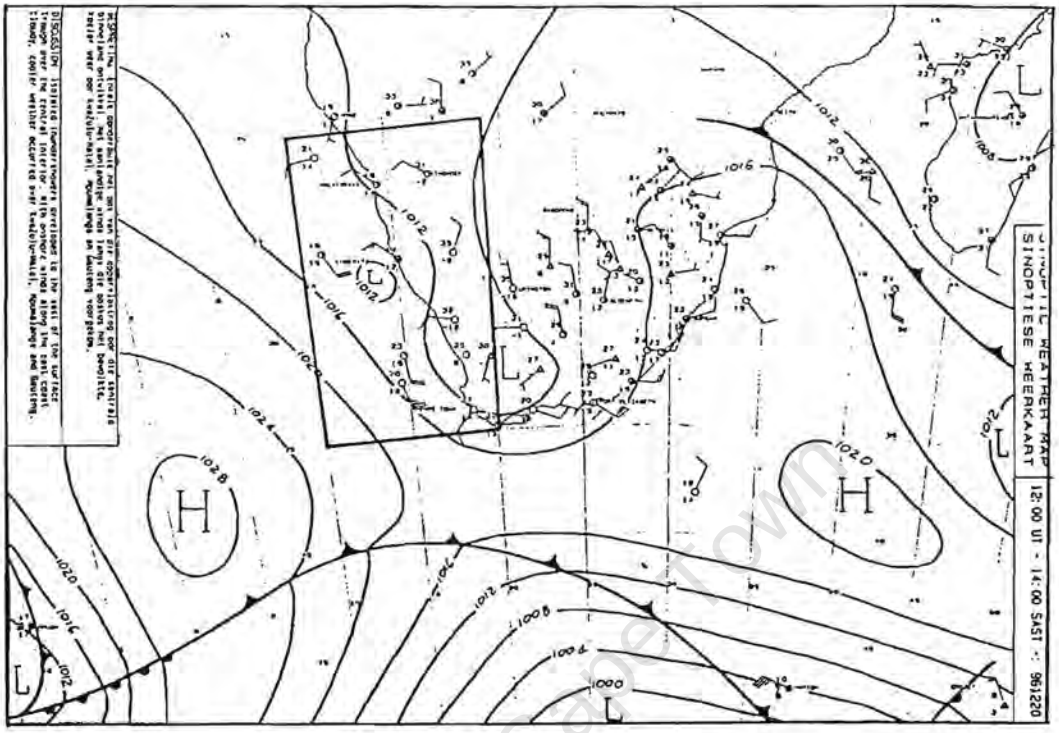

Figure 3.19: Continued .....

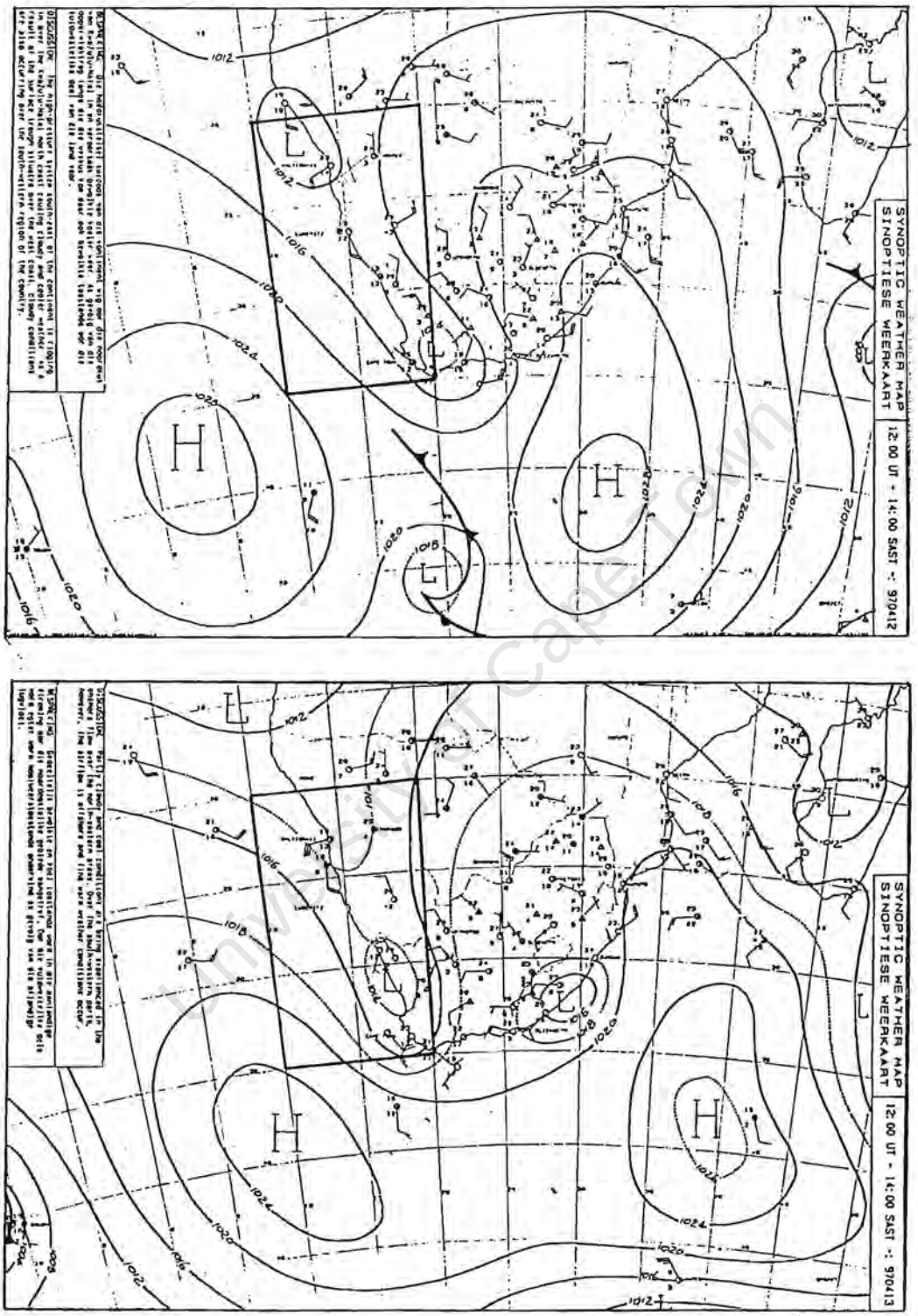

Figure 3.20: Daily synoptic weather maps produced by the South African Weather Bureau for the period 12 - 14 April 1997. During this period a coastal low formed in the vicinity of Walvis Bay and propagated down the coast.

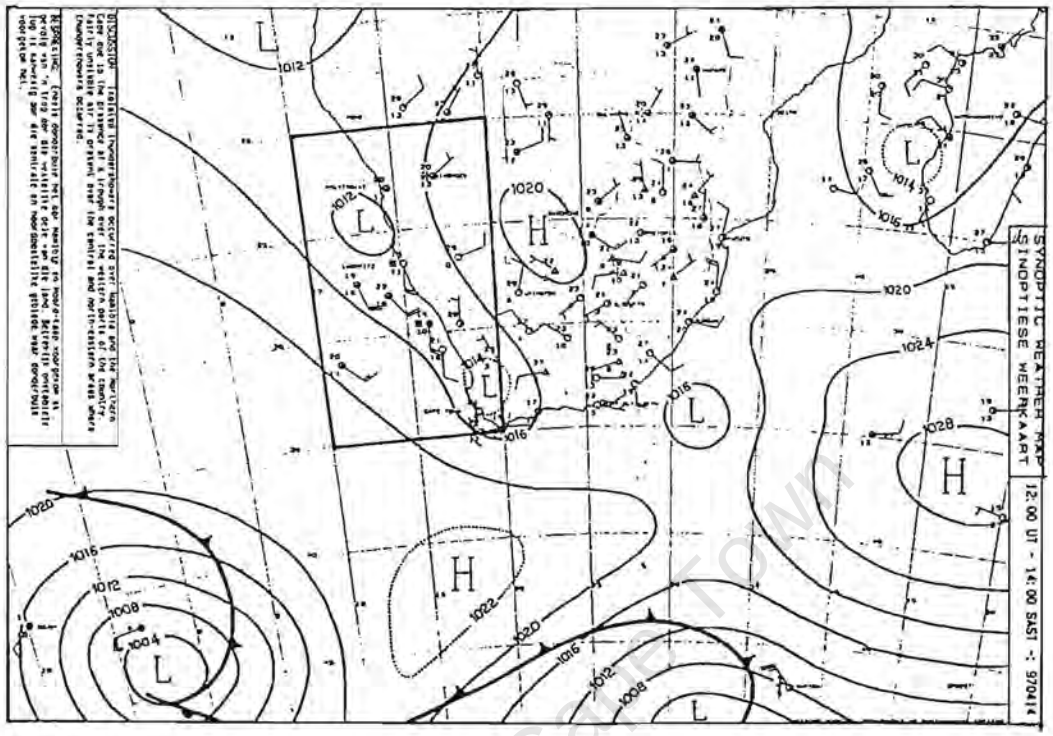

Figure 3.20: Continued .....

Daily-Averaged NSCAT Data

Figures 3.21 and 3.22 are the daily-averaged NSCAT wind vectors and wind speed isotachs, respectively for the period 18 - 20 December 1996.

On 18 December the wind field within 3° longitude from the coast shows significant topographically induced flow, especially between 23 - 29°S (Figure 3.21). The flow in this region shows rather strong cyclonic curvature, with eventual onshore flow near Walvis Bay. This large cyclonic curvature of wind could be due to the formation of a coastal low as was shown in the SAWB daily synoptic charts in Figure 3.19. Isotach data (Figure 3.22) along the protruding coastline of Namibia indicate some degree of accelerating airflow. Offshore of this region of cyclonic flow, the wind field is very uniform with wind speeds as high as 16 ms^{-1} located offshore from Lüderitz. To the north of this wind speed maximum there is a gradual decrease in values to 11 ms^{-1} between latitudes 21°S and 22°S. A minimum wind speed value of 6 ms^{-1} is located to the north of St Helena Bay.

On 19 December there is a region of cyclonic circulation, marking the coastal low, in the area of Walvis Bay. It is estimated that the latitudinal-longitudinal dimensions of the system are 330 km and 440 km, respectively. There is a strong isotach gradient (Figure 3.22), of 5 ms^{-1} over a distance of 110 km, between the coastal low pressure system and the adjacent region and the position of this gradient is consistent with the SAWB chart for this time. The adjacent region also shows a strong and narrow equatorward flow of 11-12 ms^{-1} parallel to the coast and around the seaward side of the coastal low. Unfortunately, the data on 20 December is missing from the area that the coastal low was likely to have propagated to.

It was shown earlier from the SEWB synoptic charts that a number of coastal lows were generated along the Namibian coast, propagating poleward along the coastline during the period 12 - 14 April 1997 (Figure 3.20). Figures 3.23 and 3.24 show daily-averaged NSCAT vectors and wind speed isotachs for this period. On 12 April the daily NSCAT isotachs show wind speeds of

6 - 7 ms^{-1} around Lüderitz between the latitudes 26 - 30°S, but little spatial structure suggesting a coastal low. South of Lüderitz, wind speeds increase to a maximum of 10 ms^{-1} centred on the coordinates (32°S; 16°E). On this day, winds were fairly strong and consistently from the south over most of the region. The only exception is the onshore flow along the west coast near 29°S.

On 13 April there is evidence of another isolated area of cyclonic air flow developing along the Namibian coast between 24 - 28°S. The offshore extent of this cyclonic system is approximately 230 km from the coast. It appears that this coastal low is much larger in areal extent than the one previously discussed, which is in partial agreement with the SAWB daily weather bulletin. Compared with the situation for 19th December 1996, a similar scenario, of strong winds offshore (8 - 10 ms^{-1}) and around this centre of low cyclonic winds (5 ms^{-1}) exists. The SAWB daily weather bulletin (Figure 3.20) showed rapid formation and southward propagation of the coastal low from one day to the next. Although there is a slight indication of another coastal low forming on 14 April (Figure 3.24) around 24°S, it is not conclusive due to a lack of data. There is no indication of the poleward propagating coastal low pressure system along the west coast of South Africa as was shown in Figure 3.20. This could be ascribed to (1) the possibility that coastal lows become smaller in spatial extent as they propagate around the coast and (2) the escarpment that traps them is situated more inland as it approaches the capes, thus steering the synoptic system more over the land. This has the implication that the part of the coastal low over the shelf would be contained within the area where there is no NSCAT data (0.5 - 1° away from the coast).

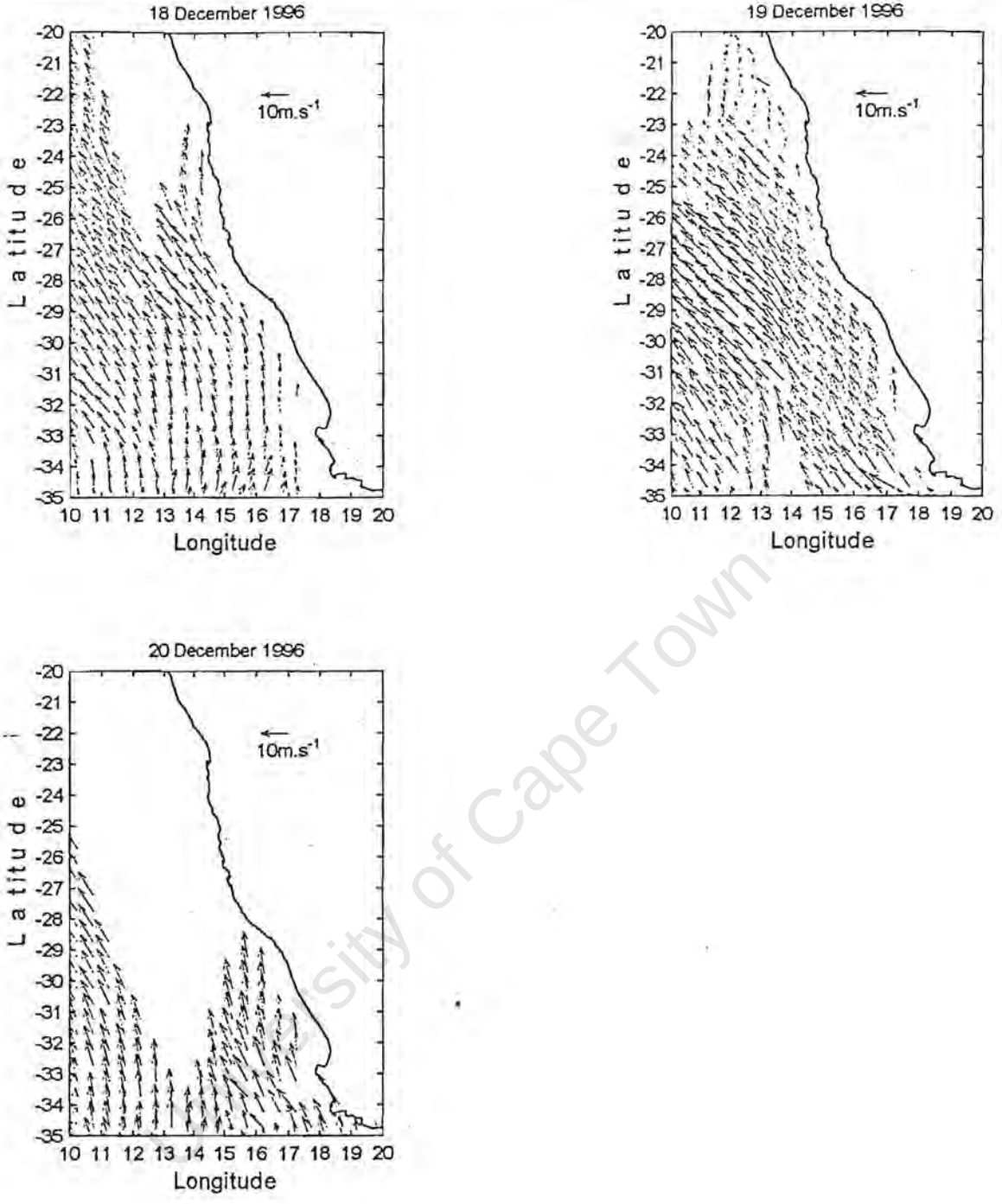

FIGURE 3.21: Daily-averaged NSCAT wind vectors for the period 18 - 20 December 1996. The reference vector is given in the upper right-hand side of the figure.

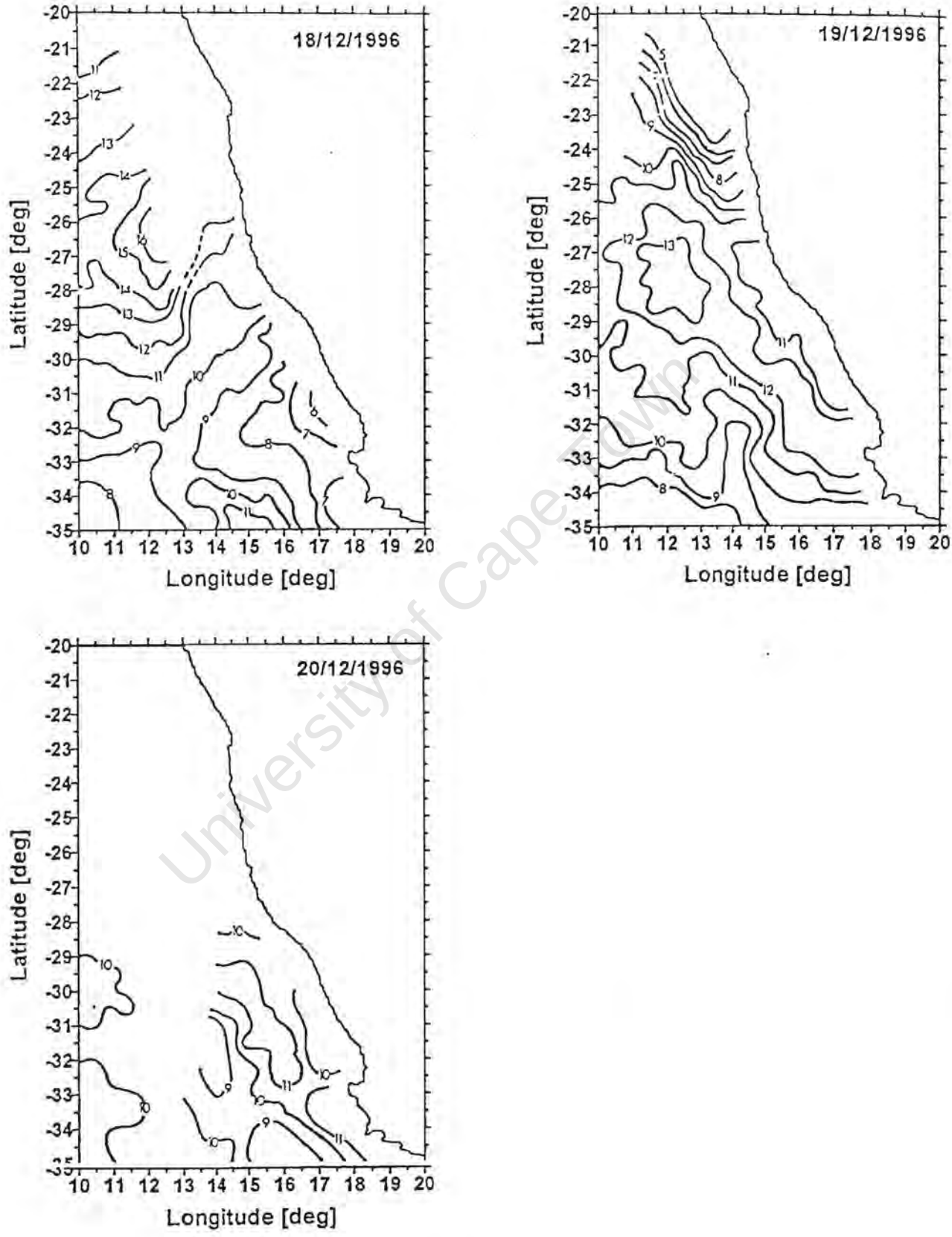

FIGURE 3.22: Daily-averaged NSCAT wind speed isotachs (ms^{-1}) for the period 18 - 20 December 1996. The contour interval is 1 ms^{-1}.

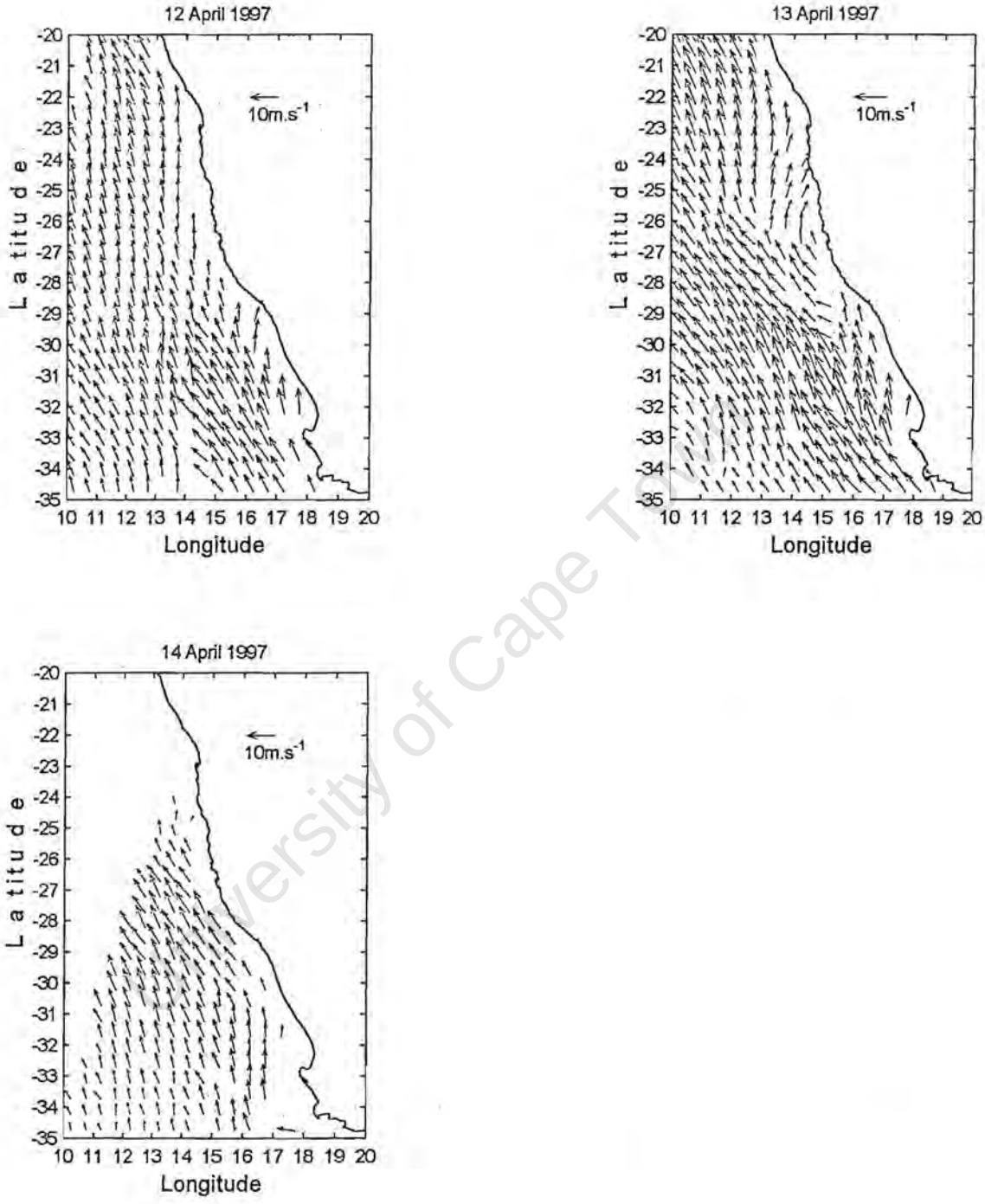

Figure 3.23: Daily-averaged NSCAT wind vectors for the period 12 - 14 April 1997. The reference vector is given in the upper right-hand side of the figure.

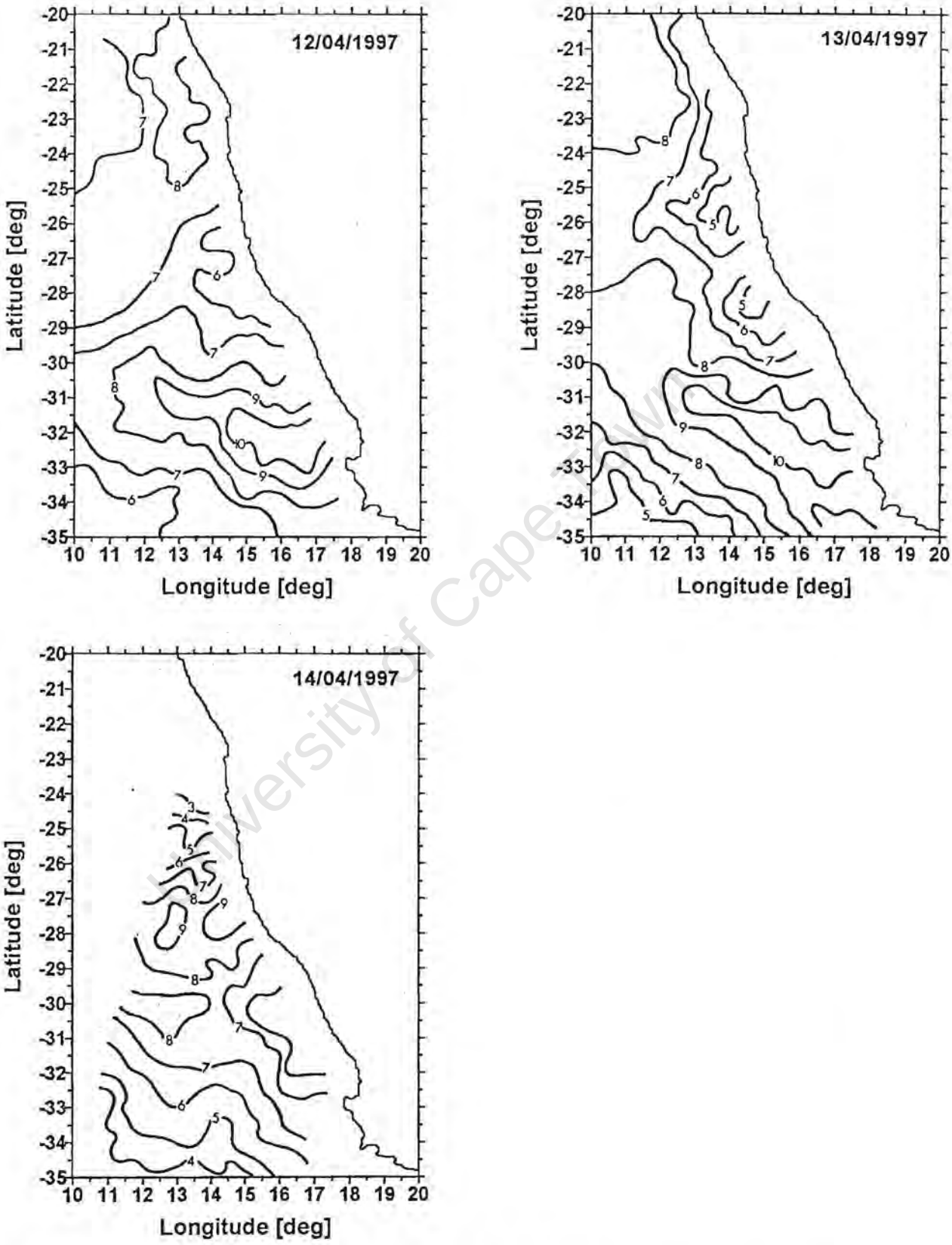

Figure 3.24: Daily-averaged NSCAT wind speed isotachs (ms^{-1}) for the period 12 - 14 April 1997. The contour interval is 1 ms^{-1}.

Summary

It appears that NSCAT was able to capture the formation of coastal lows on both the above occasions. The systems were formed along the Namibian coast around Lüderitz and Walvis Bay, which are both situated on a large bulge in the coastline between the latitudes 22 - 29°S. There appears to be a size differentiation between the coastal low formed around Lüderitz compared to that near Walvis Bay. The coastal low formed near Lüderitz was much larger, almost double in size, than the one near Walvis Bay. More data is required for further validation of these concepts.

A generally accepted theory to explain the formation of coastal lows was proposed by Gill (1977). He suggested that coastal lows are essentially atmospheric Kelvin waves, generated by interaction of the synoptic scale wind systems with the topography. Although this is beyond the scope of the present study, the formation of coastal lows observed from NSCAT appears to be linked to the strength (~10 ms^{-1}) and direction of the offshore wind field. There is obviously some association between this propagating synoptic scale wave and its influence on the winds along the west coast, but this is not addressed in this study. The generation of the coastal low starts with clockwise rotation of wind around a centre located somewhat or completely over the land. This clockwise rotation could be attributed to two distinct possibilities:

(1) the synoptic scale atmospheric waves interacting with the interior escarpment or

(2) the topography between latitudes 22 - 29°S causing some wake-effect. The wake position is dependent on the general direction of the stronger offshore flow. Because of this wake, air is drawn from the coastal plain resulting in a clockwise rotation of air around a central low pressure system.

OVERVIEW OF RESULTS IN CHAPTER 3

Chapter 3 investigated wind field dynamics linked to a range of synoptic atmospheric systems affecting the weather over southern Africa. Daily NSCAT wind data were used in conjunction with a three-day running mean filtered time series composite in order to gain maximum benefit from the satellite derived synoptic wind field. The analysis revealed the following:

- High southerly wind speeds are associated with the South Atlantic Anticyclone (SAA) at Lüderitz and Cape Columbine (~13 ms^{-1}). During the ridging process of the SAA, wind speeds increase along an area nearly parallel to the west coast. Wind direction around the southern part of the Cape Peninsula changes from southerly to easterly at the same time as the increase in wind speeds. This gives a unique negative wind stress curl configuration that runs parallel to the west coast from the Cape Peninsula-Cape Columbine area to the north and extending beyond the northern border of the study region. The vertical velocities calculated from the wind stress curl and wind stress revealed that the spatial structure in the wind field plays a near-insignificant role in the upwelling process at the coast. Vertical velocities due to wind curl were two to three orders of magnitude smaller than that produced by Ekman coastal divergence.
- The west coast trough was found to be responsible for decreasing wind speeds over the entire continental shelf along the west coast of southern Africa. The effect reached an offshore distance of approximately 120 nmiles (~220 km). Wind speeds associated with west coast troughs were from 1 - 8 ms^{-1} and wind directions were inconsistent and often converging or diverging. The convergence and divergence in the wind field during west coast troughs can be ascribed to a problem in the NSCAT data collection process as the scatterometer was unable to

accurately estimate wind direction for speeds under 2 ms^{-1}. Negative wind curl was also associated with the western "boundary" of the west coast trough, but with its propagation southward it appeared to force the negative curl area further offshore as the low pressure trough continued to occupy the shelf.

- It was found that cold fronts did not influence the Benguela region north of 28°S, agreeing with Shannon and Nelson (1996). The vorticity associated with the central low pressure of the cold front would produce an upward vertical velocity of ~11 $m.day^{-1}$. This is significant especially in light of the fact that average thermocline depth along the west coast is 50m during summer. This could help to explain why there is thermocline erosion during the passage of a cold front.
- NSCAT data can be used to resolve the formation of a coastal low along the coast of Namibia. Two areas of formation were observed: the first being Lüderitz and the second, Walvis Bay. The average offshore extent appeared to be approximately 250 km from the coast. The southward propagation of the coastal low signal was not seen in NSCAT data, but this was attributed to a problem with the lack of data in the area close the coast.

Chapter 4

This chapter describes the atmospheric and consequent oceanic dynamics prior to and during the largest rock lobster stranding event at Elands Bay. Cockcroft *et al.* (1999) showed that 1500 tonnes of Rock Lobster were stranded in and around Elands Bay between 5 - 8 April 1997. A longer period from 25 March to 10 April 1997 is investigated, using daily and three-day running mean NSCAT wind data to link the rock lobster strandings to unusual environmental forcing. It is hypothesised that west coast atmospheric pressure troughs are crucial elements in setting the scene for red tide formation and subsequent rock lobster mortality events.

INTRODUCTION

For the analysis in this chapter, a low wind event will be defined as one when the wind speed $\leq 5\ ms^{-1}$ (~ 10 knots) along a large area of the west coast of South Africa; persisting for longer than three to four days. This criterion was based on a preliminary study, not included here, of daily weather maps from 1 December 1996 to 31 May 1997. The NSCAT data plots containing vectors and wind speed isotachs in this chapter extend from the latitude 20°S to beyond the Cape Peninsula (35°S). The area concerned with rock lobster mortality events is confined to a small section along the South African coast near Elands Bay (~32.5°S). The large area analysis was done in order to describe the advection of atmospheric systems, such as the west coast low pressure trough and coastal lows. These systems propagate from the north, resulting in low wind speeds over the relevant shelf zone (Pitcher *et al.*, 1995). Daily NSCAT winds are used to qualitatively describe the wind field as it changes from day-to-day in conjunction with daily weather maps produced by the South African Weather Bureau (SAWB). It is also recognised that the wind is only one part of a multi-faceted process that lead to rock lobster stranding events.

DAILY NSCAT WINDS AND SYNOPTIC WEATHER CHARTS (25 MARCH - 10 APRIL 1997)

A preliminary study of daily weather charts, mentioned earlier, from December 1996 to May 1997 showed extended periods of low wind occurring episodically. On average the low wind periods lasted from three or four days to beyond one week. The period under investigation is associated with one such event from its origin on 27 March up to its conclusion on 5 April 1997, i.e. nine consecutive days in total. Figures 4.1 and 4.2 show a series of daily weather charts (SAWB) and NSCAT wind vectors, respectively for the period 25 March - 10 April 1997. This

time period includes the largest rock lobster mortality event of 1500 tons that occurred between 5 - 8 April at Elands Bay as recorded by Cockcroft *et al.* (1999).

On 25 March what appears to be a coastal low forms in the vicinity of Lüderitz (Figure 4.1), along the coast of Namibia. The SAA ridges to the south of the country following the passage of a cold front. Wind speeds range from 5 knots (~2 ms^{-1}) at Port Nolloth to 40 knots (~20 ms^{-1}) at Lüderitz. Wind direction is principally from the south. The daily NSCAT wind vectors for 25 March (Figure 4.2) show a distinct difference between the shelf and offshore regions roughly separated from each other at a distance of ~220 km from the coastline. Wind vectors offshore are tightly aligned along a NW-SE orientation compared to a southerly orientation of vectors over the shelf. There is no evidence in daily NSCAT data of a coastal low forming in the vicinity of Lüderitz.

On 26 March a second coastal low is formed between Lüderitz and Walvis Bay (Figure 4.1), whereas the one formed the previous day has propagated poleward over a distance of approximately 330 km. The 1014 and 1016 hPa isobars appear to enclose both coastal lows and the configuration resembles that of a west coast trough of low pressure. At this time the SAA ridges further eastward increasing the pressure gradient between itself and the more southerly coastal low. As a result there is a ship measured wind speed of 35 knots (~17 ms^{-1}) approximately 750 km to the west of Cape Town. Wind speeds recorded along the South African west coast are relatively moderate ranging from 10 knots (~5 ms^{-1}) at Cape Town and Port Nolloth to 20 knots (~10 ms^{-1}) west of Cape Columbine, but wind direction remains southerly.

The daily NSCAT wind vectors for 26 March (Figure 4.2) clearly shows the eastward advance of the SAA as it ridges south of South Africa. It results in wind speed increasing as shown by wind vectors around Cape Peninsula from 25 to 26 March, but wind direction also changes from southerly to more easterly. Northward of Cape Columbine the distinct difference in wind vectors between the offshore and coastal regions still exist. It appears that the tight offshore wind vectors are aligned along the 1018 hPa isobars between the ridging SAA and the coastal

lows. Subsequently as the SAA ridges further eastward and around the southern tip of the continent, the region of offshore wind vectors move along with it. This causes the coastal region to expand to the west. Most of the coastal wind vectors show a slight onshore flow resulting in a zone of divergence separating it from the offshore area blowing north westward.

The 27th of March marks the start of the low wind conditions, as defined earlier. Figure 4.1 shows that the double coastal low pressure configuration enclosed by the 1016 hPa isobar is well established on this day. Wind speeds along the coast are mainly 10 knots (~5 ms^{-1}). The wind direction appears to vary from station to station (on 27 March) along the coast of the entire study region, but over the South African continental shelf it remains mostly from the south. The low wind conditions remain along the South African west coast up to 5 April 1997, 10 days of wind speeds of ≤15 knots or 7 ms^{-1}.

During the entire low wind period there only appears to be changes in wind direction when a cold front or ridging SAA influences the west coast shelf wind circulation. When a cold front moves over the study area from west to east, southerly winds become north westerly for a short period of time (± 1 day). Two cold fronts that caused changes in wind direction are shown in Figure 4.1 between 29 March and 1 April. Coincident with this four day window (29/3 - 1/4) the position of an anticyclone is anomalously further south than previously seen the dissertation. Between 29 March and 1 April, the anticyclone was situated between latitudes 40 - 50°S. In conjunction with the clockwise rotation of winds along the cold fronts, it produced onshore wind flow over the continental shelf south of ~30°S. A cold front on 5 April marks the end of the low wind period. A ridging SAA causes wind direction to change from southerly to more easterly, but this effect appears to be confined to air circulation around the Cape Peninsula-Cape Columbine area and further south. The first ridging SAA during the study period occurred between 6 - 7 April, after the passing of the cold front on 5 April 1997.

The daily NSCAT wind vectors for the period 25 March to 10 April are given in Figure 4.2. The start of the low wind conditions are not shown in the daily NSCAT data on 27 March

due to a lack of measurements over the continental shelf. Lack of data along the coast is also problematic for 31 March and 3 April. Low wind speeds are clearly seen in the daily spatial time series along the South African coast between 27 March and 5 April. In addition, wind vectors over the continental shelf are inconsistently aligned from one day to the next. This could be an artifact of NSCAT data due to the scatterometer being unable to record reliable wind directions at very low wind speeds (≤ 2 ms^{-1}). Even with this problem in the data, the correspondence of NSCAT wind vectors with daily weather charts (Figure 4.1) is good as the period of low wind over the shelf is well defined in daily NSCAT data. The spatial extent of low wind during this period is much greater than that expected from an analysis of the daily weather maps.

On 4 April (Figure 4.2) the approach of a cold front is evident in the vector direction south of 30°S which appears as a sinusoidal wave-like pattern west of South Africa. This results in an onshore wind direction over the continental shelf that continues on 5 April. Hereafter there appears to be a short period (6 - 8 April) of consistent southerly winds associated with an SAA, which would be ideal for upwelling to commence. On 9 April a low wind event appears north of 28°S along the Namibian coast, which propagates poleward and reaching ~30°S on 10 April. The cold front, ridging SAA and commencement of a second low wind period as described earlier from daily weather maps is also present in the daily NSCAT data.

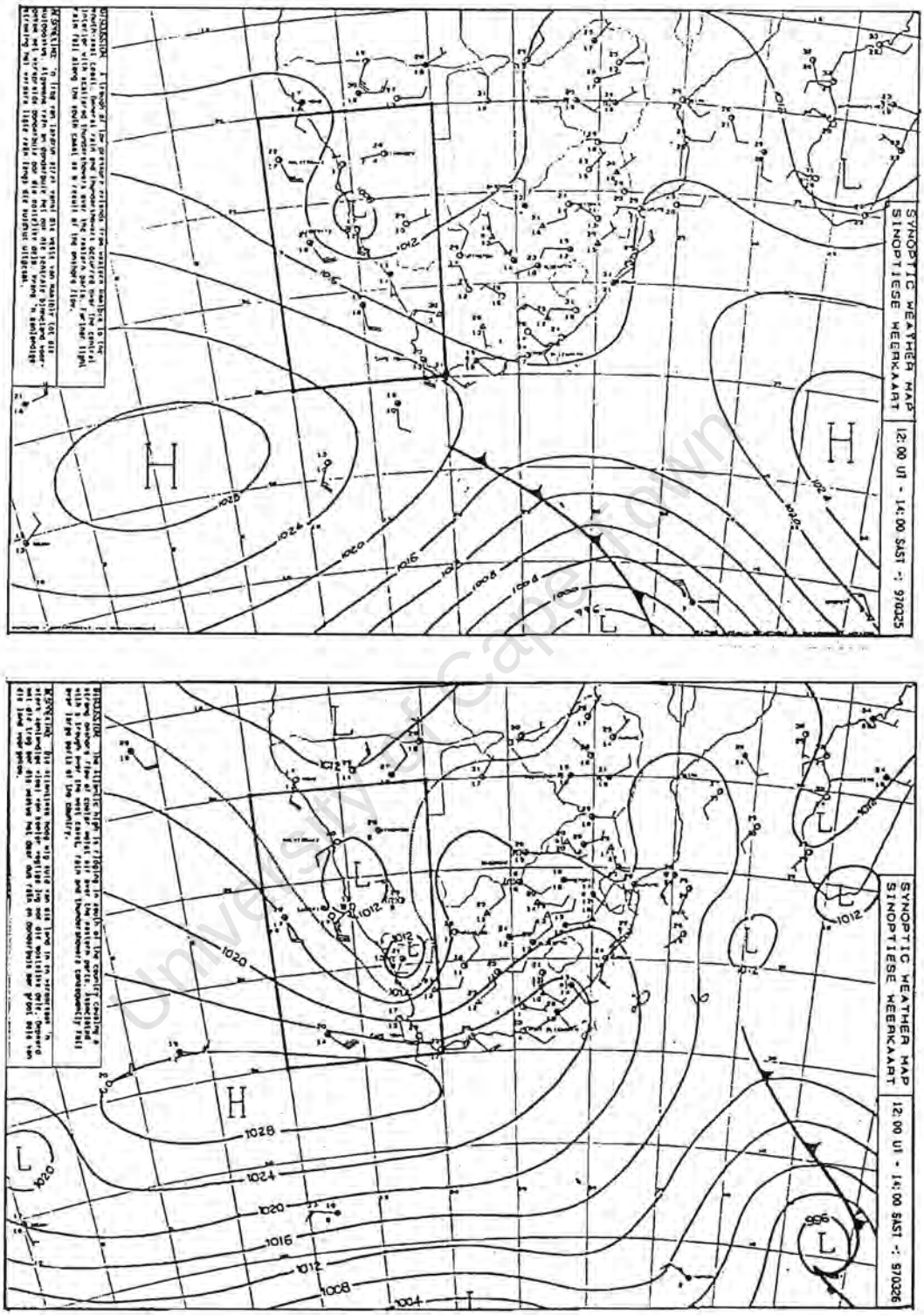

Figure 4.1: Daily synoptic weather maps produced by the South African Weather Bureau for the period 25 March to 10 April 1997. This period was selected as a result of the long quiescent phase in the wind due to low pressure trough formation.

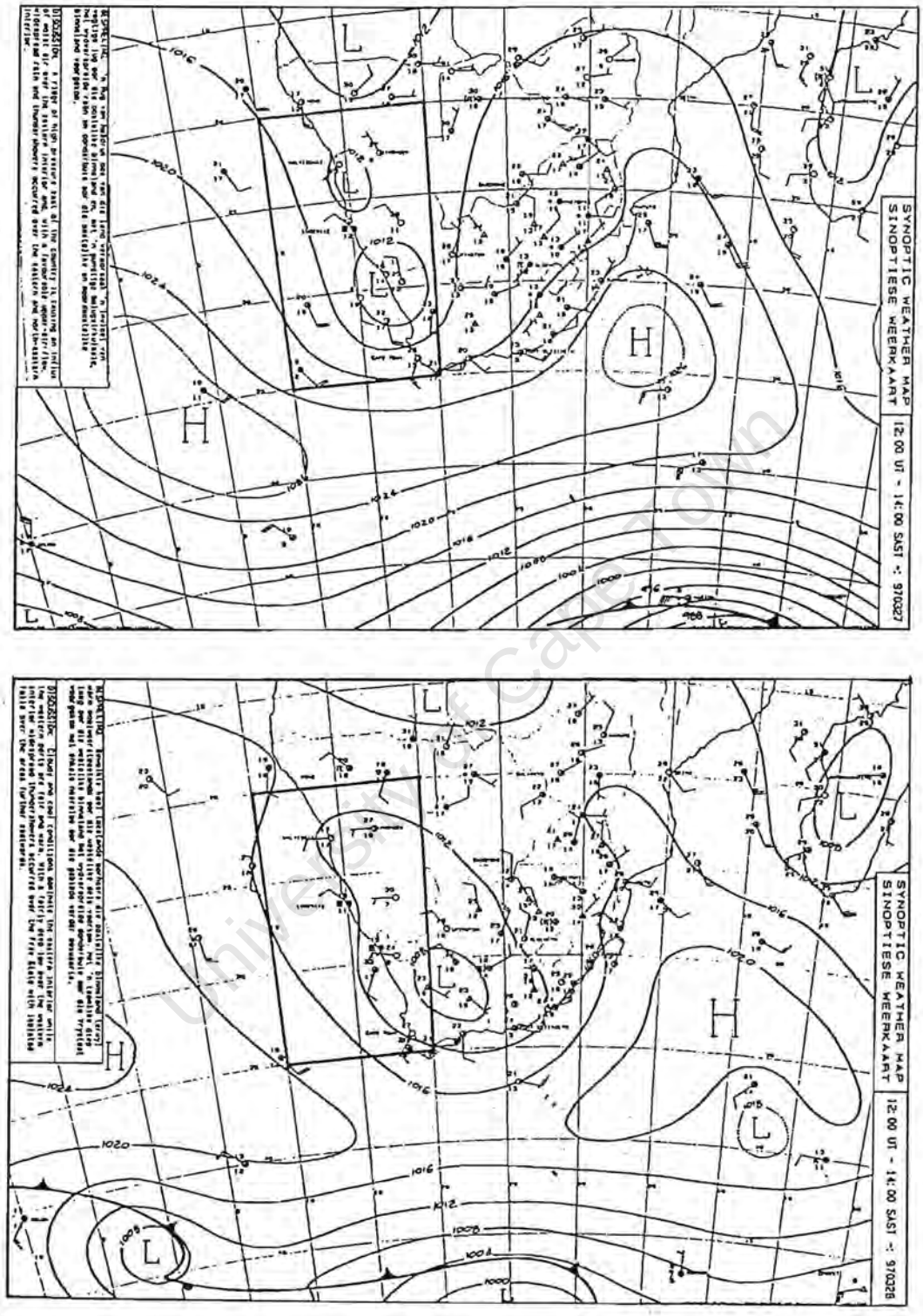

Figure 4.1: Continued .....

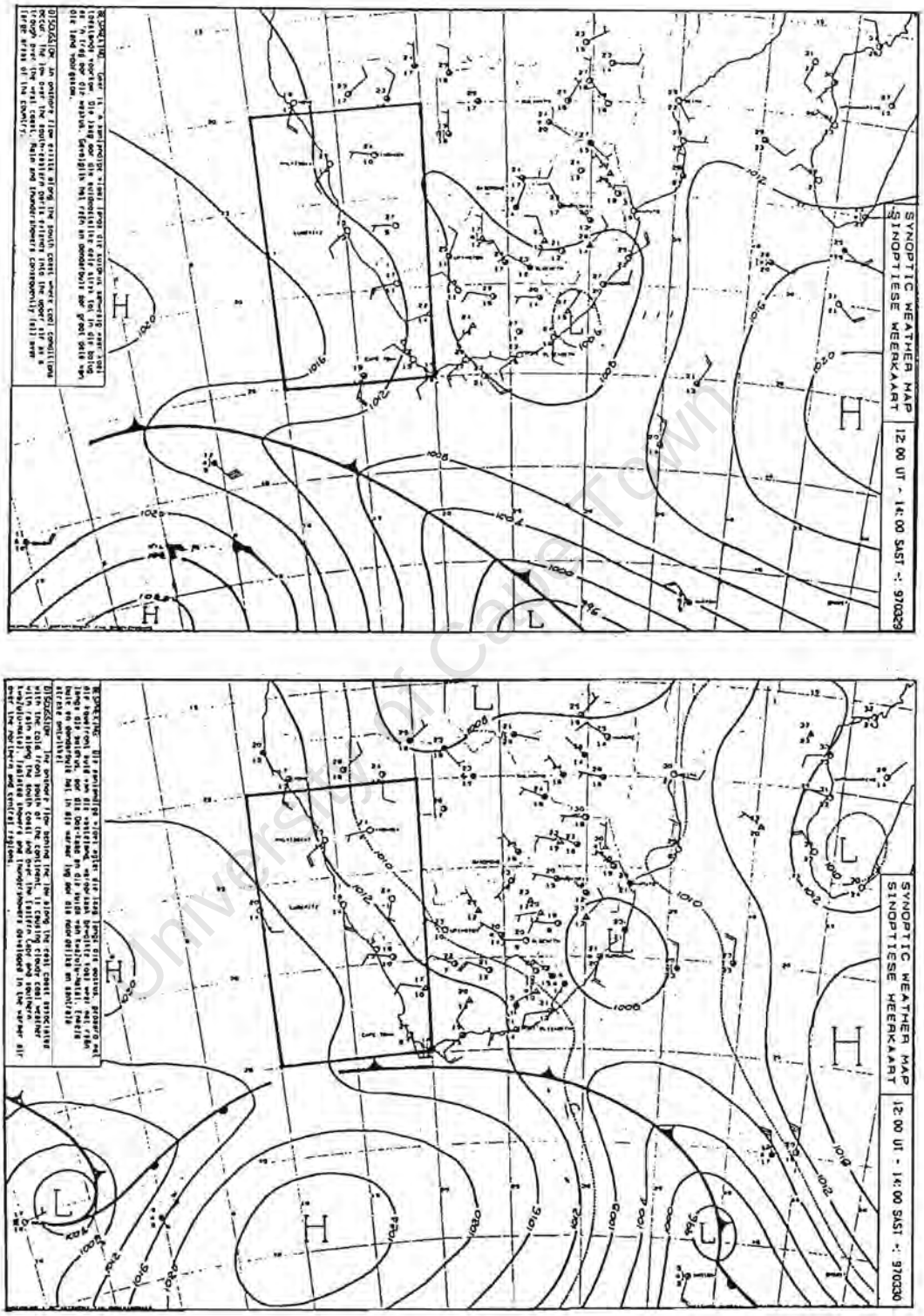

Figure 4.1: Continued .....

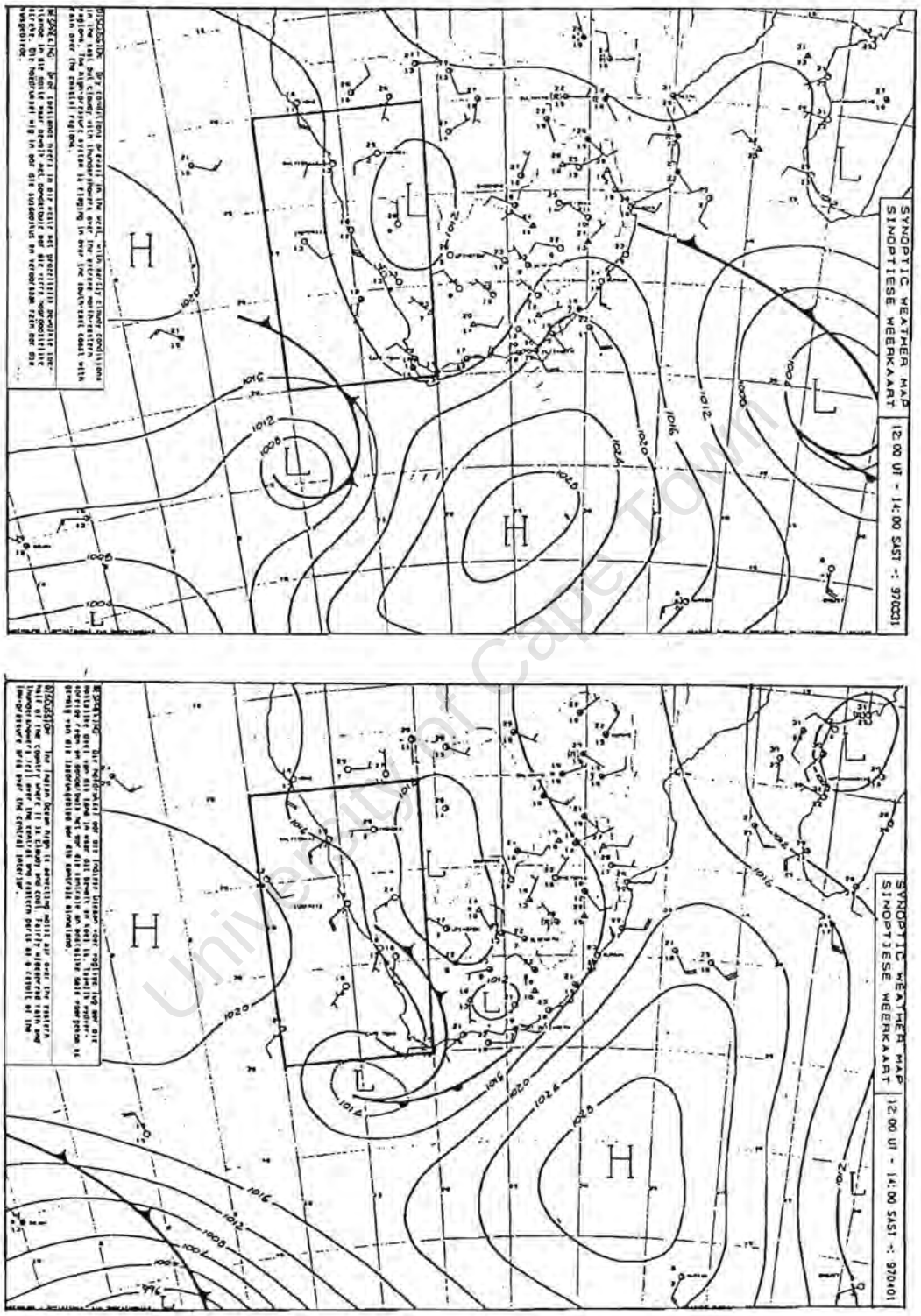

Figure 4.1: Continued .....

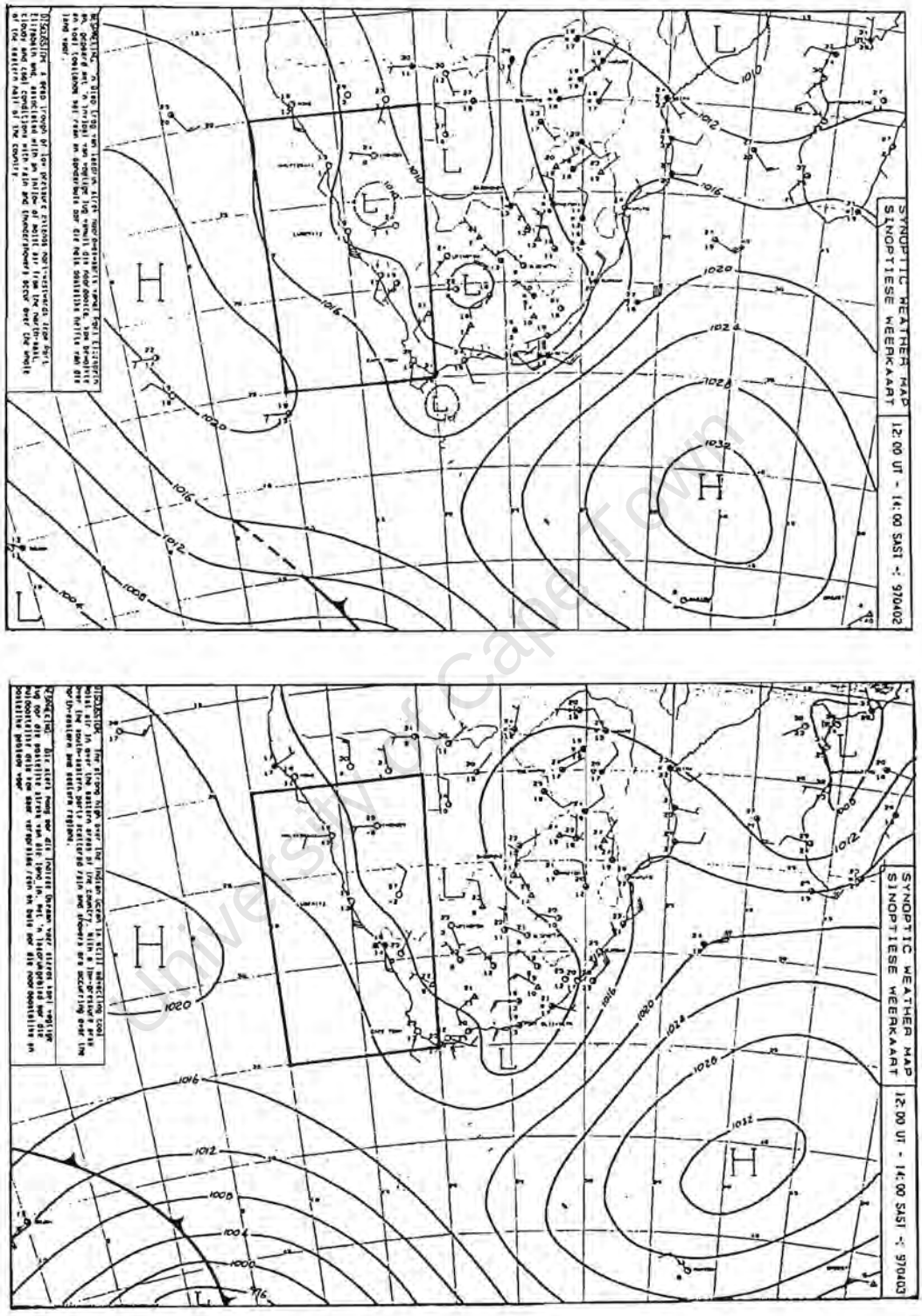

Figure 4.1: Continued .....

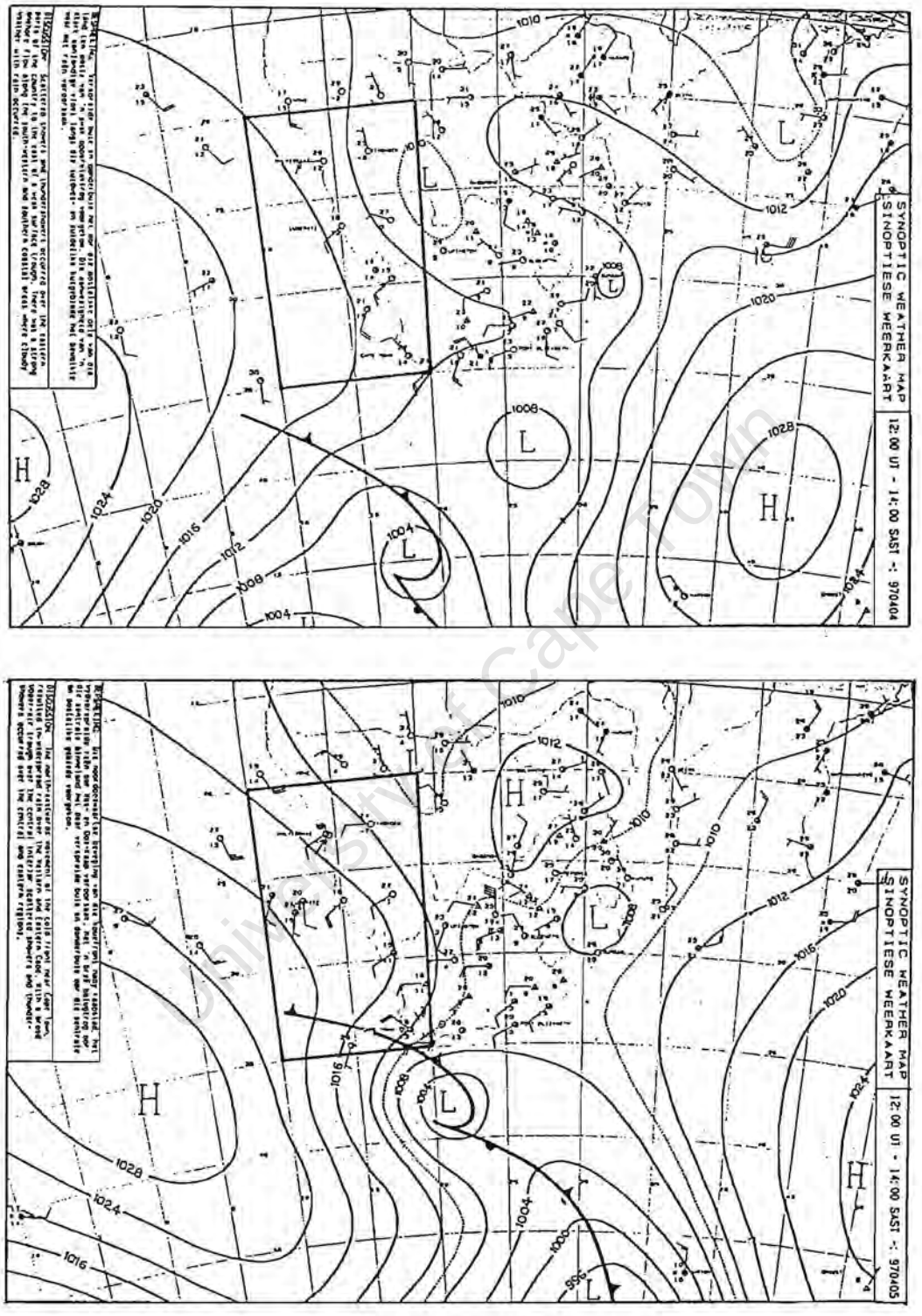

Figure 4.1: Continued .....

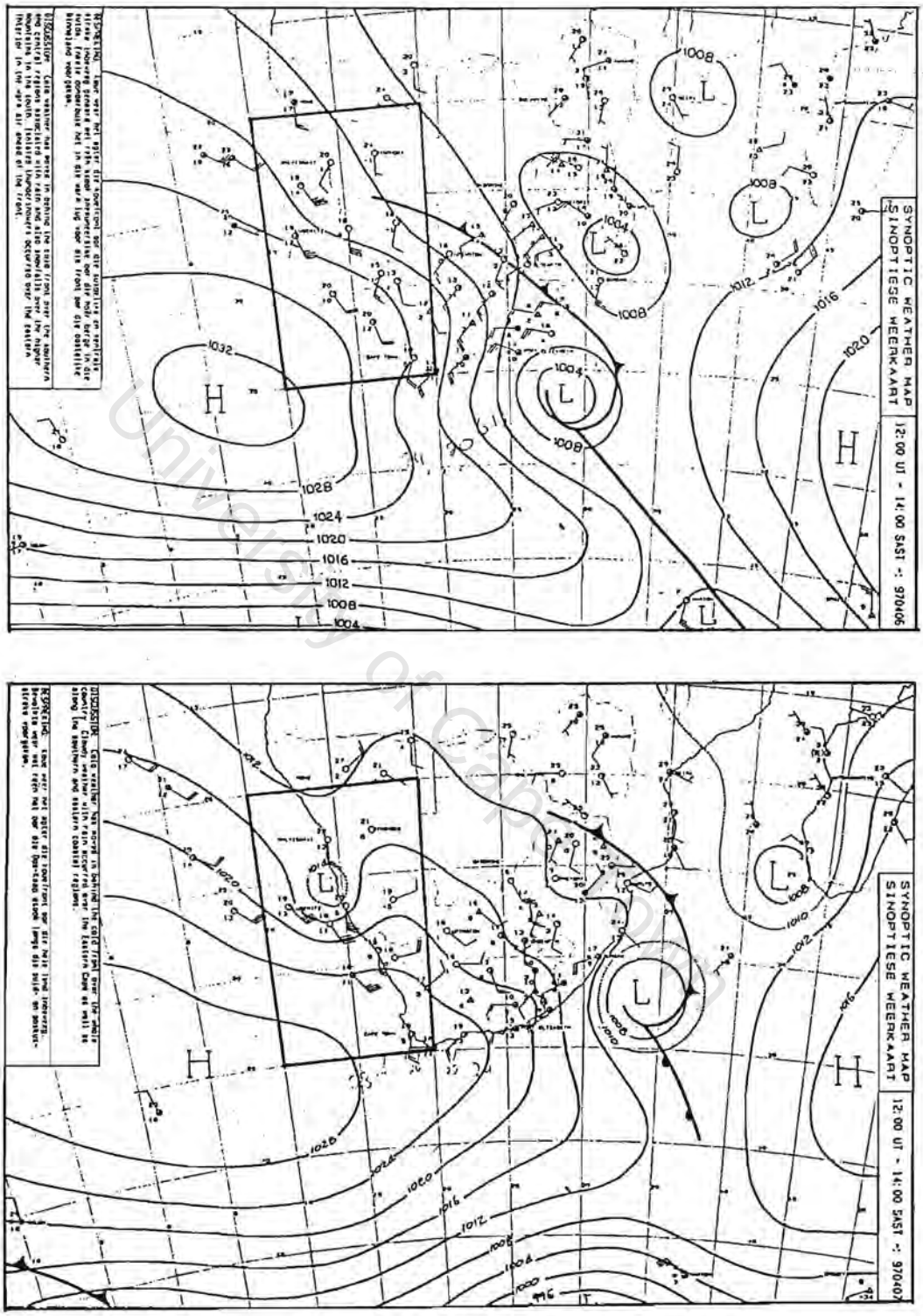

Figure 4.1: Continued .....

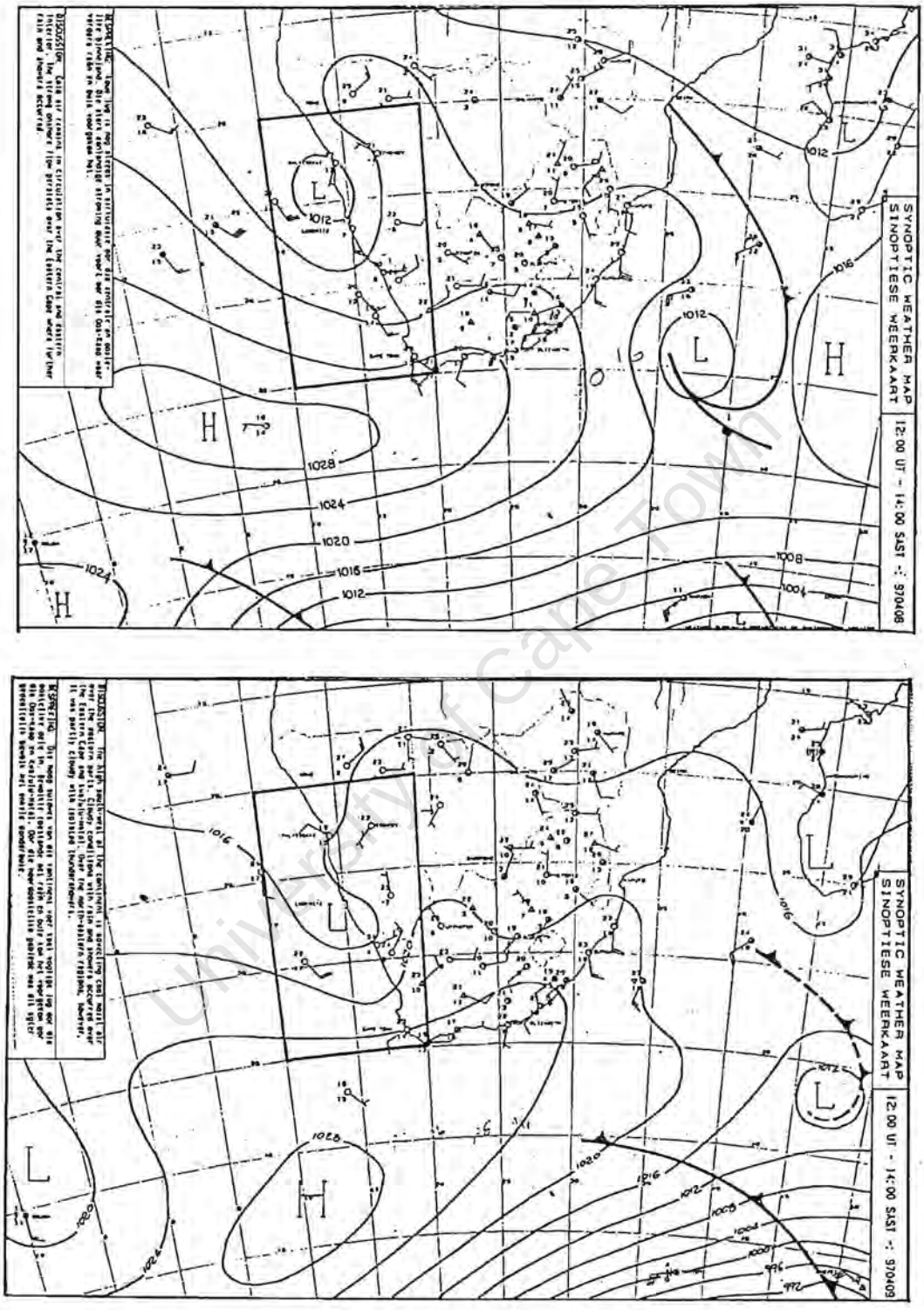

Figure 4.1: Continued .....

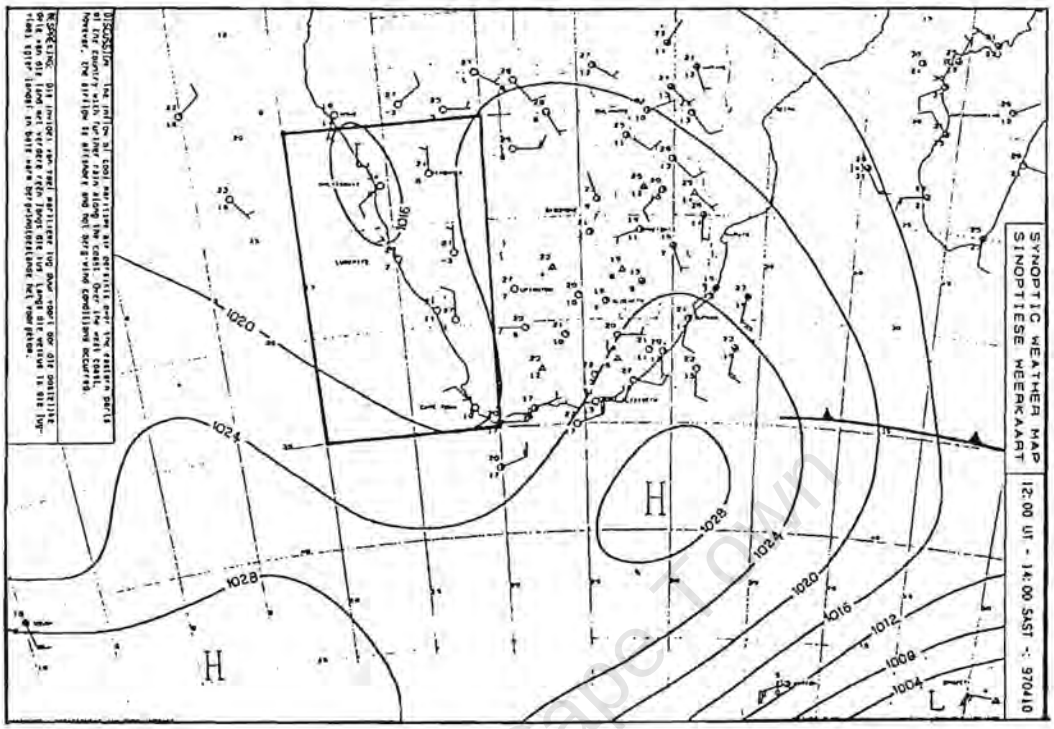

Figure 4.1: Continued .....

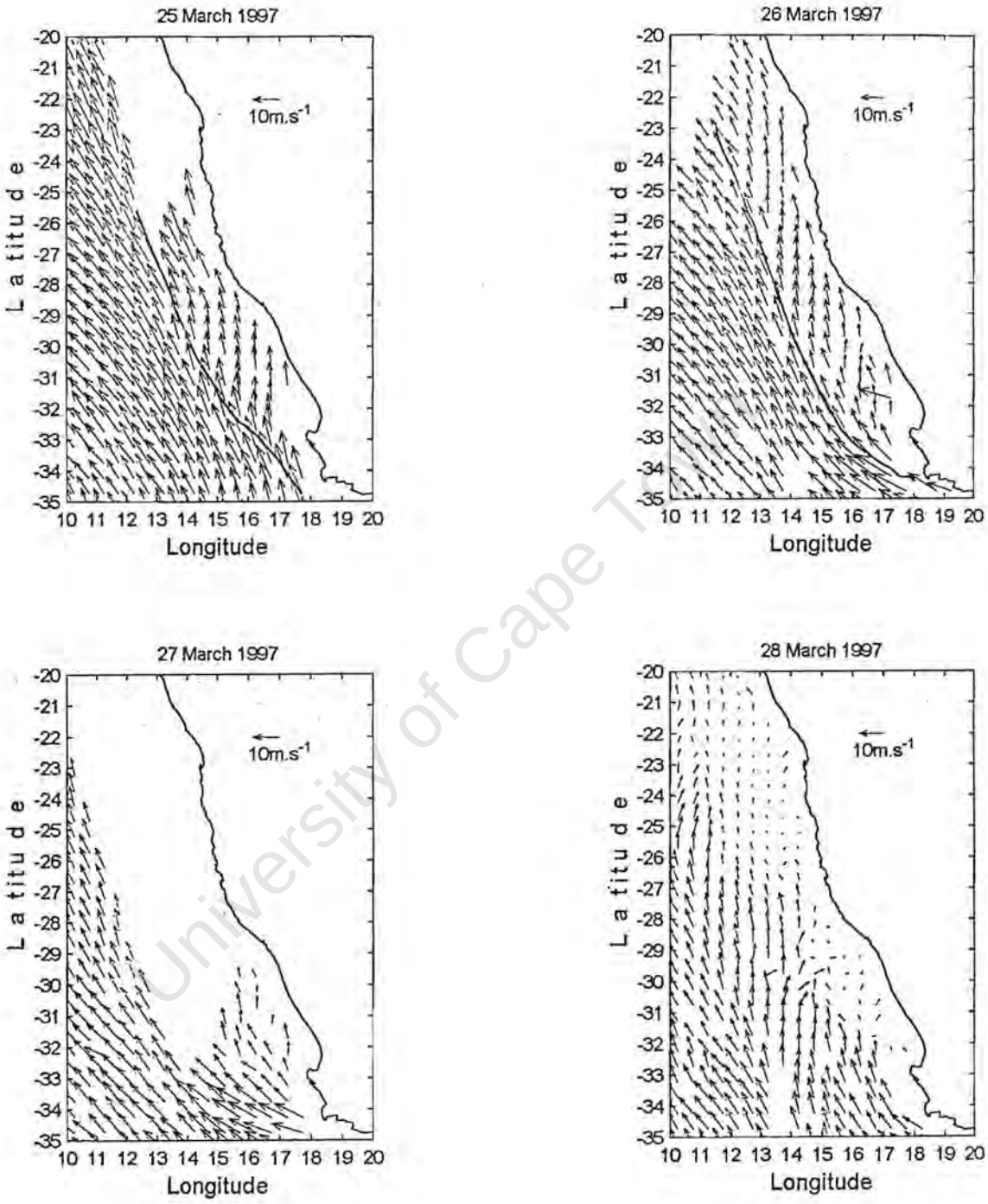

Figure 4.2: Daily-averaged NSCAT wind vectors for the period 25 March to 10 April 1997. The reference vector is given in the upper right-hand part of the figure.

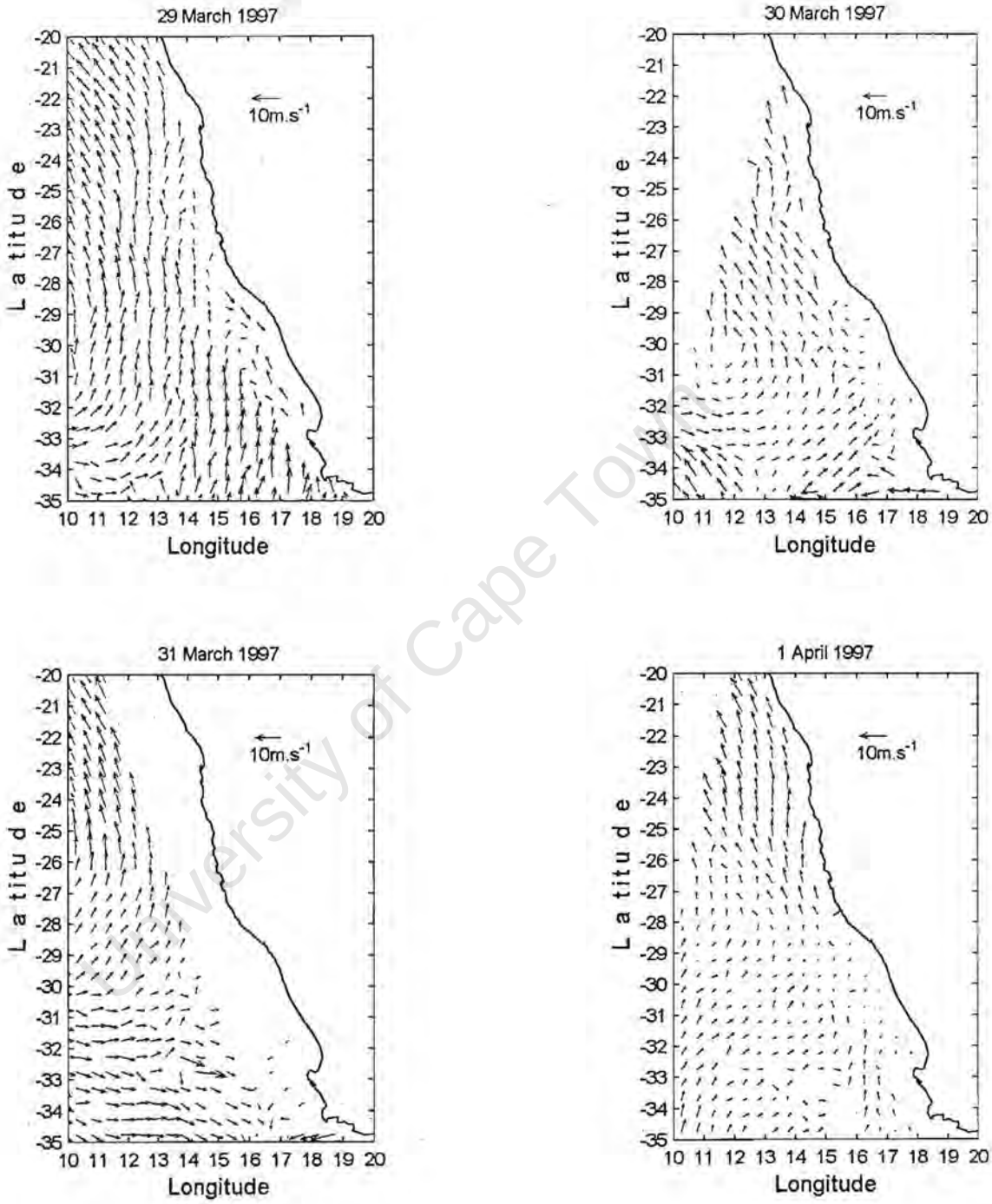

Figure 4.2: Continued.....

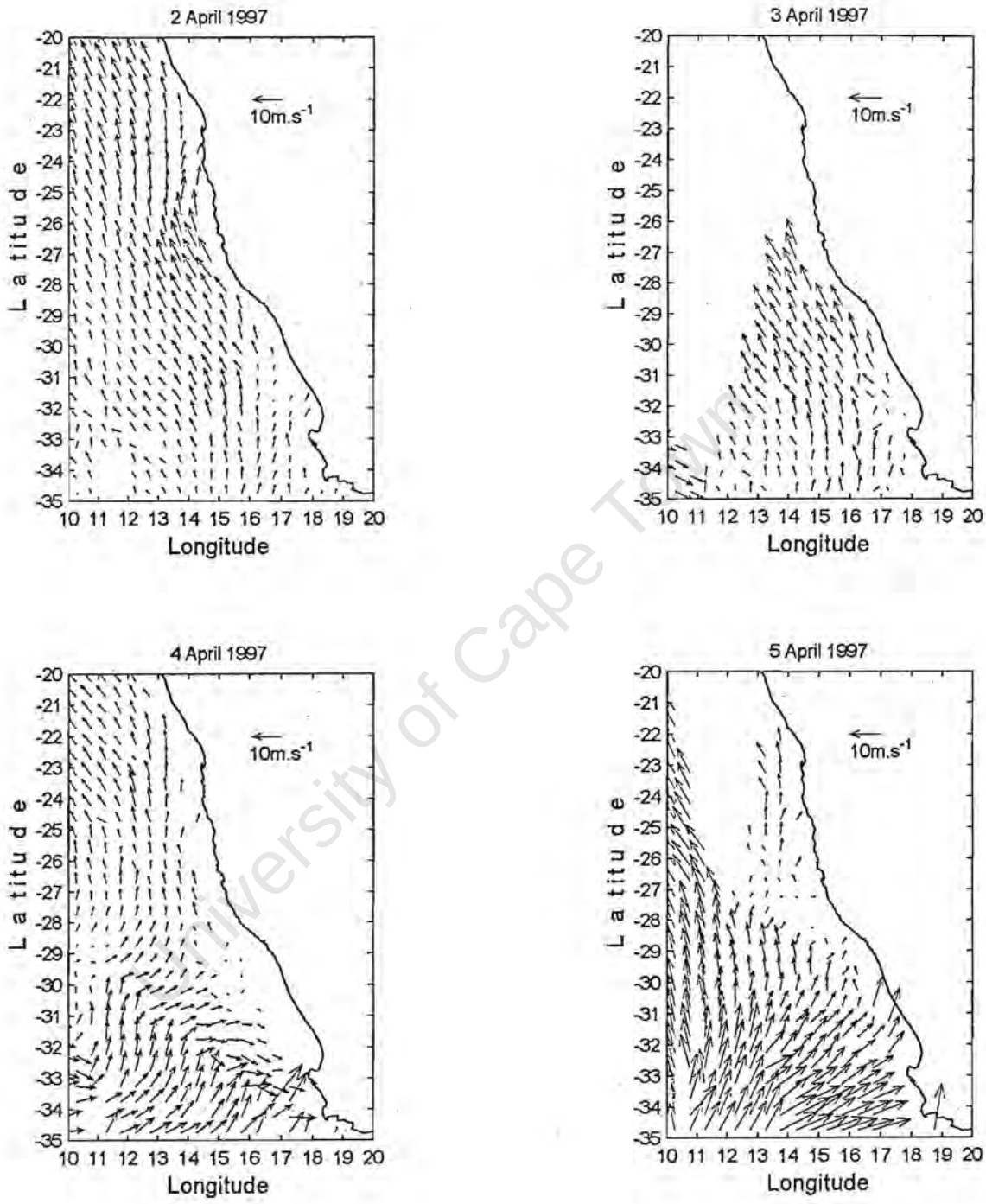

Figure 4.2: Continued.....

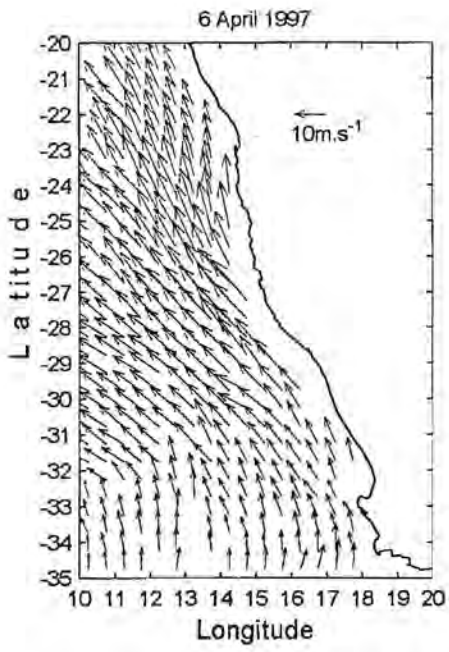

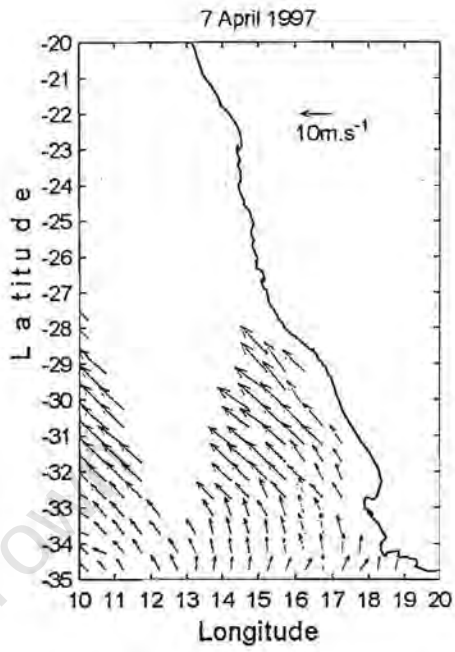

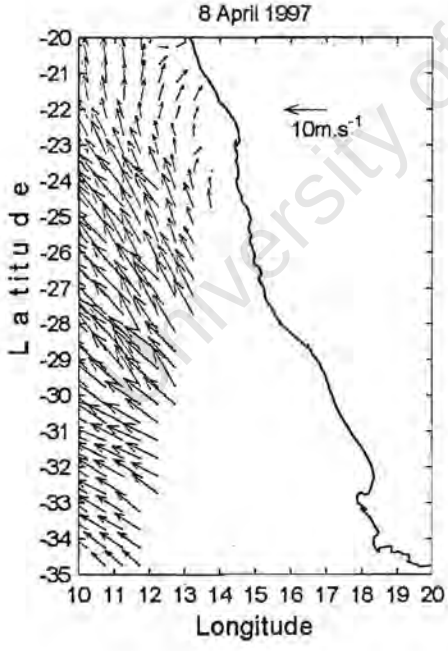

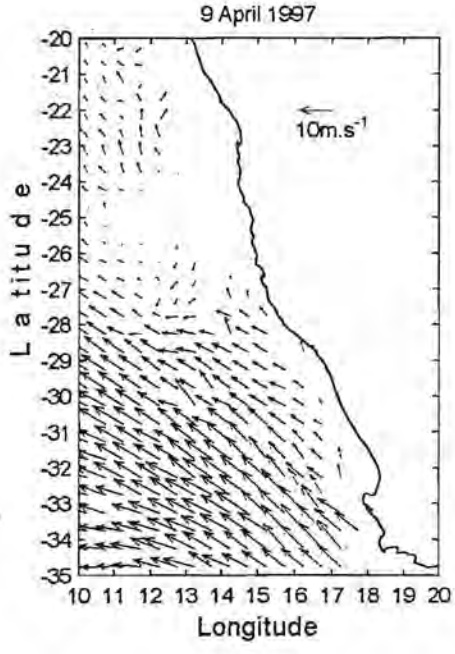

Figure 4.2: Continued.....

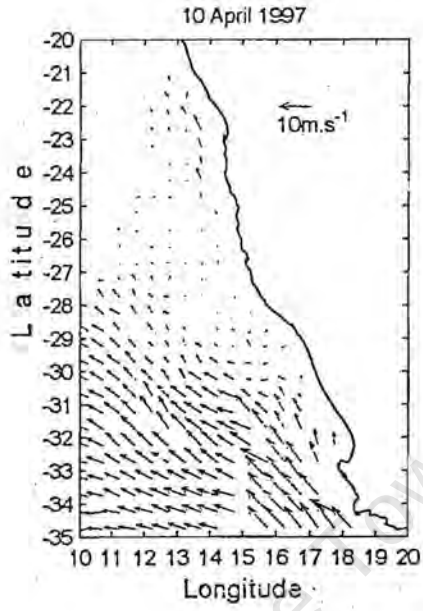

FIGURE 4.2:.....Continued

Wind Stress Curl

Figure 4.3 show wind stress curl patterns for the period 25 March to 10 April 1997 calculated from three-day running mean wind vector data. Three-day running mean wind vectors and isotachs are not shown because they add very little to the interpretation of the daily NSCAT data. The period starts with a strong negative wind curl present along the entire coast of southern Africa. Highest negative curl values are adjacent to the Cape Peninsula-Cape Columbine area and remains that way from 25 - 27 March 1997. As the period of low wind commences negative curl values decrease steadily until the system is dominated by low positive curl values, leading to downwelling velocities not exceeding 1.2 $m.day^{-1}$.

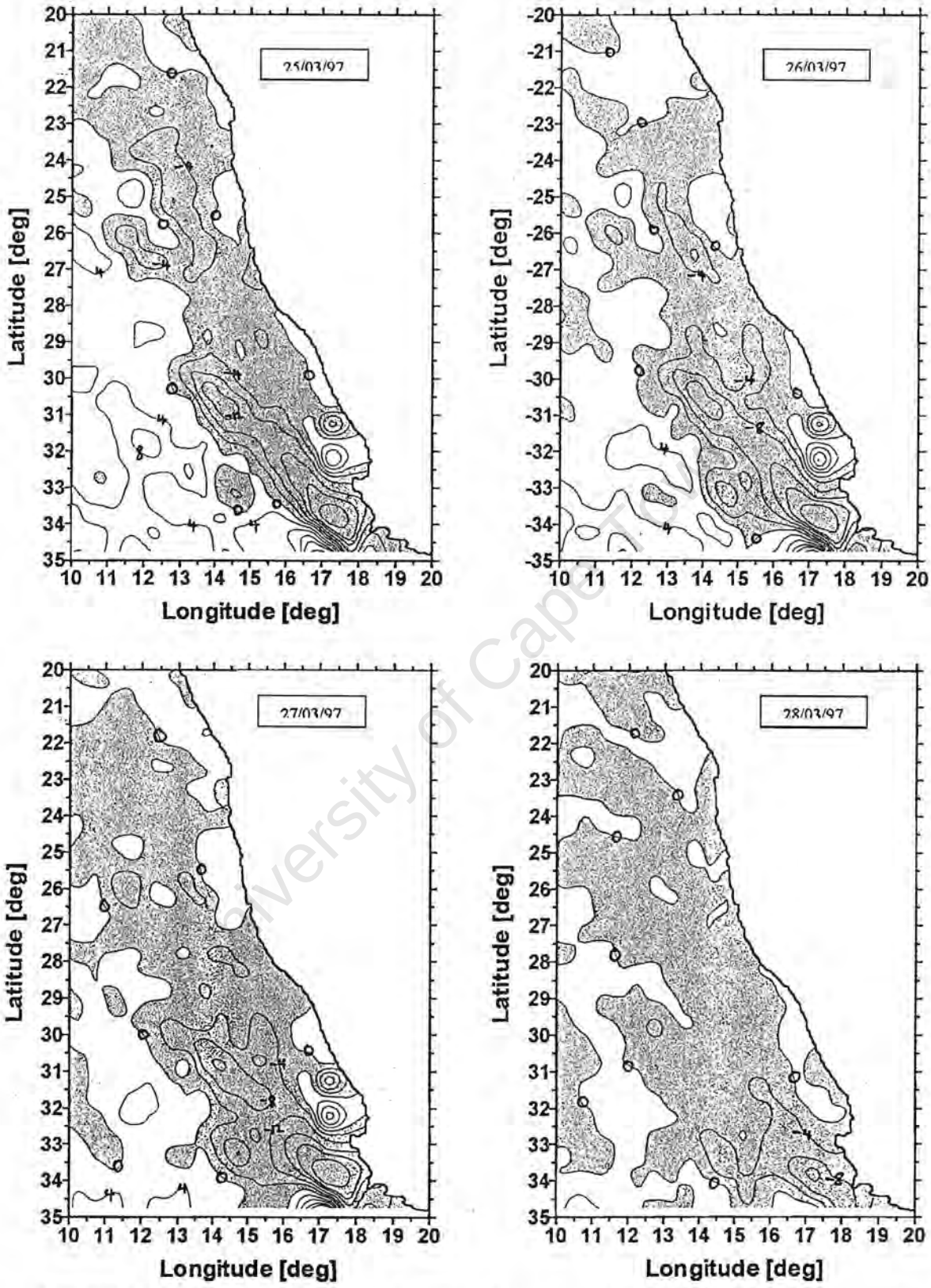

FIGURE 4.3: Wind stress curl contours (x 10^{-7} Nm^{-3}) constructed from three-day running mean data for the period 25 March to 10 April 1997. The contour interval is 4 x 10^{-7} Nm^{-3} and the shaded areas signify clockwise or negative curl, whereas unshaded areas indicate positive or anticlockwise curl.

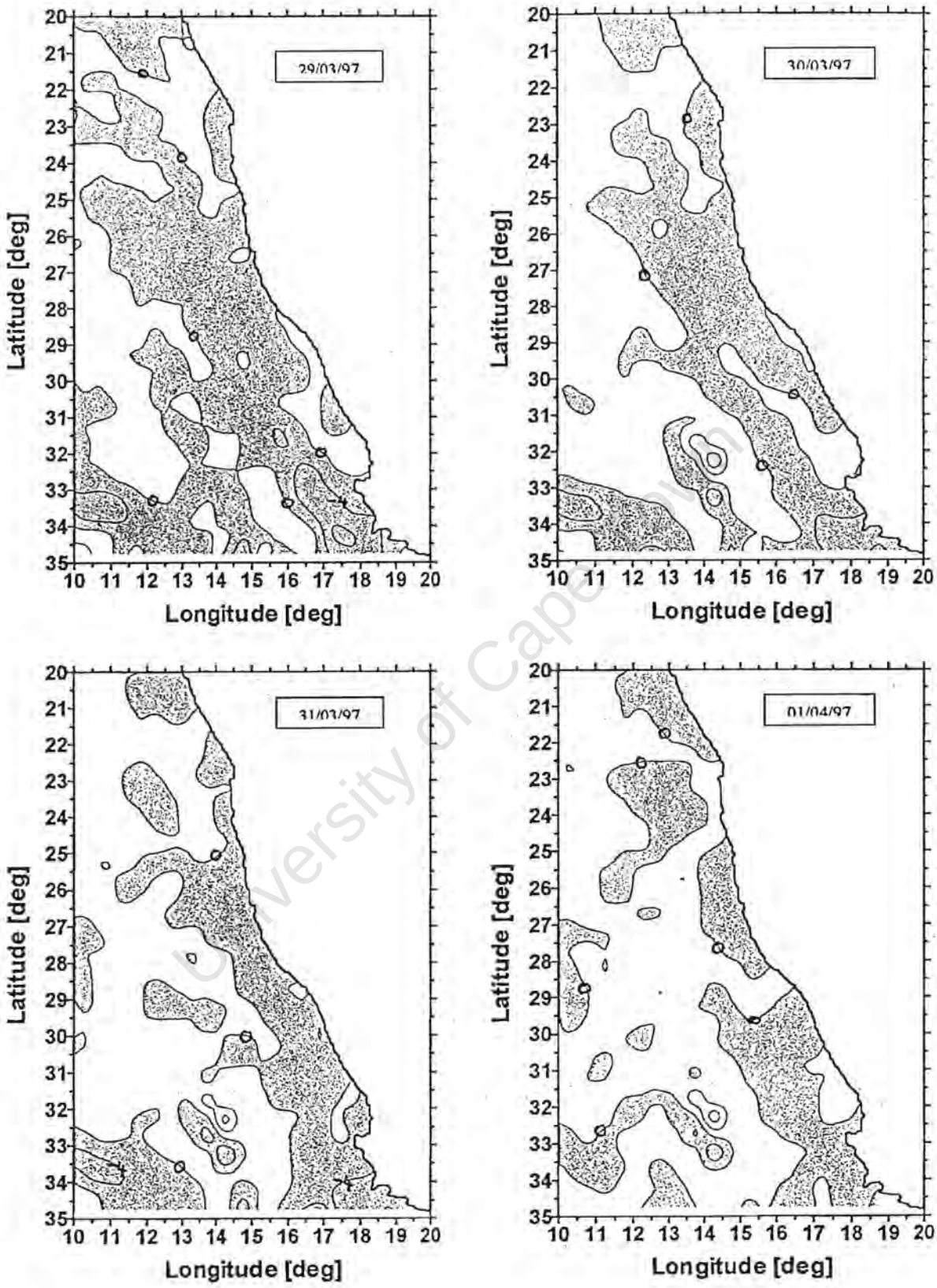

Figure 4.3: Continued .....

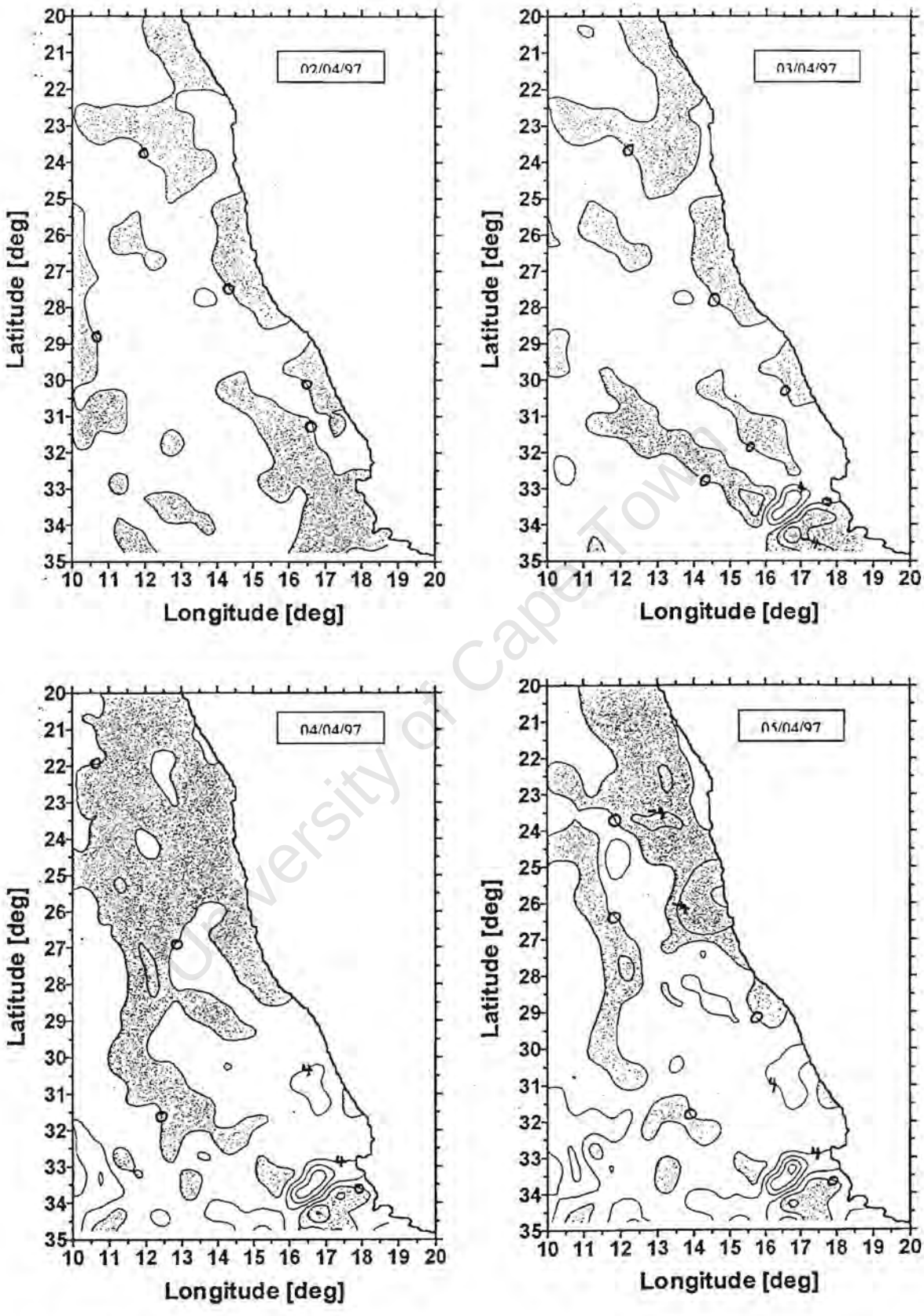

Figure 4.3: Continued .....

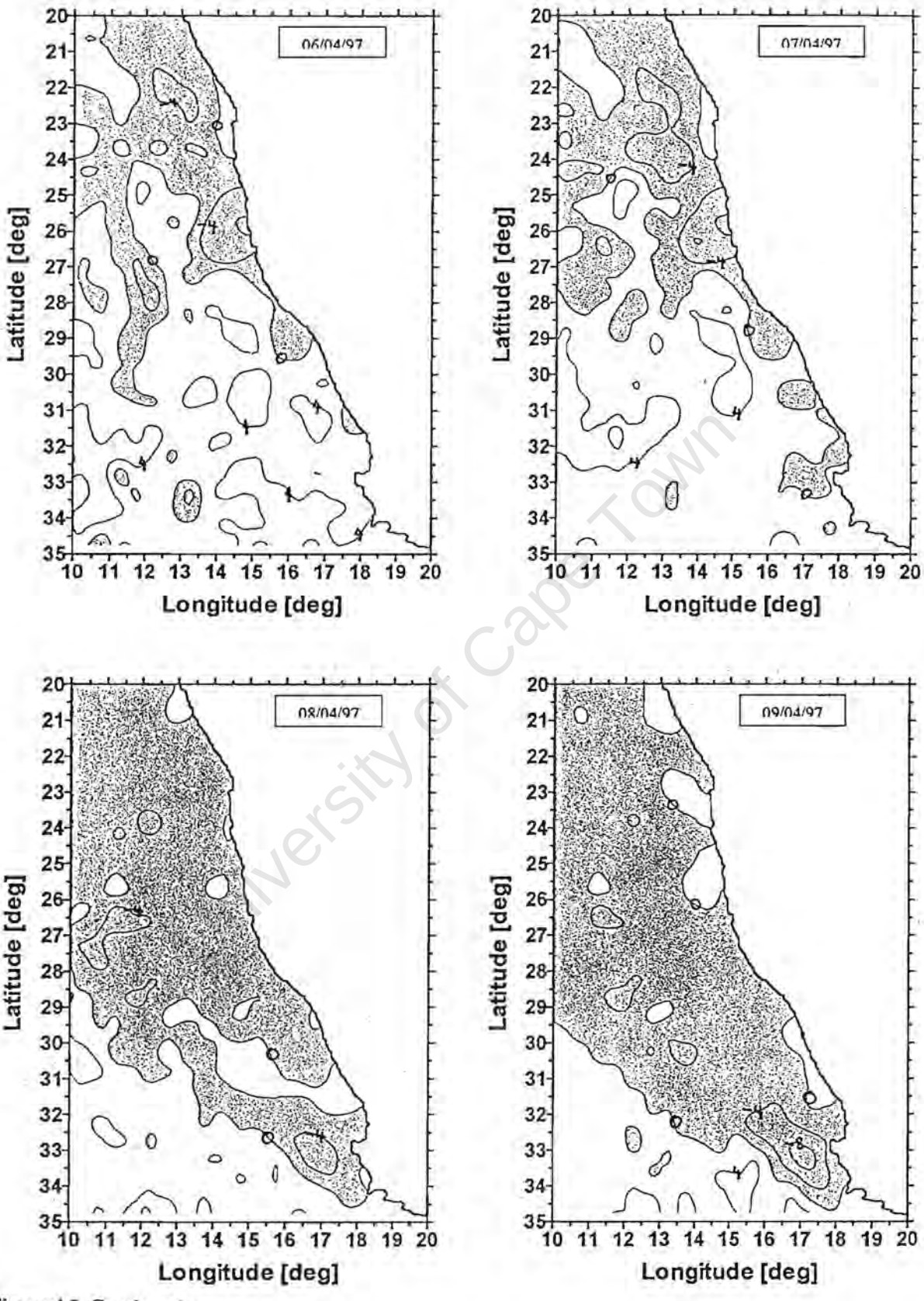

Figure 4.3: Continued .....

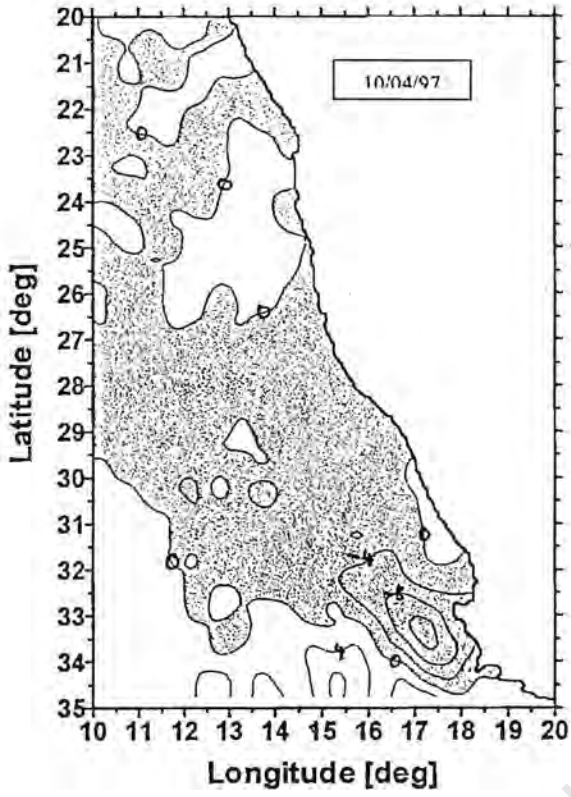

Figure 4.3: Continued .....

Discussion

Daily NSCAT data were used in conjunction with daily weather maps produced by the South African Weather Bureau for the period 25 March to 10 April 1997. The comparison was consistent and the NSCAT data appears to give a good description of the wind conditions over the shelf environment.

On this occasion, the west coast atmospheric trough produced a low wind episode over the continental shelf along the west coast of South Africa. The low wind episode occurred from 27 March to 4 April 1997. During this period of low wind speed, wind vectors recorded by NSCAT showed that the spatial extent of low winds varied. At the start of the low wind episode, wind speeds within 120 nmiles from the coast were below 10 knots. The spatial coverage of low winds appears to expand dramatically between 30 March and 1 April. Not only does the area of low winds occupy a larger area, but the wind direction south of ~28°S rotated from southerly to dominantly onshore westerlies. The onshore flow is coincident with the passage of a cold front as well as the anomalous position of an anticyclone well to the south of the subcontinent. Together the two synoptic systems produce the onshore westerlies. In this way, the present study supported the results of Pitcher *et al.* (1995) as well as with Cockcroft *et al.* (1999). Based on a preliminary investigation of daily weather maps for the period December 1996 to May 1997, it was found that there were several periods of extended low winds such as the nine day scenario investigated.

It appears from the present analysis that the rock lobster stranding event happened after a long period of low winds, as a result of a persistent west coast trough. The "walk-out" only occurred after a cold front altered shelf winds from southerly to westerly, but aided by the anomalous anticyclone situated around 40-50°S. Such a change in wind direction would advect dinoflagellate bloom onshore into shallower waters. This fits into the conceptual model proposed by Pitcher *et al.* (1998). The daily NSCAT wind vectors also showed that strongest onshore flow

produced by the cold front (4-5 April) occurred in the region south of 30°S. This corresponds with the approximate latitude of Elands Bay.

There are other physical factors to consider explaining rock lobster mortality events such as lunar phase that controls the generation of internal waves at the shelf edge and stratification. A poster presentation of Nelson and Pitcher (19) showed that there is a good relationship between tidal maxima and occurrence of *Noctiluca* tide tides during spring and autumn.

Chapter 5 - CONCLUSIONS

The dissertation seeked to understand the effectiveness of satellite based data collection of wind fields along the west coast of southern Africa, pertaining to particular synoptic atmospheric systems. A comparison was undertaken between data from two automatic weather stations and measurements obtained by the NASA scatterometer NSCAT for the period 1 December 1996 to 31 May 1997. It was found that automatic coastal weather stations are effective tools for gaining some understanding of the complex wind field dynamics over the west coast continental shelf. The correlation coefficients between the two sets of coastal weather station and NSCAT data points were ~70%. This correlation statistic was much lower than the 95% quoted by Bourassa *et al.* (1997), who compared NSCAT wind data with data collected by research ships. A possible explanation could be that research vessels out at sea are far from topographic interference such as weather stations along the coast of the Cape Columbine-Cape Peninsula area. At the same time it was found that NSCAT was very effective in capturing day-to-day changes in the Benguela wind field on a synoptic scale. The ability of NSCAT wind data resolving the synoptic scale, in conjunction with its good agreement to coastal weather station data, has proved that NSCAT data was useful in this analysis.

From NSCAT wind vectors data, upwelling rates were calculated for the main upwelling centres along the southern African west coast, which included Cape Peninsula, Cape Columbine, Hondeklip Bay and Lüderitz. The volume estimates showed that Lüderitz, the largest upwelling centre, upwelled approximately 1.23 Sv between 1 December 1996 and 28 February 1997. During the same period Cape Columbine upwelled 0.25 Sv; 20% of the volume at Lüderitz. The four upwelling centres collectively upwelled 1.69 Sv during the same period and the volume flux at Lüderitz contributed 72.7% of the total. This is in good agreement with the findings of Johnson and Noli-Peard (1998) for Lüderitz and Johnson and Nelson (1999) for Cape Columbine, who

estimated upwelling volumes from coastal weather station data. The results exceed the totals published by Monteiro (1996), but that could be as a result of NSCAT winds being higher than coastal weather stations.

In Chapter 3, attention was given to a quantitative study of four major synoptic atmospheric systems and their wind field dynamics over short periods of several days. The first synoptic system type was the South Atlantic Anticyclone (SAA) moving from its established position along the west coast of southern Africa to ridging eastward around the southern tip of the subcontinent. It was found that the strong, negative wind stress curl produced by the wind system stretched from the Cape Peninsula-Cape Columbine area northward to beyond the boundaries of the study region. This was not the case for data used by Jury (1984, 1985), Jury *et al.* (1985a, b), Jury (1988) and Kamstra (1985). This longshore pattern of negative wind stress curl was evident in Parrish *et al.* (1983) and Bakun (1988) who both used monthly wind stress climatologies from ships data.

It was found that the offshore extent of coastal topographic steering is ~ 200 km. Along the coast the highest wind speed was associated with such topographic features such as the Cape Columbine-Cape Peninsula area, Hondeklip Bay and Lüderitz. The squeezing of air between the topography and synoptic atmospheric system produced wind speeds of 10 - 12 ms^{-1} compared to wind speeds one or several meters per second slower. With the ridging SAA, there was an area wide increase in wind speed with wind vectors becoming more uni-directional or southerly. Due to the strongest topographical steering at the capes in the south, highest negative wind stress curl was produced. At the capes negative wind stress curl increase from -1 x 10^{-7} Nm^{-3} to -16 x 10^{-7} Nm^{-3} within four days. The ridging SAA also produced strongest upward vertical velocities associated with Ekman pumping and coastal Ekman divergence. Highest upward Ekman pumping velocity was 1.56 $m.day^{-1}$ compared to 68 m. day^{-1} at the same time for coastal divergence. Even at the most favourable conditions producing maximum negative curl values, the structure in the wind field is not as significant as coastal divergence at the coast.

The second atmospheric system type was the west coast trough of low pressure that forms in the north of the study area and propagates southward along the west coast. It was found that the system is responsible for reducing wind speeds under its influence to values mostly below 5 ms^{-1}. Its area of influence over the shelf was estimated at approximately 250 km from the coast. This offshore scale suggests that this synoptic system may be an important factor for inducing calm conditions, which often lead to dinoflagellate blooms developing during late summer-early autumn. It was shown that the wind direction under the influence of the west coast trough of low pressure were inconsistent in direction, but may be ascribed to the inability of NSCAT to accurately measure wind direction for speeds less than 2 ms^{-1}. It was also shown that as the atmospheric low pressure trough propagates poleward it pushes the negative wind stress curl further offshore.

The third synoptic atmospheric system type was the cold front. It appears to affect the study area south of 28°S, which is in agreement with Shannon and Nelson (1996). North of 28°S, winds are consistently from the south and wind speeds range from 4 - 10 ms^{-1}. The front was marked by a very sharp spatial gradient in direction from southerly to north westerly. The wind direction changes in the region when the cold front reaches the west coast continental shelf. At the central low pressure of the cold front, a vertical velocity of 11 $m.day^{-1}$ was estimated from negative wind stress curl.

Daily NSCAT wind data was used to capture the formation of two coastal lows along the Namibian coast. The first was formed near Lüderitz and the second at Walvis Bay. It was shown that the offshore extent of the coastal low pressure systems are ~ 220 km from the coast. The southward propagation of coastal lows were not captured by NSCAT, but this could be as a result of the data gap ranging from 60 nmiles (north of Cape Columbine) to 90 nmiles (in the vicinity of St Helena Bay) between the coast and the first NSCAT data point. Estimates from daily weather maps from the South African Weather Bureau showed that the systems have an average ground speed of approximately 11 ms^{-1}. This agrees well with the statistical results of Preston-Whyte and

Tyson (1973) and Gill (1977). It also agrees well with the numerical result shown by Ngoc Ahn and Gill (1981).

The overall conclusion that can be drawn from the analysis done in Chapter 3, is that NSCAT wind measurements compliment that of coastal weather stations. However, NSCAT data captures synoptic scale changes in the wind field on a daily time scale. This is a great improvement when compared to data characteristics derived from coastal weather stations, or climatological data such as COADS. It must be stressed that NSCAT data must be verified with ground measurements, and should be used in conjunction with coastal weather station data.

Chapter 4 contained a spatial time series of daily NSCAT data that was used with daily weather maps for the period 25 March to 10 April 1997. It was shown that this period was marked by a long period of low wind speeds (≤ 5 ms^{-1}). The period of low wind commenced on 27 March and lasted until 5 April. During this time persistent coastal low pressure troughs dominated the atmospheric circulation and this is revealed by the long troughs in the air pressure time series recorded at Cape Columbine and Port Nolloth. This was in good agreement to the previous study done by Pitcher *et al.* (1995), who analysed daily weather maps during periods of dense dinoflagellate blooms along the west coast of South Africa. The present analysis also revealed a similar mechanism for advecting such dense dinoflagellate blooms onshore would be by cold fronts. It showed that the cold front reached the west coast shelf on the 5th of April resulting in winds blowing onshore. This was immediately followed by a rock lobster mortality event giving rise to 1500 tons of lobster being stranded on the beach at Elands Bay (~30.5°S). Although not shown in the present study, an analysis of other periods of rock lobster mortality events revealed the same sequence of atmospheric phenomena.

Future Studies

In order to obtain wind data in the area between the coast and the first NSCAT data point, a line of moored buoys will be placed perpendicular to the coast. These buoys will record wind speed and direction, together with air pressure. Such measurements would give the offshore structure of wind data and give an indication of whether a simple linear interpolation is an adequate description as used in this study.

A numerical model to study coastal upwelling, was implemented for the southern Benguela region by Penven (2000). The model was the community-based Regional Ocean Modeling System (ROMS) developed by the University of California Los Angeles (UCLA) and Rutgers University. Penven (2000) used climatological wind forcing and it is believed that the inclusion of the three-day running mean wind fields of the present study in the forcing would increase the simulation of reality in the model. Such forcing would also show what happens to the upwelling fronts during periods of low wind and indicate mechanisms of advecting dense dinoflagellate blooms onshore.

REFERENCE LIST:

Agenbag, J.J. (1996): Pacific ENSO events reflected in meteorological and oceanographic perturbations in the southern Benguela system. *S. Afr. J. Sci., vol. 92*, pp. 243 - 247.

Andrews, W.R.H. and L. Hutchings (1980): Upwelling in the southern Benguela current. *Prog. Oceanogr., Vol. 9(1).*

Apel, J.R. (1987): Principles of ocean physics. *International Geophysical Series, vol. 38*, Academic press Limited, London.

Bailey, G.W. and P. Chapman (1985): The nutrient status of the St Helena Bay region in February 1979. *In: South African Ocean Colour Experiment*, Shannon L.V. (Ed), Sea Fisheries Research Institute, Cape Town, pp. 125 - 145.

Bailey, G.W. and P. Chapman (1991): Short-term variability during an anchor station study in the southern Benguela upwelling system: Chemical and Physical Oceanography. *Prog. Oceanogr., vol. 28*, pp. 9 - 37.

Bakun, A. (1973): Coastal Upwelling Indices, West coast of North America 1946 - 1971. U.S. Dept. Commer., *NOAA Tech. Rep., NMFS SSRF-671.*

Bakun, A. and C.S. Nelson (1977): Climatology of upwelling related processes off Baja, California. *CalCOFI Rep. 19*, pp. 107 - 127.

Bakun, A. and R.H. Parrish (1982): Turbulence, transport and Pelagic fish in the California and Peru current systems. *CalCOFI Rep. 23*, pp. 99 - 112.

Bakun, A. (1987): Applications of marine data to the study of surface forcing of seasonal and interannual ocean variability in eastern boundary regions. *Ph.D. Thesis*, Oregon State University, Oregon, USA.

Bakun, A. and C.S. Nelson (1991): The seasonal cycle of wind stress curl in subtropical eastern boundary current regions. *J. Phys. Oceanogr., vol. 21*, pp. 1815 - 1834.

Bakun, A. (1996): *Patterns in the Ocean: Ocean Processes and Marine Population Dynamics*, University of California Sea Grant, San Diego.

Bathelor, G.K.(1987): *An introduction to fluid dynamics.* University Press, Cambridge.

Boyd, A.J. and G. Oberholster (1994): Currents off the West and South coasts of South Africa. *SA Shipping News and Fishing Industry Review*, pp. 26 - 28.

Boyd, A.J. and G. Nelson (1998): Variability of the Benguela Current off the Cape Peninsula. *S. Afr. J. mar. Sci., vol. 19*, pp. 15 - 39.

Brink, K.H., Jones, B.H., Van Leer, J.C., Mooers, C.N.K., Stuart, D.W., Stevenson, M.R., Dugbale, R.C. and G.W. Heburn (1981): Physical and biological structure and variability in an upwelling centre off Peru near 15°S during March, 1977. *In: Coastal Upwelling*, F.A. Richards (Ed), *Amer. Geophys. Union*, Washington D.C., pp. 473 - 495.

Brink, K.H. (1983): The near-surface dynamics of upwelling. ***Prog. Oceanogr., vol. 12,*** pp. 223 - 257.

Brink, K.H. (1991): Coastal-trapped waves and wind-driven currents over the continental shelf, ***Annu. Rev. Fluid Mech., vol. 23,*** pp. 389 - 412.

Brink, K.H. (1998): Wind-driven currents over the continental shelf. ***In: The Sea, vol. 10,*** The Global Coastal Ocean: Processes and Methods. Brink, K.H. and A.R. Robinson (Eds), Wiley, New York, pp. 3 - 20.

Brown, G.S. (1979): Estimation of surface winds using satellite-borne radar measurements at normal incidence. ***J. Geophys. Res., vol. 91,*** pp. 3974 - 3978.

Brown, P.C., Hutchings, L. and D.A. Horstman (1979): A red-water outbreak and associated fish mortality at Gordon's Bay near Cape Town. ***Fish. Bull. S. Afr., vol. 9,*** pp. 46 - 52.

Brundrit, G.B. (1981): Upwelling fronts in the southern Benguela Region. ***Trans. Roy. Soc. S. Afr., vol. 44,*** pp. 309 - 313.

Brundrit, G.B., De Cuevas, B.A. and A.M. Shipley (1987): Long-term sea-level variability in the eastern south Atlantic and comparison with the eastern Pacific. ***S. Afr. J. mar. Sci., vol. 5,*** pp. 73 - 78.

Cockcroft, A.C., Schoeman, D.S., Pitcher, G.C., Bailey, G.W. and D.L. Van Zyl (1999): A mass stranding, or "walk out" of west coast rock lobster, *Jasus lalandii,* in Elands Bay, South Africa: Causes, Results, and Implications. ***In: The Biodiversity Crisis and Crustacea:*** *Proceedings of the fourth International Crustacean congress, Amsterdam, the Netherlands, July 20 - 24, 1998.* Von Vanpel Klein, J.C. and F.R. Schrom (Eds), pp. 673 - 688.

Crepon, M., Richez, C. and M. Chartier (1984): Effects of coastline geometry on Upwellings. ***J. Mar. Res., vol. 14,*** pp. 1365 - 1382.

Da Silva, A.M., Young, C.C. and S. Levitus (1994): Atlas of surface marine data 1994, volume 1: algorithms and procedures. ***NOAA Atlas NESDIS 6,*** pp. 74.

Dingle, R.V. and G. Nelson (1993): Sea-bottom temperatures, salinity and dissolved oxygen on the continental margin off south-western Africa. ***S. Afr. J. mar. Sci., vol. 13,*** pp. 33 - 49.

Enriquez, A.G. and C.A. Friehe (1995): Effects of wind stress and wind stress curl variability on coastal upwelling. ***J. Phys. Oceanogr., vol. 25,*** pp. 1651 - 1671.

Garvine, R.W. (1974): Ocean interiors and coastal upwelling models. ***J. Phys. Oceanogr., vol. 4 (1),*** pp. 121 - 124.

Garzoli, S.L., Fordon, A.L. and D. Pillsbury (1994): BEST: Benguela Source and Transport. The South Atlantic: Present and Past Circulation, Bremen, Germany 15 - 19 August 1994. ***Berichte, Fachbereich Geowissenschaften, Universität Bremen 52,*** pp. 167.

Garzoli, S.L. and A.L. Gordon (1996): Origins and variability of the Benguela Current. ***J. Geophys. Res., vol. 101,*** pp. 897 - 906.

Gill, A.E. (1977): Coastally trapped waves in the atmosphere. ***Quart. J. Roy. Met. Soc., vol. 103***, pp. 431 - 440.

Glowienka-Hense, R., Hense, A. and C. Volker (1992): ECMWF versus Hellerman and Rosenstein stress climatology of the Southern Ocean. ***Antarctic Science, vol. 4***, pp. 111 - 117.

Gordon, A.L., Weiss, R.F. and Smethie, W.M. (1992): Thermocline and intermediate water communication between the South Atlantic and Indian Oceans. ***J. Geophys. Res., vol. 97(C5)***, pp. 7223 - 7240.

Gordon, A.L., Bosley, K.T. and F. Aikman (1995): Tropical Atlantic water within the Benguela upwelling system at 27°S. ***Deep-Sea Res., vol. 42***, pp. 1 - 12.

Haidvogel, D.B., Wilkin, J.L. and R. Young (1991): A semi-spectral primitive equation ocean circulation model using vertical sigma and orthogonal curvilinear horizontal coordinates. ***J. Computational Phys., vol. 94(1)***, pp. 151 - 185.

Haidvogel, D.B. and A. Beckman (1998): Numerical modeling of the coastal ocean. ***The Sea, vol. 10***, The Global Coastal Ocean: Processes and Methods. Brink, K.H. and A.R. Robinson (Eds), Wiley, New York, pp. 457 – 482.

Hellerman S. and M. Rosenstein (1983): Normal monthly wind stress over the world ocean and error estimates. ***J. Phys. Oceanogr., vol. 13***, pp. 1093 - 1104.

Holden, C. J. (1985): Currents in St Helena Bay inferred from radio-tracked drifters, ***In: South African Ocean Colour Experiment***, Shannon, L.V. (Ed), Sea Fisheries Research Institute, Cape Town, pp. 97 - 109.

Holden, C.J. (1987): Observations of low-frequency currents and continental shelf waves along the west coast of South Africa. ***In: The Benguela and Comparable Ecosystems***, Payne, A.I.L., Gulland, J.A. and K.H. Brink (Eds), ***S. Afr. J. mar. Sci., vol. 5***, pp. 197 - 208.

Holton, J.R. (1972): ***An introduction to dynamic meteorology***. Academic Press, California.

Horstman, D.A. (1981): Reported red-water outbreaks and their effects on fauna of the west and south coasts of South Africa. ***Fish. Bull. S. Afr., vol. 15***, pp. 71 - 88.

Horstman, D.A., McGibbon, S., Pitcher, G.C., Calder, D., Hutchings, L. and P. Williams (1991): Red tides in False Bay, 1959 - 1989, with particular reference to recent blooms of *Gymnodinium* sp. ***Trans. Roy. Soc. S. Afr., vol. 47***, pp. 611 - 628.

Hsu, S.A. (1988): ***Coastal Meteorology***. Academic Press Incorp., New York, USA.

Hutchings, L. and J. Taunton-Clark (1990): The monitoring of gradual change in areas of high mesoscale variability. ***S. Afr. J. Sci., vol. 86***, pp. 9 - 37.

Johnson, A.S. and G.Nelson (1999): Ekman estimates of upwelling at Cape Columbine based on measurements of longshore wind from a 35-year time-series. ***S. Afr. J. mar. Sci., vol. 21***, pp. 433 - 436.

Johnson, A.S. and K.Noli-Peard (1998): Ekman estimates of upwelling derived from winds measured at Luederitz. ***Poster presentation,*** Abstract in proceedings : ***Variability in SE Atlantic symposium,*** Swakopmund, Namibia.

Jury, M.R. (1984): Wind-shear and differential upwelling along the S.W. tip of Africa. ***Ph.D Thesis,*** University of Cape Town, South Africa.

Jury, M.R. (1985a): Mesoscale variation in summer winds over the Cape Columbine-St Helena Bay region, South Africa. ***S. Afr. J. mar. Sci., vol.3,*** pp. 77 - 88.

Jury, M.R., Kamstra, F. and J. Taunton-Clark (1985a): Diurnal wind cycles and upwelling off the northern portion of the Cape Peninsula in summer. ***S. J. mar. Sci., vol.3,*** pp. 1 - 10.

Jury, M.R., Kamstra, F. and J. Taunton-Clark (1985b): Diurnal wind cycles and upwelling off the southern portion of the Cape Peninsula in summer. ***S. Afr. J. mar. Sci., vol.3,*** pp. 33 - 42.

Jury, M.R. (1985b): The sudden decay of upwelling off the Cape Peninsula, South Africa: A case study. ***S. Afr. J. mar. Sci., vol.4,*** pp. 111 - 118.

Jury, M.R. (1988): Case studies of the response and spatial distribution of wind-driven upwelling off the coast of Africa: 29-34° south. ***Cont. Shelf. Res., vol.8(11),*** pp. 1257 - 1271.

Jury, M.R., MacArthur, C.I. and G.B.Brundrit (1990): Pulsing of the Benguela upwelling region: Large-scale atmospheric controls. ***S. Afr. J. mar. Sci., vol.9,*** pp. 27 - 41.

Jury, M.R. and G.B.Brundrit (1992): Temporal organisation of upwelling in the southern Benguela ecosystem by resonant coastal trapped waves in the ocean and atmosphere. *S. Afr. J. mar. Sci., vol.12,* pp. 219 - 224.

Kamstra, F. (1985): Environmental features of the southern Benguela with special reference to the wind stress. ***South African ocean colour and upwelling experiment.*** Shannon, L.V. (Ed.) Cape Town, Sea Fisheries Research Institute, pp. 13 - 27.

Kidson, J.W. (1988): Indices of the southern hemisphere zonal wind. ***J. Climate, vol.01,*** pp. 183 - 194.

Kundu, P.K. (1990): ***Fluid Mechanics.*** Academic Press, California.

Lamberth, R. and G. Nelson (1987): Field and analytical drogue studies applicable to the St Helena Bay area off South Africa's west coast. ***In: The Benguela and Comparable Ecosystems,*** Payne, A.I.L., Gulland, J.A. and K.H. Brink (Eds), ***S. Afr. J. mar. Sci., vol. 5,*** pp. 163 - 169.

Levitus, S. (1982): ***Climatological Atlas of the World Ocean.*** Professional Paper 13, NOAA, USA, pp. 173.

Liu, W.T. and W. Tang (1996): Equivalent Neutral Wind. ***Jet Propulsion Lab. Publi. 96-17,*** JPL, Pasedena, California

Liu, W.T., Tang, W. and H. Hu (1998a): Spaceborne sensors observe El Niño's effects on

ocean and atmosphere in North Pacific. ***EOS Transaction Amer. Geophys. Union, vol. 79(21)***, pp. 249.

Liu, W.T., Tang, W. and P.S. Polito (1998b): NASA scatterometer provides global ocean-surface wind fields with more structure than numerical weather prediction. ***Geophys. Res. Letters, vol. 25(6)***, pp. 761 - 764.

Lutjeharms, J.R.E. and J.M. Meeuwis (1987): The extent and variability of South-East Atlantic upwelling. ***In: The Benguela and Comparable Ecosystems***, Payne, A.I.L., Gulland, J.A. and K.H. Brink (Eds), ***S. Afr. J. mar. Sci., vol. 5***, pp. 51 - 62.

Lutjeharms, J.R.E. and P.L. Stockton (1987): Kinematics of the upwelling front off southern Africa. ***In: The Benguela and Comparable Ecosystems***, Payne, A.I.L., Gulland, J.A. and K.H. Brink (Eds), ***S. Afr. J. mar. Sci., vol. 5***, pp. 35 - 49.

Lutjeharms, J.R.E. and H.R. Valentine (1987): Water types and volumetric considerations of the south-east Atlantic upwelling regime. ***In: The Benguela and Comparable Ecosystems***, Payne, A.I.L., Gulland, J.A. and K.H. Brink (Eds), ***S. Afr. J. mar. Sci., vol. 5***, pp. 63 - 71.

Lutjeharms, J.R.E. (1996): The exchange of water between the South Indian and the South Atlantic. ***In: The South Atlantic: Past and Present Circulation***, Wefer, G., Berger, W.H., Siedler, G. and D. Webb (Eds), Springer-Verlag, Berlin, pp. 125 - 162.

Mason, S.J.(1990): Temporal variability of sea surface temperatures around southern Africa: a possible forcing mechanism for the 18-year rainfall oscillation? ***S. Afr. J. Sci., vol.86***, pp. 243-252.

Matthews, S.G. and G.C. Pitcher (1996): Worst recorded marine mortality on the South African coast. ***In: Harmful and Toxic Algal Blooms***, Yasumoto, T., Oshima, Y. and Y. Fukuyo (Eds), *Intergovernmental Oceanographic Commission of UNESCO*, pp. 89 - 92.

McClean-Padman, J. and L. Padman (1991): Summer upwelling on the Sydney inner continental shelf: the relative roles of local wind forcing and mesoscale eddy encroachment. ***Continental Shelf Res., vol. 11(4)***, pp. 321 - 345.

Monteiro, P.M.S. (1996): The oceanography, the biogeochemistry and the fluxes of carbon dioxide in the Benguela upwelling system. ***Ph.D. Thesis***, University of Cape Town.

Nelson, G. and L. Hutchings (1983): The Benguela upwelling area. ***Prog. Oceanogr., vol. 12***, pp. 333 - 356.

Nelson, G. and N. Walker (1984): Comparison of summer winds on the west coast of South Africa between 1979 and 1983 and the response of coastal upwelling. ***S. Afr. J. Sci., vol.80***, pp. 90 - 93.

Nelson, G. (1985): Notes on the physical oceanography of the Cape Peninsula upwelling system. ***In: South African Ocean Colour and Upwelling Experiment***, Shannon, L.V. (Ed), Sea Fisheries Research Institute, Cape Town, pp. 63 - 95.

Nelson, G. (1992a): Longshore wind variation on the west coast of southern Africa and its influence on the shelf sea. ***S. Afr. J. Sci., vol.88***, pp. 418 - 423.

Nelson, G. (1992b): Equatorward wind and atmospheric pressure as metrics for primary production in the Benguela system. ***S. Afr. J. mar. Sci., vol.12***, pp. 19 - 28.

Nelson, G. and A.S.Johnson (1997): Episodic variation in Ekman divergence in the Cape Columbine upwelling cell, estimated from a 34-year lighthouse wind time-series. ***Poster presentation at 13th Annual Conf S.A.Soc. Atmos. Sci. symposium***, Abstract only.

Neumann, G. and W.J.Pierson (1966): ***Principles of Physical Oceanography.*** Englewood Cliffs, New Jersey; Prentice Hall, pp. 545.

Nguyen Ngoc Ahn and A.E. Gill (1981): Generation of coastal lows by synoptic-scale waves. ***Quart. J. Roy. Met. Soc., vol. 107***, pp. 521 - 530.

Parrish, R.H., Bakun, A., Husby, D.M. and C.S. Nelson (1983): Comparative climatology of selected environmental processes in relation to eastern boundary current pelagic fish reproduction. ***In: Proceedings of the expert consultation to examine changes in abundance and species composition of Neritic fish resources***, San José, Costa Rica, April 1983, Sharp, G.D. and J. Csirke (Eds), ***FAO Fish. Rep., vol. 291(3)***, pp. 731 - 777.

Pedlosky, J.(1986): ***Geophysical Fluid Dynamics.*** Springer-Verlag, New York.

Penven, P., Lutjeharms, J.R.E., Marchesiello, P., Roy, C. and S.J. Weeks (submitted): Generation of cyclonic eddies by the Agulhas Current in the lee of the Agulhas Bank. ***Geophys. Res. Letters.***

Penven, P. (2000): A numerical study of the southern Benguela circulation with an application to fish recruitment. ***Ph.D. Thesis***, Université de Bretagne Occidentale, Brest, France.

Pierson(Jr.), W.J.(1989): Probabilities and statistics for backscatter estimates obtained by a scatterometer. ***J. Geophys.Res., vol.94(7)***, pp. 9743 - 9759.

Pitcher, G.C., Horstman. D.A. and D. Calder (1993): Formation and decay of red tide blooms in the southern Benguela upwelling system during the summer of 1990/91. ***In: Toxic phytoplankton blooms in the sea.*** Smayda, T.J. and Y. Shimizu (Eds), Elsevier Science Publishers, New York, pp. 317 - 322.

Pitcher, G.C., Agenbag, J.J., Calder, D., Horstman, D.A., Jury, M. and J. Taunton-Clark (1995): Red tides in relation to the meteorology of the southern Benguela system. ***In: Harmful marine algal blooms***, Lassus, P., Arzul, G., Erard, E., Gentien, P. and C. Marcaillou (Eds), *Technique et Documentation, Lavoisier*, Intercept Ltd., Paris, pp. 657 - 662.

Pitcher, G.C. and A.J. Boyd (1996): Across-shelf and alongshore dinoflagellate distributions and the mechanismss of red tide formation within the southern Benguela upwelling system. ***In: Harmful and Toxic Algal Blooms***, Yasumoto, T., Oshima, Y. and Y. Fukuyo (Eds), *Intergovernmental Oceanographic Commission of UNESCO*, pp. 243 - 246.

Pitcher, G.C., Boyd, A.J., Horstman, D.A. and B.A. Mitchell-Innes (1998): Subsurface dinoflagellate populations, frontal blooms and the formation of red tide in the southern Benguela upwelling system. ***Mar. Ecol. Prog. Ser., vol. 172***, pp. 253 - 264.

Pollard, R.T., Rhines, P.B. and R.O.R.Y. Thompson (1973): The deepening of the

wind-mixed layer. ***Geophys. Fluid Dyn., vol. 3***, pp. 381 - 404.

Preston-Whyte, R.A. and P.D. Tyson (1973): Note on pressure oscillations over southern Africa. ***Mon. Weath. Rev., vol. 101***, pp. 650 - 659.

Preston-Whyte, R.A. and P.D. Tyson (1988): ***The atmosphere and weather of southern Africa.*** Oxford University Press, Cape Town.

Reason, C.J.C. and M.R. Jury (1990): On the generation and propagation of the southern African coastal low. ***Quart. J. Roy. Met. Soc., vol.116***, pp. 1133 - 1151.

Servain, J., Gohin, F. and A. Muzellec (1993): Wind fields at the sea surface determined from combined ship and satellite altimeter data. ***J. Atmos. Ocean. Tech., vol.10***, pp. 880 - 886.

Schumann, E.H., Illenberger, W.K. and W.S. Goschen (1991): Surface winds over Algoa Bay, South Africa. ***S. Afr. J. Sci., vol.87***, pp. 202 - 207.

Shannon, L.V., Nelson, G. and M.R. Jury (1981): Hydrological and meteorological aspects of upwelling in the southern Benguela Current. ***In: Coastal and Estuarine Sciences I, Coastal Upwelling.*** Richards, F.A. (Ed), *American Geophys. Union*, pp. 146 - 159.

Shannon, L.V. (1985): The Benguela ecosystem. Part I: Evolution of the Benguela, physical features and processes. ***Oceanogr. Mar. Biol. Annu. Rev., vol. 23***, pp. 105 - 182.

Shannon, L.V., Boyd, A.J., Brundrit, G.B. and J. Taunton-Clark (1986): On the existance of an El Nino-type phenomenon in the Benguela system. ***J. Mar. Res., vol.44***, pp. 495 - 520.

Shannon, L.V., Lutjeharms, J.R.E. and J.J. Agenbag (1989): Episodic input of Subantarctic water into the Benguela region. ***S. Afr. J. Sci., vol. 85(5)***, pp. 317 - 322.

Shannon, L.V., Lutjeharms, J.R.E. and G. Nelson (1990): Causative mechanisms for intra-annual and interannual variability in the marine environment around southern Africa. ***S. Afr. J. Sci., vol.86***, pp. 356 - 373.

Shannon, L.V. and P. Chapman (1991): Evidence of Antarctic bottom water in the Angola basin at 32°S. ***Deep-Sea Res, vol. 38(10)***, pp. 1299 - 1204.

Shannon, L.V., Crawford, R.J.M., Pollock, D.E., Hutchings, L., Boyd, A.J., Taunton-Clark, J., Badenhorst, A., Melville-Smith, R., Augustyn, C.J., Cochrane, K.L., Hampton, I., Nelson, G., Japp, D.W. and R.Q. Tarr (1992): The 1980's- a decade of change in the Benguela ecosystem. ***S. Afr. J. mar. Sci., vol.12***, pp. 271 - 296.

Shannon, L.V. and G. Nelson (1996): The Benguela: large scale features and processes and system variability. ***In: The South Atlantic: Past and Present Circulation***, Wefer, G., Berger, W.H., Siedler, G. and D. Webb (Eds), Springer-Verlag, Berlin, pp. 163 - 210.

Shillington, F.A. (1998): The Benguela upwelling system off southwestern Africa. ***In: The Sea, vol.10***, Brink, K.H. and A.R. Robinson (Eds), Wiley, New York, pp. 583 - 604.

Siegfried, W.R., Crawford, R.J.M., Shannon, L.V., Pollock, D.E., Payne, A.I.L. and R.G.

Krohn (1990): Scenarios for global-warming induced change in the open-ocean environment and selected fisheries of the west coast of southern Africa. *S. Afr. J. Sci., vol.86*, pp. 281 - 285.

Smith, R.L. (1968): Upwelling. *Oceanogr. Mar. Bio. Ann. Rev., vol. 6*, pp. 11 - 46.

Strub, P.T., Shillington, F.A., James, C. and S.J. Weeks (1998): Satellite comparison of the seasonal circulation in the Benguela and California current systems. *S. Afr. J. mar. Sci., vol. 19*, pp. 99 - 112.

Taunton-Clark, J. (1985): The formation, growth and decay of upwelling tongues in response to the mesoscale wind field during summer. In: *South African Ocean Colour and Upwelling Experiment.* Shannon, L.V. (Ed.). Cape Town, Sea Fisheries Research Institute, pp. 47 - 61.

Taunton-Clark, J. (1990): Environmental events within the south-east Atlantic(1906-1985) identified by analysis of sea surface temperature and wind data. *S. Afr. J. Sci., vol.86*, pp. 470 - 472.

Thompson, R.O.R.Y. (1983): Low-pass filters to suppress inertial and tidal frequencies. *J. Phys. Oceanogr., vol.13*, pp. 1077 - 1083.

Valentine, H.R. (1990): A fine-scale volumetric census of the water masses of the Agulhas retroflection area. *Rep. S. Afr. Coun. Scient. Ind. Res. EMA-R 691*, pp. 105.

Valentine, H.R., Lutjeharms, J.R.E. and G.B. Brundrit (1993): The water masses and volumetry of the southern Agulhas current region. *Deep-Sea Res., vol. 40(6)*,pp. 1285 - 1305.

Tomczak, M. and J.S. Godfrey (1994): *Regional Oceanography: an introduction.* Pergamon, New York.

Walker, N. (1987): Interannual sea surface temperature variability and associated atmospheric forcing within the Benguela system. *S. Afr. J. mar. Sci., vol.5*, pp. 121 - 132.

Wu, J. (1980): Wind-stress coefficients over sea surface near neautrla conditions - A revisit. *J. Phys. Oceanogr., vol.10*, pp. 727 - 740.